University of Massachusetts Medical School
eScholarship@UMMS

GSBS Dissertations and Theses | Graduate School of Biomedical Sciences

2009-12-01

Pathophysiology of Respiratory Failure Following Acute Organophosphate Poisoning : A Dissertation

Romolo Joseph Gaspari
University of Massachusetts Medical School

Let us know how access to this document benefits you.
Follow this and additional works at: https://escholarship.umassmed.edu/gsbs_diss

 Part of the Chemical Actions and Uses Commons, Medical Toxicology Commons, Organic Chemicals Commons, and the Pharmacology, Toxicology and Environmental Health Commons

Repository Citation
Gaspari RJ. (2009). Pathophysiology of Respiratory Failure Following Acute Organophosphate Poisoning : A Dissertation. GSBS Dissertations and Theses. https://doi.org/10.13028/46yb-g062. Retrieved from https://escholarship.umassmed.edu/gsbs_diss/445

This material is brought to you by eScholarship@UMMS. It has been accepted for inclusion in GSBS Dissertations and Theses by an authorized administrator of eScholarship@UMMS. For more information, please contact Lisa.Palmer@umassmed.edu.

PATHOPHYSIOLOGY OF RESPIRATORY FAILURE FOLLOWING ACUTE ORGANOPHOSPHATE POISONING

A Dissertation Presented

By

ROMOLO JOSEPH GASPARI

Submitted to the Faculty of the

University of Massachusetts Graduate School of Biomedical Sciences, Worcester

in partial fulfillment of the requirements for the degree of

DOCTOR OF PHILOSOPHY

October 7th, 2009

BIOMEDICAL SCIENCES

PATHOPHYSIOLOGY OF RESPIRATORY FAILURE FOLLOWING ACUTE ORGANOPHOSPHATE POISONING

A Dissertation Presented

By

ROMOLO JOSEPH GASPARI

The signatures of the Dissertation Defense Committee signifies completion and approval as to style and content of the Dissertation

Lawrence Hayward MD, PhD Chair of Committee

Peter Grigg PhD, Member of Committee

Mark Dershwitz MD, Member of Committee

John McCullough PhD, Member of Committee

David Paydarfar MD, Thesis Advisor

The signature of the Chair of the Committee signifies that the written dissertation meets the requirements of the Dissertation Committee

The signature of the Dean of the Graduate School of Biomedical Sciences signifies that the student has met all graduation requirements of the school.

Anthony Carruthers, PhD, Dean of the Graduate School of Biomedical Sciences

Millennium Program

October 7th, 2009

Acknowledgements

I have entered into the world of graduate research at a relatively late stage in my career. As a practicing physician I had to change my focus from patient care to basic science research. The decision to make this change was done after consultation with two individuals who are responsible, for better or worse, for placing me on this path. The first is Dr. Eric Dickson whose repeated requests to turn my attention to research was the initial impulse for my research. The guidance behind my research efforts has been my mentor, Dr. David Paydarfar. His ability to combat my tendency to jump to the quick answer without thoughtful consideration of alternatives has been instrumental in my success. When I started the process I did not think of the years of work ahead, but only on proving that I could achieve the focus needed for scientific research.

I would also like to acknowledge the support of the Millennium Program of the University of Massachusetts. Not only did the Millennium Program provide me with the initial resources to allow me to begin my research, they insisted on the structure that in hindsight has prevented many errors and wasted effort. My thesis committee of Peter Grigg, Lawrence Hayward, Mark Dershwitz and John McCullough should be commended for their ability to patiently rephrase questions and comments in a fashion that finally got through to me.

I would also like to acknowledge the help of Kevin Kane in the Department of Neurology at the University of Massachusetts (for statistical methodology) and Li Aihua

at Dartmouth Medical Center for assistance in surgical techniques for isolation of the phrenic nerve. I would like to acknowledge the assistance of Dr. Julian Paton at University of Bristol in Bristol England as well as Dr. Walter St-John and Alison Rudkin at Dartmouth Medical Center for their patience and assistance in the artificial perfusion techniques of the working brainstem-spinal cord.

I would also like to acknowledge the support of the National Institutes of Neurological Disease and Stroke who provided funding for this research over the last 3 years. This research would also not have been possible without the generous support of the Department of Emergency Medicine.

This research was supported by grant NIH K08-NS48857.

Abstract

Organophosphate (OP) poisoning is a health issue worldwide with over 200,000 deaths per year. Although not a problem in most developed countries, in some third world countries, one third of a hospital's population could be patients with OP exposure. Even with the most aggressive therapy, 10-40% of patients admitted to an intensive care unit will die. Research into the best practice for treating OP poisoning is lacking, due somewhat to a lack of detailed understanding of the physiology of OP poisoning. Our research uses animal models of acute OP poisoning to explore the mechanism of OP-induced respiratory failure.

Our research shows that animals poisoned with dichlorvos demonstrated a uniformly fatal central apnea that, if prevented, was followed immediately by a variable pulmonary dysfunction. Potential mechanisms for dichlorvos-induced central apnea can be divided into direct effects on the central respiratory oscillator (CRO) and feedback inhibition of the CRO. Two afferent pathways that can induce apnea include vagal feedback pathways and feed-forward pathways from the cerebral hemispheres. In our studies we found that vagal feedback and feed forward inhibition from the cerebral hemispheres were not required for OP-induced central apnea. The pre-Botzinger complex in the brainstem is thought to be the kernel of the CRO, but exposure of the pre-Botzinger complex to dichlorvos was not sufficient for apnea. Although OP induced central apnea was uniformly fatal, partial recovery of the CRO occurred post apnea with mechanical ventilation.

Central apnea was ubiquitous in our rat poisoning model, but pulmonary dysfunction was extremely variable, with a range of pulmonary effects from fulminate pulmonary failure with prominent pulmonary secretions to no pulmonary dysfunction at all. Vagal efferent activity is involved in neural control of pulmonary tissue but the vagus was not involved in OP-induced pulmonary dysfunction. Anti-muscarinic medications are the mainstay of clinical therapy and are commonly dosed by their effects on pulmonary secretions. Our studies found that atropine (the most common therapeutic agent for OP poisoning) resulted in a ventilation-perfusion mismatch secondary to effects on the pulmonary vasculature.

TABLE OF CONTENTS

List of Tables

List of Figures

List of Symbols, Abbreviations or Nomenclature

Alveolar-arterial gradient	A-a gradient
Analysis of variance assessment	ANOVA
Arterial pressure of oxygen	paO_2
Breaths per minute	bpm
Central respiratory oscillator	CRO
Carbon dioxide	CO_2
End-tidal carbon dioxide	$ETCO_2$
Fraction of inspired oxygen	FiO_2
Minute ventilation	MV
Organophosphate	OP
Partial pressure of carbon dioxide	PCO_2
Partial pressure of end-tidal carbon dioxide	$P_{ET}CO_2$
Pre-Botzinger complex	preBøtC
Parafacial respiratory group	pFRG
Respiratory rate	RR
Standard error of the mean	SEM

Preface

Part of this thesis work has been published previously as:

- Romolo Gaspari and David Paydarfar. Pathophysiology of respiratory failure following acute dichlorvos poisoning in a rodent model. Neurotoxicology, 2007. 28(3): p. 664-71.
- Romolo Gaspari and David Paydarfar. Respiratory failure induced by acute organophosphate poisoning in rats: Effects of vagotomy Neurotoxicology, 2009. 30(2): p. 298-304.

Study Background

1.1 Significance of organophosphate poisoning

Research exploring the pathophysiology of acute organophosphate (OP) poisoning is fragmented and incomplete with a body of clinical research divorced from a separate body of basic science, mechanistic research. For example, respiratory failure following acute OP poisoning is most likely multi-factorial yet despite mechanistic research that implies both pulmonary dysfunction[1-3] and central apnea[4, 5], clinical research on respiratory failure focuses almost exclusively on the pulmonary effects[6-8] with little attention to the central effects. The research on the delayed symptoms following OP poisoning is even less well studied. A 2008 report by the Research Advisory Committee on Gulf War Veterans' Illnesses to the US Senate concluded a link between pesticides and a collection of neuro-behavioral changes called Gulf War Syndrome[9]. A wide range of neurological and psychiatric symptomatology has been linked to OP exposure[10-14] but research into the potential mechanisms involved is lacking[15]. Neurodegeneration[16, 17], reduced neurogenesis[18], alterations in sleep patterns[19, 20], downregulation of cholinergic receptors[21], alterations in other neurotransmitters[22], or seizure related neuropathology[23, 24] have all been proposed as explanations for post OP-exposure syndromes.

Despite the widespread use of OP pesticides for the last 60 years and the health problems they generate worldwide, the therapy for OP exposure has not changed significantly for the last 50 years. Research into the best practice for treatment of OP intoxication has been lacking and we still do not know how the therapies identified decades ago should be used[25]. The evidence supporting many of the therapies used to treat OP exposure is weak and larger, better-designed trials are needed[26]. The response of the public health, medical and scientific community to the problems involved with pesticide exposure has been called “inadequate”[27]. OP exposure is a health issue worldwide with an estimated 200,000 deaths per year globally from self ingestion alone[25]. Despite intensive medical therapy, the mortality rate of OP poisoned patients in intensive care units ranges from 10-40%[6, 28-33]. Atropine, the core therapy for OP intoxication, has significant central nervous system[34] and pulmonary side effects[35] that may exacerbate OP toxicity, but even these mechanisms are not well understood.

Understanding the complex pathophysiology of acute OP poisoning requires a comprehensive understanding of the physiologic changes that occur. The lack of a detailed understanding of OP induced physiology is exemplified in “Rosen’s Emergency Medicine: Concepts and Clinical Practice, 6th edition,” the premier emergency medicine textbook. The chapter on pesticides describes the respiratory failure following OP intoxication as secondary to diaphragmatic paralysis[36] with no discussion of the numerous other contributing mechanisms

(central apnea, upper airway obstruction, bronchospasm, pulmonary secretions, etc). Previous attempts to describe the physiologic changes following OP poisoning have generally focused on a single organ system. This simplistic approach is unlikely to succeed as, by their nature as neurotoxins, OP agents involve the CNS, peripheral nervous system and the organ system(s) of interest. In the real world situation where multiple organ systems interact, it is even more complicated. Respiratory failure and pulmonary dysfunction have been identified as major mechanisms of mortality[6, 28], but little attention has been paid to central events that contribute to this dysfunction[37]. It is also possible that acute exposure to OPs may induce long-term changes in the central control of respiration through neuronal plasticity[38] where acute changes initiate long lasting effects in neuronal control.

One of the basic tools missing in OP research is a detailed integrative physiologic model of OP poisoning to help understand the mechanisms of OP intoxication and how current and future therapies affect OP-induced changes. In November of 2007 the US Department of Defense asked researchers for the "development, validation and use of animal models" to test new and existing therapies for weaponized organophosphate compounds[39]. A detailed understanding of how OP agents cause morbidity and mortality could help physicians better treat patients poisoned with this agent. Future therapeutics will need to be developed using physiologic models to understand how the therapies affect mammalian physiology. The lack of progress in the medical therapy of

acute OP intoxication and it's sequelae can be directly related to the lack of a strong foundation in understanding the complex physiology of OP poisoning.

1.2 Organophosphates and respiratory dysfunction

Acute OP exposure produces a range of clinical findings related to increased acetylcholine levels centrally and peripherally acting on post-junctional receptors. For a list of findings and mechanisms of action see Table 1.1. Some of these effects such as miosis are minor and will resolve over time. Other effects such as increased pulmonary secretions escalate post exposure and have the potential to cause morbidity or even mortality if not adequately treated. Still other effects such as central apnea are life threatening if not treated immediately. Many of the clinical effects of acute OP poisoning have the potential to cause respiratory dysfunction, and respiratory failure post OP exposure is most likely multi-factorial, but the exact mechanism of respiratory failure has not been determined.

A number of synergistic mechanisms have the potential to contribute to decreased ventilation post OP exposure. Acutely, peripheral acetylcholine at the neuromuscular junction induces fasciculation and weakness of voluntary muscle groups (including those involved in respiration)[40], and necrotic lesions within skeletal muscle cells[41]. Exposure of the neuromuscular junction to an OP results in dysfunction with repetitive compound muscle action potentials in

response to a single stimulus[42]. OP agents could also increase the work of breathing through an increase in lung static and dynamic compliance[43], constriction of the airways[37] or airway outlet obstruction[44]. Alternatively, OP agents could cause a central respiratory depression or central apnea[4, 45, 46].

Experiments exposing regions of the brain to OPs or cholinergic agonists demonstrate the potential of central mechanisms to contribute to OP-induced respiratory failure. Exposure of the entire brain to increased acetylcholine via direct injection into the cerebrospinal fluid caused depressed respiration[47]. A more limited exposure of the ventral surface of the medulla in the region responsible for chemosensitivity caused a decrease in respiratory rate and volume[48]. Injection of a small volume (10-60nl) of a cholinergic agonist into the medial portion of the rostral pons (near the pontine reticular formation involved in REM sleep) also resulted in respiratory depression[49]. Interestingly, medullary slice experiments demonstrate that exposure of the pre-Botzinger complex (an area central to respiratory control) to acetylcholinesterase inhibitors had the opposite effect, increasing respiratory related output of the hypoglossal nerve[50]. The results of the medullary slice experiments have to be interpreted with caution as the respiratory network in these experiments lacks most of the connections present in an intact animal.

Pulmonary physiology following OP exposure is complicated. OP exposure to the lung results in increased acetylcholine at pulmonary muscarinic receptors

causing pulmonary dysfunction. Airway changes from OP-induced bronchospasm[51] and bronchorrhea[52] result from both local and vagally-mediated effects. Total pulmonary vascular resistance, pulmonary arterial and pulmonary wedge pressure increase significantly in goats post OP exposure[51]. Interstitial edema from OP exposure may contribute to decreased pulmonary compliance and ventilation perfusion mismatch[52, 53]. Clinically, patients with respiratory failure post-OP exposure demonstrate significantly impaired gas exchange despite anti-cholinergic medication and aggressive mechanical ventilation[6].

1.3 Anatomy and pathways involved in the central control of respiration

To understand the potential effects of OP exposure on respiratory control, it is useful to review the neural pathways involved in the central control of respiration. Central control of respiration involves a series of components that allow the initiation and modulation of respiratory activity by the central nervous system. At its most basic level the respiratory control system includes a central respiratory oscillator with both feedback and feed-forward afferent pathways for modulation as well as efferent pathways to components of the respiratory system. Afferent signaling provides the environmental cues that allow accurate control of respiration in a changing internal and external environment. Many parts of this control system contain cholinergic neurons that are affected during acute OP poisoning. Understanding how the central and peripheral components of

respiratory control are integrated is critical to understanding how this system is affected by exposure to OPs.

Respiratory neurons are concentrated in three distinct locations. Cat and rat animal models have been used extensively to map the connections between regions of the brain involved in respiratory control. The dorsal respiratory group in the medulla is located in the dorsolateral nucleus tractus solitarius[54]. The ventral respiratory group is located in the ventrolateral medulla and is divided into three regions, caudal, intermediate and rostral. The rostral ventral respiratory group contains the pre-Botzinger complex[55]. The pontine respiratory group (also called the pneumotaxic center) is located in the nucleus parabrachialis medialis and the Koliker-Fuse nucleus[56]. Other neurons involved in respiration are located throughout the brain and provide afferent input during respiration[57]. (see Figure 1.1)

Afferent signaling to respiratory neurons in the pons and medulla projects from receptors within the lung. Studies using rats have shown that pulmonary stretch receptors[58] and irritant receptors[59, 60] project via vagal afferents to modulate respiratory activity. Activation of pulmonary stretch receptors cause reflexive cessation of respiration, known as the Hering-Breuer reflex[61]. Afferent inputs via irritant receptors (C-fibers) have a similar effect and activate of the cough reflex[62, 63]. Other irritant receptors (J receptors) initiate different changes in respiration with a reflexive tachypnea secondary to pulmonary edema[59].

Other afferent signaling originates from areas in the brainstem or higher brain or even areas outside the CNS. Feed-forward signaling from the cerebral hemispheres[64] can modulate respiratory activity. Both voluntary (breath holding) and involuntary (seizure related) activity can influence central respiratory control[64]. Sensory projections from the diaphragm[65], peripheral muscles[66] and the larynx[67] affect respiratory control as well. Intercostal and abdominal muscle afferent activity suppresses central respiratory activity and phrenic nerve activity[68]. Projections from sites in the pons such as the pedunculopontine tegmental nucleus[69] involved in REM sleep and cerebellar structures[70] provide afferent signaling to the pneumotaxic center and apneustic center in the pons and the ventral and dorsal respiratory group in the medulla.

Efferent signaling from the respiratory control center coordinates the cyclic activation of inspiratory and expiratory muscle groups and provides central control of some cardiovascular and pulmonary physiology. Output from the central respiratory oscillator via the phrenic nerve triggers a major component of inspiration by stimulating a contraction of the diaphragm. Spinal motor neurons innervate a range of muscles involved in inhalation and exhalation. Additional efferent output via the hypoglossal nerve in a cat stimulates the muscles of the upper airway to prevent airflow obstruction during inspiration[71]. Other studies using rat, pig and cat models show that efferent signaling via the vagus nerve modulates ventilation via bronchial smooth muscle[72], pulmonary perfusion via

arterial smooth muscle[73, 74] and pulmonary secretions via pulmonary glandular output[75, 76].

Although multiple brain regions may contribute to OP-induced central apnea [45, 46], a number of sites are likely candidates due to their central role in respiratory control and their cholinergic innervation. Cholinergic neurons do not seem to comprise a significant portion of the ventral respiratory group[77] but are located in the dorsal respiratory group[78] and the pre-ganglionic neurons of the vagus in the ventral medulla[79]. There are additional cholinergic ponto-medullary circuits involved in respiratory control[49, 80-82]. Any of these cholinergic circuits could be involved in OP induced central apnea. A more detailed discussion of specific areas in the brain potentially involved in OP-induced apnea is below.

1.4 Respiratory Pattern Generation

Conceptually, the mechanism of OP-induced respiratory failure can be divided into two broad categories defined by location of action of the OP: 1) direct action of the OP on the central respiratory oscillator in the brainstem, 2) OP-induced feedback or feed-forward inhibition of the central respiratory oscillator. Regardless of the location of action of the OP, a loss of efferent output (phrenic output to the diaphragm) from the central respiratory oscillator is a critical feature of OP-induced apnea.

Rhythm and pattern generation in the brainstem involves synchronously active inhibitory and excitatory postsynaptic potentials producing fluctuations in the membrane potential of rhythm generating neurons. The main inhibitory neurotransmitters involved in respiratory rhythm generation are glycine and γ-aminobutyric acid (GABA) with increased neurotransmitter release producing a depression in respiratory rate and phrenic nerve activity[83-85]. Excitatory amino acids required for respiratory rhythm generation include N-methy-D-aspartate (NMDA) and α-amino-3-hydroxy-5-methy-4-isoxazole propionic acid (AMPA) with NMDA primarily responsible for respiratory rhythm and AMPA responsible for pattern[86]. A number of different neurotransmitters are involved in modulating the respiratory rhythm generating elements of the respiratory neurons.

The anatomic location of the central respiratory oscillator within the brainstem has been debated in the scientific literature but many experts now believe it is either the pre-Botzinger complex or the parafacial respiratory group (pFRG)[87, 88]. One hypothesis is that a rhythm generator in the pFRG composed of pre-inspiratory neurons periodically triggers output from an inspiratory oscillator in the pre-Botzinger complex [89]. Multiple lines of evidence support this hypothesis (see Onimaru et al[87] for a more detailed description) but alternative hypotheses exist. A second hypothesis proposes that there are two interacting oscillators, the pre-Botzinger complex providing inspiratory activity and the pFRG providing expiratory activity. A more detailed discussion of the data supporting this hypothesis was published by Feldman et al[88] in 2006.

1.5 Chemoreception and Respiratory Modulation

Changes in chemoreception have been implicated as contributing to the respiratory changes from acute OP poisoning. Chemoreception is a complex, redundant system that modulates respiratory activity to compensate for changes in pH, CO_2 and O_2. Cholinergic transmission seems to be integrally involved in chemosensitivity but other nerves have a substantial role with some non-cholinergic neurons directly sensing changes in pH and providing afferent input to the pre-Botzinger complex[90].

The ventral surface of the medulla contains chemosensitive zones that sense changes in CO_2. Cells on the ventral surface of the medulla were previously thought to react to changes in pH in the cerebrospinal fluid secondary to dissolved CO_2 [91] but more recently it is thought that intracellular pH and CO_2-specific receptors play a role[92]. Receptors responding to changes in PCO_2 within the central nervous system[93] provide afferent input via ponto-medullary circuitry[94]. Application of acetylcholine to the chemosensitive zone results in a stimulation of respiration[95] and cholinergic antagonists applied to this area[96], or introduced into the CSF[97], decrease CO_2 sensitivity.

It is unlikely that changes in chemosensitivity at the aortic or carotid bodies are involved in OP-induced apnea. Hypoxia increases ventilation secondary to

stimulation of receptors in the carotid body and aortic body. Glomus cells in the carotid body (and to a lesser extent the aortic body) detect changes in peripheral pH, PCO_2[98], and PO_2[99] and provide input to respiratory centers in the brain via the glossopharyngeal nerve. The carotid body contains acetylcholine (and other neurotransmitters) that is thought to be released secondary to hypoxia-induced activation of nicotinic receptors through concentration changes in adenosine[100]. Nicotinic receptors are present on chemoreceptor afferent fibers as well as on glomus cells (chemoreceptors). Arterial chemoreceptor afferent activity in the rat increases excitatory drive through the release of glutamate at the nucleus tractus solitarius[101]. Theoretically, OP exposure with increased acetylcholine at the carotid body chemoreceptor afferent fibers would result in an increase in respiratory activity.

1.6 Sleep and Respiratory Control

Interestingly, there is a link between sleep and respiratory control that may be involved in OP-induced apnea. Changes in respiration occur during REM sleep with increases in respiratory rate and increased variability of breathing[102, 103]. The onset of REM sleep is marked by increased activity of cholinergic pontine neurons in the laterodorsal tegmental and pedunculopontine tegmental nuclei (LTD/PPT)[104-106] with connections to respiratory neurons in the medulla[107, 108]. Injection of cholinergic agonists into the region of the LTD/PPT induces a REM sleep like state with respiratory depression characterized by decreased

tidal volumes and respiratory rate[109]. This suggests a connection between the LTD/PPT and the rhythm generating cells in the brainstem. The respiratory effects of LTD/PPT afferent activity may be indirect via the reticular formation as there is a close correlation between mid-brain reticular formation sleep specific activity and respiratory efferent activity[110].

1.7 Pulmonary function

A wide range of pulmonary activities are mediated by post-junctional effects of acetylcholine, providing the underlying mechanisms for OP-induced pulmonary dysfunction. Postganglionic parasympathetic nerve endings form a meshwork around the airways and vessels of the lungs. Acetylcholine is accumulated in synaptic vesicles at the post-synaptic nerve terminals and depolarizing of the nerve terminal causes release of acetylcholine into the synaptic cleft, where it diffuses to interact with both pre- and post-synaptic receptors. Depending on the animal species, cholinergic stimulation of muscarinic receptors plays a role in the stimulation of mucus secretions[111] as well as the secretion of both water and electrolytes[3]. Two cholinergic mechanisms in rabbits compete for modulating pulmonary vascular tone, a direct stimulatory effect and an indirect endothelium-dependent (nitric oxide) relaxing effect[112, 113]. Acetylcholine also induces bronchial smooth muscle constriction, regulating bronchial airflow by narrowing the airway diameter[114]. Airway smooth muscle contraction is induced by muscarinic receptors (M2 and M3)[115, 116].

Bronchoconstriction is a common complication of acute OP poisoning. Acute changes in pulmonary airflow is regulated primarily by bronchial airway caliber that can be controlled via efferent signaling or local pathways. Stimulation of adrenergic sympathetic fibers causes dilation of bronchial smooth muscle while stimulation of cholinergic parasympathetic fibers causes constriction. Vagal efferent signaling results in bronchoconstriction mediated by substance P (in rats) [72] and acetylcholine (in dogs)[114] acting on bronchial smooth muscle. Effects from a variety of local compounds mediate changes in bronchial tone with compounds such as acetylcholine, histamine, serotonin, leukotrienes, α-adrenergic agonists and others mediating bronchoconstriction[2, 117-119] and compounds such as $ß_2$-agonists, nitric oxide, and others mediating bronchodilatation[119, 120].

A number of different mechanisms may be involved in OP-induced dysfunction in pulmonary gas exchange. Efficient pulmonary function requires a coordination of ventilation and perfusion to allow the transfer of oxygen and carbon dioxide between the airways and the pulmonary vasculature. Pulmonary perfusion is normally matched to ventilation via local and neural mechanisms but the coordination of these mechanisms during pathologic states is not completely understood. In general, sympathetic stimulation increases pulmonary vascular resistance while parasympathetic stimulation results in a decrease. Stimulation of vagal efferents in the cat results in vasodilatation mediated by acetylcholine

acting on the vascular smooth muscle[74]. Rat pulmonary vascular tone was increased with stimulation of cervical and thoracic (C7-T4) spinal sympathetics[121]. Local prostaglandins (PGE_2, $PGF_{2\alpha}$), thromboxane, angiotensin II, α-adrenergic agonists increase pulmonary vascular resistance[122-125]. Local agents such as PGE_1, prostacyclin, nitric oxide, bradykinin mediate a decrease[124, 126, 127] but it is unclear how these mediators are coordinated. Pulmonary arterial caliber is also moderated by local hypoxic conditions via production of local mediators from endothelial cells[122, 126, 128]. It is most likely that OP-induced decrease in pulmonary gas exchange is related to an inappropriate decrease in pulmonary vascular tone.

Increased pulmonary secretions are a prominent feature of acute OP exposure. Tracheal and pulmonary secretions are enhanced by local mediators and via central nervous system pathways. In cats, irritant compounds can induce increased pulmonary secretions via both methods[129]. Vagal efferent activity provides most of the regulatory control of output from airway glands via acetylcholine, substance P, and vasoactive intestinal peptide (VIP). In piglets, reflexive increase in tracheal secretions occurs secondary to stimulation of laryngeal mucosa and pulmonary C-fibers [130]. Local mediators such as substance P can increase secretory output in the absence of neural control.

The effect of OP exposure on interstitial fluid has not been well studied. Changes to the interstitial compartment of the lung are mediated by locally

secreted compounds and neural efferent activity. The release of a wide range of inflammatory mediators from rat and rabbit airway epithelial cells[131-134], human mast cells[117] and human and mouse inflammatory cells[135-137] are modulated by cholinergic mechanisms. Systemic or local hypoxic conditions mediate changes in the vascular epithelium of rats resulting in increased permeability[138]. Other injuries such as sepsis[139], aspiration[140] or trauma[141] can cause similar changes. Pulmonary edema increases pulmonary and bronchial C-fiber afferent activity[142], causing reflexive vasodilatation[143], increased mucous secretion, bronchoconstriction, and changes in respiratory rate and volume[138, 144] in animal models.

Acute OP poisoning results in conflicting signaling from stimulatory and inhibitory cholinergic pathways involved in both central respiratory control and neural control of the lung. OP agents increase acetylcholine levels in all areas of the brain[145] and lung[37], but it is not clear which area (or group of areas) are responsible for OP-induced respiratory failure.

Table 1.1 – Mechanisms of action of organophosphate poisoning

Finding	Mechanism of Action
Diarrhea/GI cramps	Cholinergic stimulation of colonic smooth muscle and decreased fluid absorption predominantly via muscarinic receptors [146-149]
Urination	Cholinergic stimulation of bladder smooth muscle muscarinic receptors[150, 151]
Miosis	Cholinergic stimulation of iris smooth muscle tone[152]
Bradycardia	Cholinergic stimulation of cardiac receptors[153], the nucleus tractus solitaris[154] or reflex bradycardia from increased sympathetic nerve activity[155]
Tachycardia	Cholinergic stimulation of receptors in the sympathetic ganglia and adrenal medulla with release of catecholamines [156]
Bronchorrhea/Pulmonary Secretions	Cholinergic stimulation of pulmonary goblet cells and glands [3, 111] or reflex bronchorrhea from pulmonary afferent activity via the nucleus of the solitary tract[157]
Bronchoconstriction	Cholinergic stimulation of bronchial smooth muscle[115, 116] or reflex bronchoconstriction from pulmonary afferent activity via the nucleus of the solitary tract[157]
Emesis	Cholinergic stimulation of stomach smooth muscle and gastric secretion via muscarinic receptors [146, 158, 159] as well as brainstem triggered “motion sickness” with nausea and vomiting[160]
Lacrimation	Cholinergic stimulation of lacrimal glands[161]
Salivation	Cholinergic stimulation of salivary smooth muscle[162] and exocytotic secretion[163, 164]
Fasciculations	Cholinergic stimulation of skeletal muscle fibers[42, 165]

Figure 1.1 – Afferent inputs to respiratory centers in the brainstem

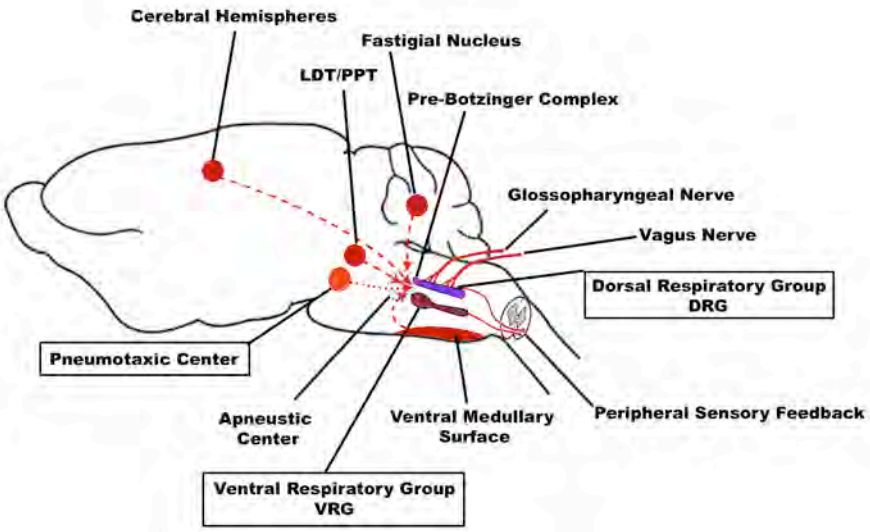

CENTRAL NERVOUS SYSTEM

1) Cerebral Hemispheres – conscious thought and seizure related feed-forward inputs
2) Latero-dorsal Tegmental/Pedunculopontine tegmental (LDT/PP)– sleep related respiratory changes
3) Fastigial Nucleus –changes in CO_2 levels, relay of vagal afferent inputs,
4) Ventral Medullary Surface –changes in CO_2 levels

CRANIAL NERVES

1) Glossopharyngeal Nerve – changes in arterial O_2, CO_2 and pH
2) Vagus Nerve – pulmonary mechanoreceptors and irritant input

SPINAL NERVES

1) Peripheral sensory – stretch receptors in diaphragm and peripheral muscles

Chapter 2 - Pathophysiology of respiratory failure following acute dichlorvos poisoning in a rodent model.

Previously published - Gaspari RJ, Paydarfar D. Pathophysiology of respiratory failure following acute dichlorvos poisoning in a rodent model. Neurotox. 2007 28(3) p664-71.

2.1 Abstract

OP poisoning causes a cholinergic crisis with a wide range of clinical effects including central apnea, pulmonary bronchoconstriction and secretions, seizures, and muscle weakness. The morbidity and mortality from acute OP poisoning is attributed to respiratory failure but the relative contributions of the central and peripheral effects in producing collapse of the respiratory system are unclear. In this study we used a novel adult rat model of acute OP poisoning to analyze the pathophysiology of acute OP poisoning. We found that poisoning caused rapidly lethal central apnea. In animals sustained with mechanical ventilation, we found that following central apnea there ensued progressive pulmonary insufficiency that was variable in timing and severity. Our findings support the hypothesis that OP poisoning in this animal model causes a sequential ‘‘two hit’’ insult, with rapid central apnea followed by delayed impairment of pulmonary gas exchange with prominent airway secretions.

2.2 INTRODUCTION

OP poisoning produces a cholinergic crisis by inhibition of acetylcholinesterase in the central and peripheral nervous systems. Acute effects of poisoning include central apnea [4, 46, 48, 166], seizures [167, 168], bronchorrhea, bronchoconstriction, muscle weakness, miosis, urination, and salivation [37, 52, 169, 170]. The morbidity and mortality from acute OP poisoning is attributed to respiratory failure [171] but the relative contributions of the central and peripheral effects in producing collapse of the respiratory system [172] are unclear. The clinical literature emphasizes the peripheral effects contributing to acute pulmonary insufficiency [28, 171]. However this does not exclude early mortality in the field due to central apnea [173, 174].

In this study we used a rodent model to analyze the dynamics of respiratory and cardiovascular collapse during acute OP poisoning. We found that poisoning caused a rapidly lethal central apnea. Central apnea consistently occurred soon after the poisoning but pulmonary insufficiency was more variable in both timing and severity. Mortality was reduced in animals that were sustained solely by artificial ventilation; however most ventilated animals exhibited signs of impaired gas exchange due to pulmonary insufficiency. Our findings support the hypothesis that OP poisoning in this animal model causes a sequential “two hit” insult, with rapid central apnea followed by delayed impairment of pulmonary gas exchange with prominent airway secretions.

2.3 MATERIALS AND METHODS

We studied 27 male Wistar rats, weighing 275-325 gm (Charles River Laboratories, Wilmington, MA). The University of Massachusetts Medical School Institutional Animal Care and Utilization Committee approved all experimental procedures and protocols. The animal model used in this study is a novel preparation for OP research and the procedures are described in detail below.

Surgical Procedures

Surgical procedures were performed under general anesthesia with 1.5 – 2.2% isoflurane (Abbott Labs, North Chicago, IL) titrated to achieve a respiratory rate of 50-60 breaths per minute (bpm). All surgical procedures were performed under 100% oxygen. The animals were restrained in a supine position with the head extended and limbs abducted. Adequacy of anesthesia was confirmed by lack of withdrawal from a painful stimulus applied to the foot. The trachea was cannulated percutaneously via a tracheostomy using polyethylene (2.4mm) tubing. Polyethylene (0.5 mm) tubing was inserted into the femoral artery for blood pressure recordings and into the femoral vein for intravenous access. Bladder catheterization was unnecessary because the experiments lasted less than 2.5 hours. Spontaneous urination was used as a marker of cholinergic toxicity.

Anesthetic Circuit

Spontaneously breathing animals received oxygen and anesthetic through a 3/32” kynar barbed y-fitting (Small parts INC, Miami Lakes, FL) with one arm supplying the gas mixture and the other arm attached to a low-pressure gas scavenger system (Surgivet, Waukesha, WI). The distal y-tube was attached in-line with a CO_2 detector, a small chamber pneumotachometer, and the tracheal tube. The dead space of the ventilation circuit (y-tube, end-tidal CO_2 detector, pneumotachometer, and tracheal tube) was 0.33 cc total or roughly 10% of the tidal volume of the animals. All animals that were not mechanically ventilated received 100% oxygen throughout the course of the experiment.

Some animals received mechanical ventilation with or without pharmacologic paralysis. Mechanical ventilation was supplied through a modification of the above anesthesia circuit using a small animal positive-pressure ventilator (Harvard Apparatus, Holliston MA). Once the surgical procedures were completed the fraction of inspired oxygen was titrated to achieve a partial arterial oxygen concentration (P_aO_2) of 100-115 mmHg. The ventilator was initially set to a tidal volume of 3 cc and respiratory rate of 80 bpm. Ventilator settings were adjusted to achieve a target end-tidal $PCO_2 < 60$ mmHg. Once these targets were achieved the ventilator and the fraction of inspired oxygen settings were not changed throughout the experiment. In pharmacologically paralyzed animals, adequacy of paralysis was monitored using esophageal pressure recordings (see below) to monitor respiratory effort.

Recording Techniques

Respiratory Recordings

Expired CO_2 was measured using an infrared CO_2 sensor (Novametrix, Wallingford CT) in-line with the endotracheal tube. End-tidal pCO_2 ($P_{ET}CO_2$) was recorded as the maximum expired pCO_2 for each respiratory cycle, along with airflow, respiratory rate, volume of expired air, and minute ventilation. Airflow was measured using a small chamber pneumotachometer (HSE, March-Hugstetten Germany) in series with the expired CO_2 detector. The volume of expired gas was calculated using half-wave integration of the airflow signal from the pneumotachometer. Respiratory rate was calculated using the peak of the inspiratory tracing as a marker of a single breath. Minute ventilation was calculated as respiratory rate multiplied by the volume of expiration. The normal respiratory rate of the rat is 80 bpm. For the purpose of the study, we defined apnea was as cessation of airflow for greater than 20 seconds and central (or non-obstructive) apnea as concomitant cessation of respiratory effort and airflow for greater than 20 seconds. Oxygen saturation was measured using a photodetector (Nellcor, Pleasanton CA) placed on the right paw. Raw tracing of the oxygen saturation signal as well as measured value of the arterial oxygen saturation were recorded and displayed continuously. Respiratory effort was monitored by esophageal pressure via a saline filled open tube inserted to the level of the mid-thorax connected to a pressure transducer (Cobe, Lakewood CO). Prior studies have correlated this esophageal pressure recording with pleural pressure as a non-invasive measurement of respiratory effort [175].

Pressure recordings were calibrated relative to atmospheric pressure recorded at the level of the animal's mouth immediately prior to insertion of the esophageal tube. Respiratory effort was measured as maximal negative esophageal pressure from baseline for each respiratory cycle during spontaneous respiration. Similar measurements were performed during positive pressure mechanical ventilation as the negative deflections of respiratory effort were easily distinguished from the positive deflections of positive pressure ventilation.

Hemodynamic Recordings

Blood pressure and pulse rate were measured using polyethylene tubing connected to a pressure transducer (Utah Medical, Midvale UT). Mean arterial pressure was calculated from the analog signal. Pulse rate was calculated using peak systolic blood pressure of the arterial pressure tracing as the marker for a single heartbeat. For the purpose of this study death was defined as an arterial pulse pressure (systolic pressure minus diastolic pressure) less than 3mmHg with a systolic blood pressure less than 5mmHg.

Arterial Blood Gas Measurements

Arterial blood samples for blood gas measurements were obtained via a stopcock attached in-line with the femoral arterial line. An initial small amount of blood (0.1 cc) was withdrawn and discarded to prevent mixing of catheter saline flush and arterial blood. A 0.2 ml sample of arterial blood was then withdrawn for immediate analysis in a Rapidlab 248 blood gas analyzer (Bayer Healthcare,

East Walpole MA). Samples were withdrawn at differing schedules depending on the study protocol. In groups with spontaneously breathing animals measurements occurred sporadically. In groups with mechanical ventilation measurements either occurred at regular intervals (ventilation throughout) or at the time of apnea (rescue ventilation). Alveolar-arterial gradients (A-a) were estimated using the following formula, where all pressures are in mmHg.

$$\text{Estimated A-a gradient} = (\text{Fraction of inspired oxygen (\%)}/100) \times (P_{atm} - 47) - (Pa_{CO2}/0.8) - Pa_{O2}$$

A-a gradients were reported as a percentage of the average A-a gradient during the control period for each animal.

Recordings in Unanaesthetized Animals

Unanaesthetized animals were placed in a cylindrical restraining device with an attached nose cone (Kent Scientific, Torrington CT). Oxygen was supplied through a pneumotachometer and end-tidal CO_2 detector (see above) attached to the nose cone. The nosecone was retracted down the restraint device until a seal was formed around the animal's nose. An adequate seal was determined by the strength of the airflow signal through the pneumotachometer. A needle attached to a length of polyethylene tubing was placed subcutaneously through an access port of the restraint device to allow a subcutaneous injection once the animal was restrained. This was accomplished under anesthesia at least 30

minutes prior to initiating the experiment to minimize respiratory changes associated with the needle insertion.

Animals were habituated to the restraining device in a dark quiet environment at least 30 minutes prior to beginning the experiment. No invasive procedures such as those required for hemodynamic monitoring were performed. The animal was removed from the restraining device once airflow through the pneumotachometer ceased and the animal appeared motionless. Visual inspection of the animals outside of the restraint device allowed us to determine if the lack of airflow was secondary to apnea or from dislodgement of the animal's nose from the nosecone apparatus.

Signal Conditioning and Data Acquisition System

All physiologic recordings were measured continuously over the course of the experiment using a PC (Dell, Round Rock, TX) and data acquisition system (ADI instruments, Colorado Springs CO). Physiologic data were sampled at 400 Hz and displayed continuously during the experiment, and subsequently averaged in 15-second bins. Measured and calculated physiologic values were displayed in real time. Airflow and esophageal pressure were amplified and filtered (Molecular Devices, Sunnyvale, CA) prior to recording and display by the data acquisition system. Arterial pressure was amplified and filtered using a separate amplifier (ADI Instruments) controlled by the data acquisition system.

Protocol and Data Analysis

Animals were allowed to reach a physiologic steady state for 15 to 30 minutes following the surgical procedures prior to initiating poisoning. Dichlorvos (Sigma-Aldrich, St Louis MO) was diluted in 0.9% saline from a stock solution in acetonitrile and administered at a dose of 100 mg/kg subcutaneously (roughly 3x LD50) in all groups. Physiologic recordings were continued until blood pressure and pulse rate declined to the study endpoint. The study was terminated at death or 1 hour, whichever came first.

Animals were randomized to four groups (Table 2.1). Animals in Group I (10 animals) were anesthetized and breathed 100% oxygen spontaneously. Animals in Group II (7 animals) were anesthetized. They initially breathed spontaneously but received mechanical ventilation that was initiated when the animal developed apnea, as defined by a lack of airflow and concomitant absence of respiratory effort. The fraction of inspired oxygen was titrated during the control period to achieve a PaO_2 of 100-115 mmHg, and was not changed throughout the remainder of the experiment. Arterial blood gases were measured at three times on surviving animals: prior to the poisoning (control), at point of apnea and later during mechanical ventilation.

Animals in Group III (6 animals) were anesthetized, pharmacologically paralyzed and mechanically ventilated throughout the experiment. Adequacy of anesthesia was determined prior to paralysis and anesthesia was maintained at a constant

level pre- and post- paralysis. Animals were paralyzed with gallamine hydrochloride, a nicotinic and M_2 muscarinic antagonist (Sigma-Aldrich, St Louis MO) (6.2 mg/kg bolus and 9.3 mg/kg continuous venous infusion) and allowed to reach a physiologic steady state prior to initiating the research protocol. Inspired oxygen concentration was titrated to a target PaO_2 concentration of 100-115mmHg prior to the poisoning as described above. Arterial blood gases were measured every 3 minutes for the first 24 minutes (8 times) followed by every 6 minutes for the next 42 minutes (7 times).

Animals in Group IV (4 animals) were poisoned while unanaesthetized and spontaneously breathing. 100% O_2 was supplied through the nose cone and recording apparatus during the entire experiment. Respiratory recordings were obtained from an in-line pneumotachometer and end tidal CO_2 detector attached to the nose cone. The animals were removed from the restraining device following apnea and observed for 30 minutes to detect any resumption of sustained respiratory activity.

Statistics

Cardiorespiratory effects of dichlorvos poisoning are expressed in the text as mean $\pm$ standard error of the entire cohort unless otherwise specified. Between-group comparisons were performed using an unpaired Student's *t*-test or Fisher's Exact test where appropriate [176]. P values are presented at p=ns for all p values greater than 0.1.

2.4 RESULTS

Cardiorespiratory parameters during the control period showed no substantial difference between Group I and the other anesthetized Groups (II and III) (see table 2.2) with the exception of $P_{ET}CO_2$ and tidal volume. Group III animals were paralyzed and mechanically ventilated which precludes measurement of respiratory rate, tidal volume and effort. However data from end-tidal CO2, blood pressure, and pulse rate were included. $P_{ET}CO_2$ levels were slightly lower in Group I, corresponding to slightly higher tidal volumes most likely due to lower levels of anesthesia. These small differences did not affect respiratory effort or time to apnea (see below).

Animals in Group I demonstrated a central apnea characterized by a simultaneous loss of tracheal airflow and respiratory effort prior to circulatory collapse with respiratory rate decreasing prior to the point of apnea. Figure 2.1 shows representative recordings from one animal. Animals in Group I showed an average respiratory rate that began declining 1 minute after poisoning and reached apnea an average of 4.95 min ($\pm$1.55 min) post-poisoning. Hemodynamic variables were robust over 20 minutes longer, gradually declining to the study endpoint (see Materials and Methods). Figure 2.2 plots respiratory rate and blood pressure over time for Group I and Group II. At the time of apnea the average mean arterial pressure (90 $\pm$ 10mmHg) was in the normal range and there was no systemic hypoxia (oxygen saturation >95%). A-a gradients

measured at this time were also in the normal range for a rat. Animals who received mechanical ventilation (group II and III) lived longer then animals with no intervention (group I) but mechanical ventilation did not prevent all mortality (Figure 2.3).

Animals in all groups that survived the initial apnea showed signs of pulmonary insufficiency. Animals in Group II (rescue mechanical ventilation) and group III (mechanical ventilation throughout) showed a significant increase in survival at one hour post poisoning (69.2% vs. 0%). The animals that did not survive despite mechanical ventilation were unable to be ventilated and uniformly had fluid filling their tracheal tube at the time of death. Markers of pulmonary dysfunction such as A-a gradient (-1.3 vs 62.0) and changes in the V_E/V_I ratio (28 vs 66%) were significantly worse in animals that died (Figure 2.4).

During normal mechanical ventilation the $(V_E)/(V_I)$ ratio is expected to be close to one. Mechanical ventilation supplies a constant V_I so a reduction in this ratio is a result of decreased V_E possibly due to severe loss of pulmonary compliance or outright obstruction of the lower airways resulting in a rupture of the tracheal seal, thereby causing a reduction in expired volume compared to inspired volume. Barotrauma would also result in a change in the $(V_E)/(V_I)$ with leak of air into the chest cavity, but this is less likely as none of the animals showed pulmonary dysfunction without secretions filling the tracheal tube. Future studies

using this animal model could benefit from measurement of airway pressure, which we would expect to increase due to pulmonary toxicity of OP[43, 52].

Arterial blood gas measurements in Groups II and III showed that the pulmonary effects of the OP were variable. Comparing animals that lived with those that died despite mechanical ventilation shows a difference between the two groups. In animals that did not survive to the study endpoint the A-a gradient began increasing around the point of apnea and progressively worsened during the post-apneic period. Two of the 6 animals with mechanical ventilation throughout the experiment (Group III) died before 1 hour with secretions filling the tracheal tube (Figure 2.5A). One of these animals showed increasing A-a gradients starting around the projected point of apnea. The other animal showed a normal A-a gradient at the time of death but a V_E/V_I ratio < 0.2. Arterial blood gas measurements in animals in Group II (rescue ventilation) showed that abnormal pulmonary gas exchange began around the time of apnea. The animals showed an elevated A-a gradient over baseline around the time of apnea (35mmHg +/- 15) with some animals (2 of 7) demonstrating a widening A-a gradient that culminated in death from a fluid filled trachea (figure 2.5B). Animals that lived to one hour (5 of 7) demonstrated abnormal A-a gradients at the point of apnea (33mmHg) but normal A-a gradients at the termination of the experiment (1mmHg). The change in A-a gradient (Group II and III) was variable with animals that did not survive demonstrating a significant increase in A-a gradient

over those that lived to the study endpoint (63 vs. -1.3 mmHg, p=0.0004 Figure 4).

Anesthesia had a limited effect on the characteristics of the apnea following acute OP poisoning. None of the animals in Group IV (no anesthesia) survived and the time to respiratory arrest occurred over a similar time course as in Group I animals (4.0 min vs. 4.95 min, p=ns).

Some animals in Group I (7 of 10) demonstrated auto-resuscitative breathing post apnea. Although some authors use gasping and auto-resuscitative breathing interchangeably[177], we use the term to refer to post apneic breathing that supports cardio-pulmonary activity[178]. The post-apneic breathing was characterized by a weak respiratory effort at 20 bpm that occurred once blood pressure dropped close to the study endpoint. Animals with autoresuscitative breathing showed a prolonged time to circulatory collapse (31 vs. 12 minutes, p=0.025). Post-apneic respiratory activity was not seen in any of the other groups. It should be noted that Group III animals were paralyzed so post-apneic respiratory activity would not have been recognized and Group IV animals were removed from the restraining device (which also recorded breathing) shortly after apnea onset precluding any record of late respiratory activity. Visual observation of animals removed from the restraining device showed no resumption of respiratory activity. There was no visible respiratory effort once animals were

removed from the restraint device. The end point for Group IV was respiratory arrest rather than circulatory collapse since arterial pressure was not recorded.

2.5 DISCUSSION

In our animal model of acute OP poisoning, dichlorvos at 3 times the LD_{50} caused a central failure of breathing in all animals. The key finding was rapidly progressive bradypnea leading to apnea due to loss of respiratory effort. Respiratory muscle weakness is an unlikely mechanism of respiratory failure because apneic animals exhibited retching, intermittent flexing of the torso, and gasping respirations during the post apneic period. The retching, commonly seen in OP poisoning, was identified as strong positive deflections of the esophageal pressure transducer. Although other muscular activities such as forced exhalation, thoracic wall contraction or abdominal wall contraction would increase esophageal pressure; all of these activities are accompanied with tracheal airflow, which was not seen during retching. Esophageal contractions cause increased esophageal pressure without tracheal airflow but differentiating this from retching would require esophageal and gastric electromyelograms.

The lack of paralysis of the respiratory muscles is also supported by other studies that demonstrated intact diaphragmatic contraction following OP poisoning [46]. We excluded systemic hypotension as a cause of central apnea because arterial pressure was in the normal range at the time of apnea onset. We also excluded apnea due to acute upper airway obstruction since this would have manifested as increasing respiratory effort during apnea, whereas in all our experiments hypopnea and apnea were associated with reduction followed by

absence of respiratory effort, respectively. Our findings are consistent with other studies of OP poisoning in experimental animal models that demonstrate loss of central inspiratory drive due to poisoning [45, 46, 168].

Central apnea has not been documented in clinical studies; rather case series of human OP poisoning emphasize respiratory failure due to toxic cholinergic effects on the lung [7, 28, 29, 179]. It is possible that central apnea is not prevalent in the clinical literature because either it is masked by mechanical ventilation or patients with central apnea die before reaching the hospital. Another possibility is that the human central respiratory oscillator is resistant to cholinergic toxicities. It is less likely that the lack of central apnea is due to ingestions less then the LD_{50}. There are limited data concerning the degree of most exposures due to circumstances of the ingestion (suicide, accidental exposure…) but the published survival rate post severe OP-poisoning averages 30% despite aggressive anti-cholinergic therapy and supportive care. Anti-cholinergic therapy is considered very effective and aggressive therapy in patients who ingested the LD50 of an OP would likely be less than 30%.

The mechanism of central apnea from increased acetylcholine remains unclear. Peripheral feedback to the central respiratory oscillator, feed-forward inhibition to the central respiratory oscillator, disruption of ponto-medullary circuits or disruption of the central respiratory oscillator itself all remain possibilities. Inputs such as the vagus nerve, glossopharyngeal nerve or ponto-medullary inputs may

be involved. Mechanoreceptors in the lung that could be activated by bronchoconstriction or fasciculations provide feedback to the CRO and can result in apnea [54]. Acetylcholine receptors have been shown to be active in modulating respiratory rhythm [50] and over-stimulation may result in loss of rhythmic output of the CRO. Further studies are needed to address the primary source of central inspiratory inhibition due to cholinergic excess.

The second phase of the OP poisoning, progressive pulmonary insufficiency, was variable across animals. Although all poisoned animals exhibited signs of pulmonary compromise, with either reduction in V_E/V_I ratio and/or widening of the alveolar-arterial gradient, the degree of pulmonary dysfunction was highly variable and only one third of the animals died from pulmonary secretions filling their lungs. It is unclear what factors led to this variability but it is interesting to note that the percentage of animals dying from the pulmonary secretions (33%) is similar to the percentage of human patients that die despite intensive care (10-35%) [28, 29]. We would speculate that this variability is related to a threshold effect for each individual rat where a certain amount of local stimulation of irritant fibers is needed to create enough secretions and interstitial edema to perpetuate stimulation of pulmonary irritant fibers. This would be dependent on individual animal responses to the local irritation and could result in a stimulatory feedback loop with overwhelming pulmonary secretions. Further studies are needed to determine the mechanisms involved in OP-induced pulmonary dysfunction.

Gasping respirations were recorded in some poisoned animals that lived on average almost 20 minutes longer then animals that showed no gasping respiration. However it is unlikely that the gasping respirations prolonged life because the respiratory activity occurred almost immediately before the point of death with mean arterial pressures averaging around 10 mmHg at the time of gasping. Prior studies of gasping have noted an association of gasping activity with hypoxia [180] but this was not consistently found in our study as hypoxia greatly preceded gasping in many of the animals.

Extrapolation of these results to the clinical treatment of human OP poisonings should be done with extreme caution but there are two aspects of our data that deserve discussion. Apnea occurred significantly prior to cardiac arrest so that in battlefield areas where triage is important, individuals in respiratory arrest may survive for a period of time prior to ventilatory support. Studies of patients who survive the initial stages of acute OP poisoning to make it to the intensive care unit describe long periods of treatment requiring anticholinergics [7, 28, 29] but as discussed above, this patient population may not be identical to patients encountered in the pre-hospital setting or a mass casualty event. Patients encountered immediately after a poisoning may show a precipitous collapse of respiratory effort. Despite aggressive anticholinergic therapy and intensive supportive care, severe OP poisonings show a mortality rate around 30%[7, 28]. These patients eventually die due to inability to maintain oxygenation despite ventilation or inability to maintain adequate perfusion[28].

A potential problem with our model is the use of inhaled anesthetics. Inhaled anesthetics have a well-documented effect of respiratory depression. It could be argued that the apnea seen in our study was secondary to the inhaled anesthetic and not the OP itself. If isoflurane was wholly or partially responsible for the apnea in our experimental model then we would have found a significant differences between the outcome of Group IV (unanaesthetized animals) and that of Groups I and II. Both anesthetized and unanaesthetized groups showed 100% mortality with no differences in the time to onset of apnea.

An additional potential problem relates to the use of gallamine as a paralytic agent in mechanically ventilated animals. Gallamine is a known antagonist of muscarinic agonists and acts non-competitively via allosteric binding of M1 and M2 muscarinic receptors in the brain and lung [181, 182]. Both M1 and M2 receptors are present in the pre-Botzinger complex [183] but gallamine has been used extensively in respiratory research and has no effect on the output of the CRO [184]. In previous studies gallamine has resulted in potentiation of vagally mediated bronchoconstriction [185] and could theoretically increase pulmonary secretions following acute OP exposure. It is important to note that there were no pulmonary effects of gallamine during the control period prior to the poisoning, as determined by A-a gradient and $V_E V_I$ ratio. Future studies in this model should be performed with neuromuscular blocking agents that have no effects on muscarinic receptors.

Table 2.1 – Interventions for Experimental Groups

	Group I (n=10)	Group II (n=7)	Group III (n=5)	Group IV (n=4)
Anesthesia	Isoflurane	Isoflurane	Isoflurane	None
FIO_2 during experiment	100%	Titrated to PAO_2 of 100-115mmHg	Titrated to PAO_2 of 100-115mmHg	100%
Pharmacologic Paralysis	None	None	Gallamine	None
Mechanical Ventilation	None	At apnea	Throughout experiment	None
1hour survival	0/10	5/7	4/6	0/4
Functional Measurements	$ETCO_2$, Vi, Ve, esophageal pressure, arterial pressure, oxygen saturation, PaO_2, $PaCO_2$	$ETCO_2$, Vi, Ve, esophageal pressure, arterial pressure, oxygen saturation, PaO_2, $PaCO_2$	$ETCO_2$, Vi, Ve, arterial pressure, oxygen saturation, PaO_2, $PaCO_2$	$ETCO_2$, Vi, Ve

FIO_2 - fraction of inspired oxygen
$ETCO_2$ - end tidal carbon dioxide
Vi - volume of inspired gas
Ve – volume of expired gas
PaO_2 – arterial partial pressure of oxygen
$PaCO_2$ – arterial partial pressure of carbon dioxide

Table 2.2 – Initial Respiratory and hemodynamic characteristics of ventilated and non-ventilated animals

	Non-ventilated (n=20)	Ventilated (n=10)	p value
Animal Weight	320gm (+/- 8)	336 gm (+/- 18)	0.37
Initial Respiratory Rate	56 bpm (+/- 3)	63 bpm (+/- 4)	0.2
Initial Tidal Volume	2.84 cc (+/- .19)	2.38 cc (+/- .37)	0.25
Initial Blood Pressure (MAP) †	90 mmHg (+/- 3)	88 mmHg (+/- 3)	0.64
Initial Respiratory Effort*	-6.1 mmHg (+/- 2.2)	-5.6 mmHg (+/- 1.3)	0.49
Initial Pulse Rate'	354 bpm (+/- 10)	379 bpm (+/- 14)	0.19
Initial ET PCO_2	49 mmHg (+/- 1.1)	53 mmHg (+/- 1.1)	0.02

*Respiratory Effort is measured as peak inspiratory pressure

† = Includes group III - paralyzed and ventilated animals (n=13)

Values are reported as mean (+/- standard error)

MAP = mean arterial pressure

There was no statistical difference between ventilated and non-ventilated animals at baseline except for ET PCO_2. Paralyzed and ventilated animals (Group III, not included in the table except for MAP) showed a decrease in the pulse rate (378 vs 322, p=0.01) but no change in MAP (88 vs 98.9, p=ns) during the baseline period when compared to the ventilated at apnea group.

Figure 2.1 – Sample tracing of OP poisoned rat

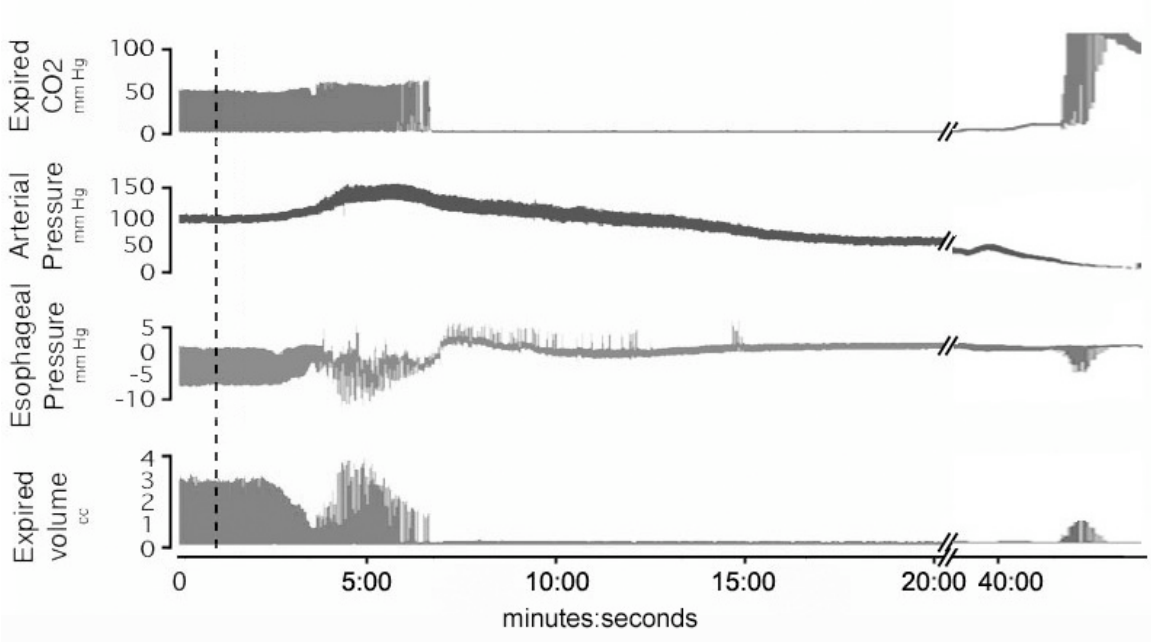

A sample tracing of a single OP poisoned rat from group 1 shows apnea occurring at 6:45 with a long period of no respiratory effort. OP injected at broken line. A break in the time scale allows us to see the terminal gasping that occurs as blood pressure approached zero. The positive deflections in the esophageal tracing represent retching.

Figure 2.2 - Blood pressure and respiratory rate in OP poisoned animals with and without mechanical ventilation.

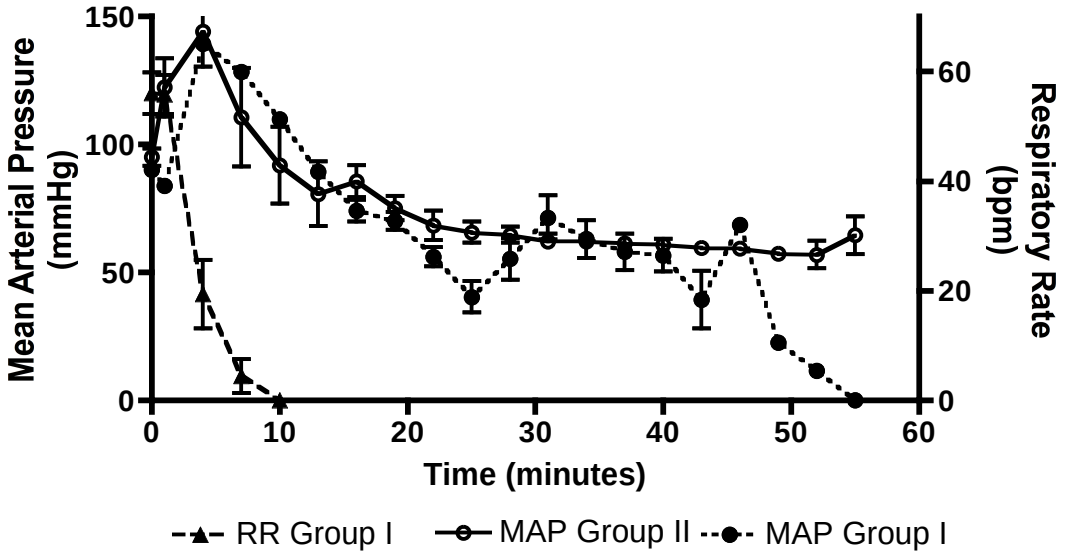

Grouped data sets show respiratory rate and mean arterial pressure for animals with acute OP and no further intervention (Group I) and mean arterial pressure for animals with acute OP and mechanical ventilation initiated at the point of apnea (Group II). Results are shown as mean value +/- standard error (n=10 all groups) with respiratory rate (triangle) represented on the right axis and mean arterial pressure (solid and hollow circle) on the left axis. The respiratory rate of Group II is not shown, as it was almost identical to the respiratory rate curve of Group I. In all groups poisoning occurred at 1 minute.

Figure 2.3 – Survival histogram ventilated and non-ventilated animals

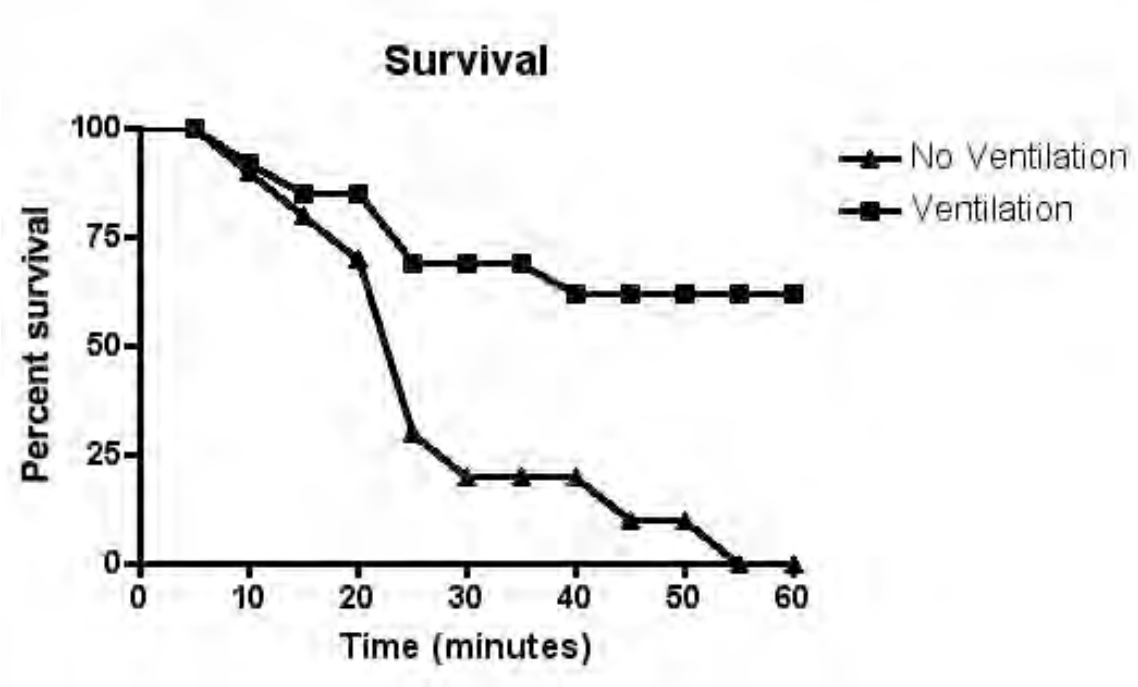

Grouped data sets for animals with OP exposure but no intervention (Group I) and all animals with OP exposure but mechanical ventilation (Group II and III) are displayed as mortality rate over time. Data are binned into 5-minute time blocks and presented as the percent of animals that survived to the end of the time block. Group IV (unanaesthetized) data was not available secondary to lack of invasive cardiovascular monitoring.

Figure 2.4 - Alveolar-arterial gradient and V_E/V_I ratio in animals that lived and died despite mechanical ventilation (Groups II and III)

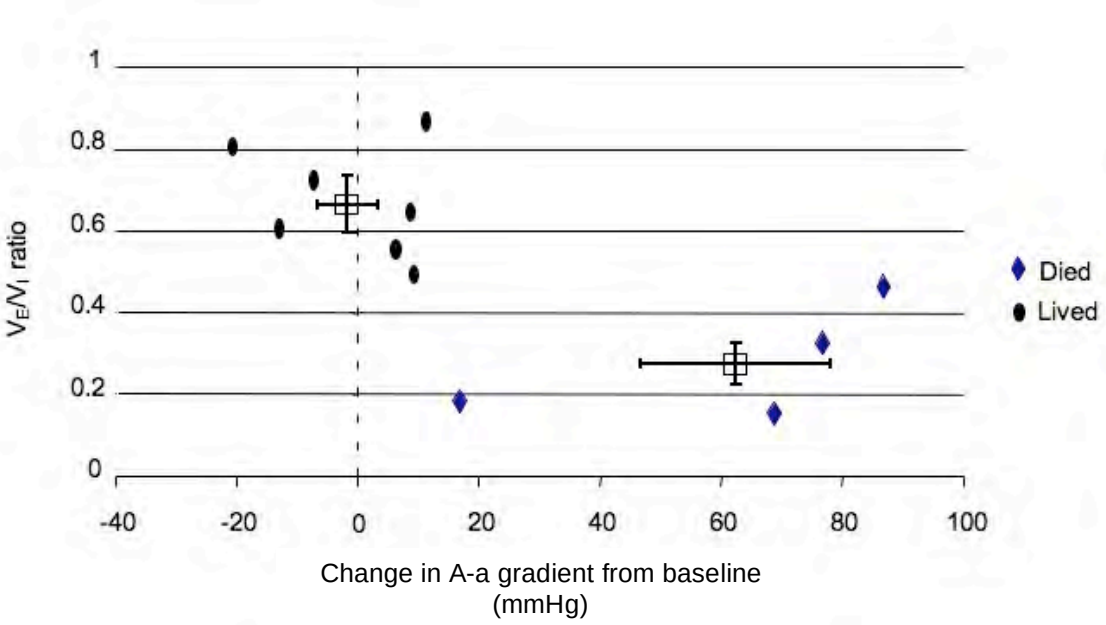

Data for animals receiving mechanical ventilation (Groups II and III) are plotted with V_E/V_I ratio on the Y-axis and A-a gradient on the X-axis. Individual animal data are represented as ovals (animals that lived to study endpoint) and diamonds (animals that did not live to study endpoint). Group averages for animals that lived and died are presented at boxes with SEM as bars. Changes in A-a gradient from baseline (-1.3 vs 62.0, P=0.0004) and changes in the V_E/V_I ratio (28 vs 66%, P=0.0014) were significantly worse in animals that died. Note, three animals from Group II and III without ABG measurements are not included in this graph (one died and two lived).

Figure 2.5 A,B - Alveolar-arterial gradient in animals receiving mechanical ventilation.

2.5A

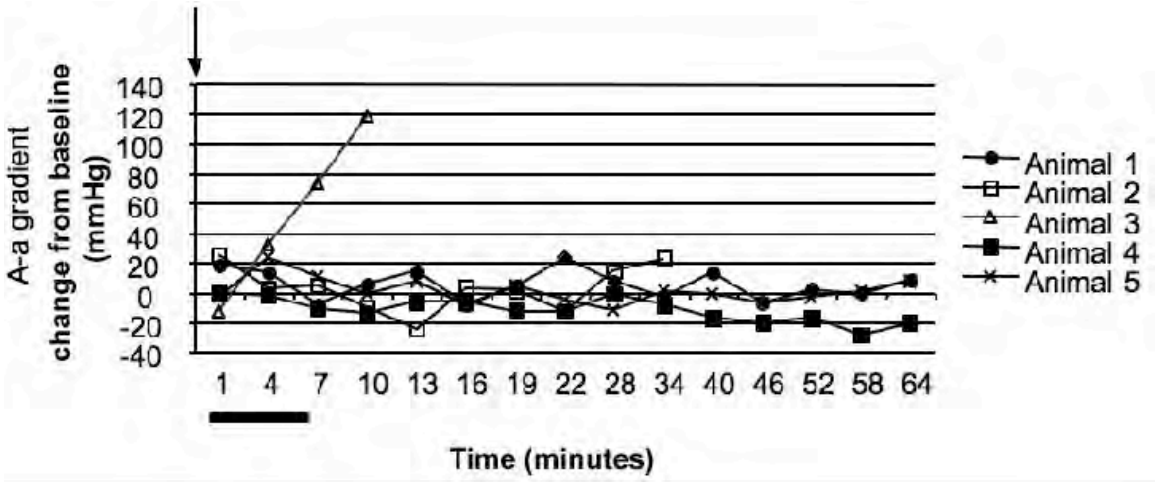

2.5B.

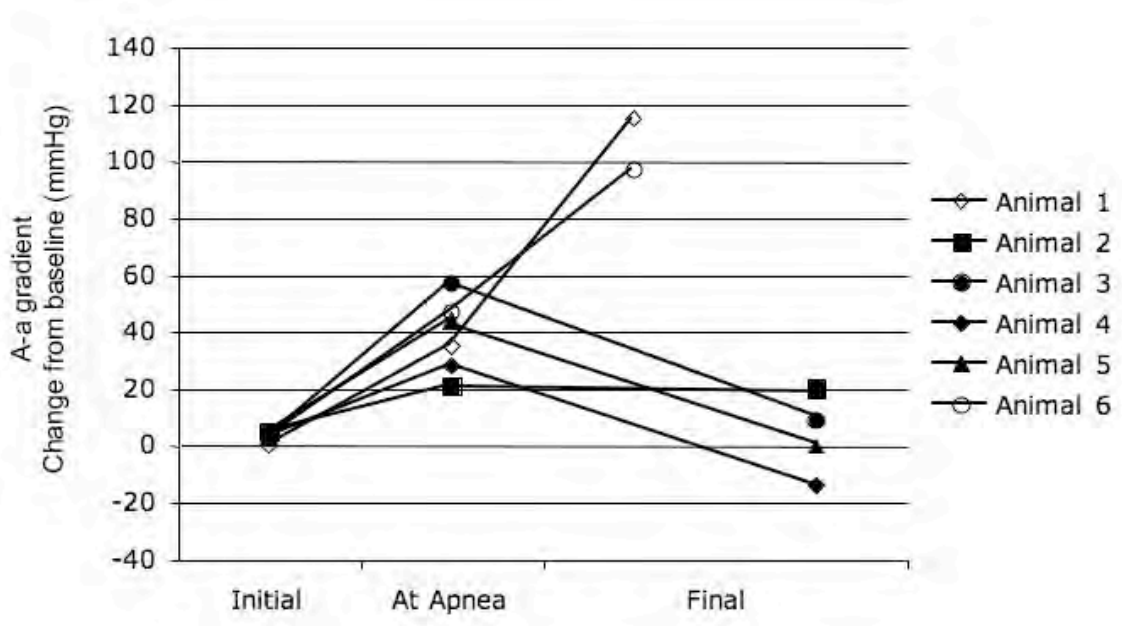

A - A graphical depiction of alveolar-arterial gradient for each animal that was exposed to OP and received mechanical ventilation throughout the experiment (Group III) is plotted over time. One of the animals in this group is not included

due to inability to obtain the necessary data points. Arterial blood gas measurements were obtained on a pre-determined schedule with a measurement every 3 minutes initially (8 times) and then every 6 minutes (7 times). The alveolar-arterial gradient is presented as change from baseline levels. All animals were poisoned at zero minutes (black arrow). Although the animals in this figure were paralyzed, the range of point of apnea in other groups is represented by a black bar under the X-axis. Data points for animals that survived to the study endpoint are solid shapes with data points for animals that died indicated by open shapes.

B - A graphical depiction of alveolar-arterial gradient for each animal that was exposed to OP and received mechanical ventilation at the point of apnea (Group II) is plotted for control period, at the point of apnea, and study endpoint. Six of the animals that received rescue mechanical ventilation had arterial blood gas measurements at these time points. The final endpoint was obtained just prior to cardiovascular collapse. A-a gradients are presented as change from baseline. Data points for animals that survived are represented as solid shapes and data points for animals that died are open shapes.

Chapter III - Respiratory failure induced by acute organophosphate poisoning in rats: effects of vagotomy.

Previously published - Gaspari RJ. Paydarfar D. Respiratory failure induced by acute organophosphate poisoning: Effects of Vagotomy. J Nuerotox. 2009 30(2) p298-304.

3.1 Abstract

In the previous chapter we showed that acute OP poisoning causes respiratory failure through two mechanisms: central apnea and pulmonary dysfunction. The vagus nerve is involved in both the central control of respiratory rhythm as well as the control of pulmonary vasculature, airways and secretions. We used a modification of the previous rat model of acute OP poisoning, with and without a surgical vagotomy to explore the role of the vagus in OP-induced respiratory failure. Dichlorvos (2,2-dichlorovinyl dimethyl phosphate) injection (100mg/kg subcutaneously, 3x LD50) resulted in progressive hypoventilation and apnea in all animals, irrespective of whether or not the vagi were intact. However, vagotomized animals exhibited a more rapidly progressive decline in ventilation and oxygenation. Artificial mechanical ventilation initiated at onset of apnea resulted in improvement in oxygenation and arterial pressure in poisoned animals with no difference between vagus intact or vagotomized animals. Our

observations suggest that vagal mechanisms have a beneficial effect during the poisoning process We speculate that vagally-mediated feedback signals from the lung to the brainstem serve as a modest protective mechanism against central respiratory depressive effects of the poison and that bulbar-generated efferent vagal signals do not cause sufficient pulmonary dysfunction to impair pulmonary gas exchange.

3.2 INTRODUCTION

In chapter 2 we describe respiratory failure following acute OP poisoning with an early central apnea followed by later pulmonary effects [186]. Experimental studies support the idea that OP-induced respiratory failure results from local effects of OPs acting on brainstem circuits underlying respiratory rhythmogenesis, and on lung tissues underlying pulmonary secretory, airway and vascular function. Application of acetylcholine or OP compounds to brainstem sites in medullary slice preparations results in a disruption of respiratory associated rhythmic activities[50, 187, 188]. These studies involve OP application to the pre-Botzinger complex, thought to be important for respiratory rhythmogenesis [88], but without the intact neural circuitry of an *in vivo* preparation. Experiments in both *in vitro*[50, 173, 189-191] and *in vivo*[49, 80, 192-195] preparations demonstrate respiratory effects secondary to cholinergic stimulation of diverse areas within the pons and medulla. The mechanism of later pulmonary effects from OP intoxication has been studied in isolated lung

preparations[52, 53, 196]. OPs exert their effects via inhibition of acetylcholinesterase and subsequent increase in acetylcholine levels. The primary source for pulmonary acetylcholine is the vagus nerve[197-199] and although the vagal trunks are transected in isolated lung preparations the acetylcholine-laden nerve endings remain intact within pulmonary tissue. It is accepted that acetylcholine from vagal nerve synapses is required for the pulmonary effects[200] of OPs. *In vivo* and *in vitro* studies support a local pulmonary effect of OP through pulmonary cholinergic receptors on pulmonary vasculature [74, 124, 201, 202], smooth muscle [203-205] and mucosal glands [205-207].

Although the local effects of OPs on brainstem and lung are sufficient to explain the central apnea and the pulmonary dysfunction associated with acute intoxication, the role (if any) of neural signals between the brainstem and the lung is uncertain. The vagus is the major neural pathway that interconnects the brainstem and the lung. The local effects of OPs could result in the stimulation of slowly adapting mechanoreceptors, rapidly adapting mechanoreceptors and C-fiber receptors that feedback via the vagus to brainstem respiratory center [59, 208, 209]. Conversely, OP-induced changes in the brainstem could result in pulmonary effects via vagal efferent projections. Vagal efferent fibers carry signals from bulbar circuits to bronchial smooth muscle [72], pulmonary secretory tissue [76] and pulmonary vasculature [210]. Cholinergic stimulation of the ventro-lateral surface of the medulla results in increased pulmonary

secretions[211] and the increase in pulmonary secretion from pulmonary irritants is decreased in vagotomized animals[212]. However, it remains unclear to what degree bulbar-generated efferent vagal activity contributes to pulmonary dysfunction during acute OP intoxication and if central effects of OPs mediated through vagal efferents predominate over local cholinergic effects at the pulmonary synapses.

We have further developed the animal model of OP poisoning described in chapter 2 to test whether signals traveling via the vagus nerve play a role in the development of OP-induced respiratory failure. First, we postulated that vagally mediated peripheral feedback influences OP-induced central apnea. Therefore we hypothesized that ablation of the vagus alters the natural history of OP-induced apnea. In the present study our results appear to support this hypothesis because vagotomized animals suffer a more rapidly progressive hypoventilation and central apnea following OP exposure, compared to animals with intact vagi.

Second, we postulated that vagally mediated efferent pathways from bulbar circuits to the lung are activated by OP-poisoning and therefore we hypothesized that ablation of the vagus reduces pulmonary dysfunction associated with OP exposure. In order to test this hypothesis, we resuscitated animals with central apnea induced by OP-poisoning, and we measured arterial blood oxygen levels during fixed mechanical ventilation. We found that during OP poisoning vagotomy was not associated with any improvement in arterial oxygen levels,

suggesting that pulmonary gas exchange during OP poisoning was not affected by the vagus.

3.3 MATERIALS AND METHODS

General Preparation

The animal model used in this study is a further development of the animal model described in detail on page 24 in chapter 2.

Experimental Groups

Experimental groups are listed in Table 3.1 and consisted of animals with intact vagus nerves (n=30) and animals that were vagotomized (N=20). There were two groups of animals with intact vagi, either spontaneously breathing throughout or animals that were spontaneously breathing prior to the poisoning but received mechanical ventilation at the point of apnea (see Figure 3.1 for schematic). There were also two similar groups of vagotomized animals, spontaneously breathing throughout and animals that received mechanical ventilation at the point of apnea. All animals that did not receive mechanical ventilation spontaneously breathed 100% oxygen. Animals with mechanical ventilation had ventilation initiated at the point of apnea. These animals were spontaneously breathing up to the point of apnea but were mechanically ventilated once they stopped breathing. In these experiments, mechanical ventilation was used as an experimental tool to allow more detailed pulmonary and cardiovascular recordings post apnea. Initiating mechanical ventilation at the point of apnea

allowed us to remove the confounding effect of apnea so that we could study arterial oxygenation during constant ventilation. This allowed measurements of pulmonary gas exchange during the later period of pulmonary dysfunction that otherwise would have been unobtainable. Supplemental oxygen for animals in the group who received mechanical ventilation at the point of apnea was titrated to achieve an arterial PO_2 between 100 and 110 mmHg during the baseline period (i.e., prior to injection of dichlorvos). Once this was achieved, the FIO_2 was not changed throughout the experiment. Arterial blood was collected via an arterial line by withdrawal of 0.2cc's of blood and PO_2, PCO_2, and pH were measured (Rapidlab 248, Bayer Medical) during the baseline pre-poisoning period, around the time of apnea and during the post-apnea period for the mechanically ventilated animals only. A-a gradient blood gas measurements are reported as a change from baseline.

Surgical Vagotomy

Mid-cervical vagotomy was performed via an anterior approach under general anesthesia. The vagi were dissected away from the cervical sheath and complete transaction was confirmed by direct visualization. Anesthetic agents did not change between groups and all animals remained under general anesthesia for surgical procedures, baseline period and the experiment. Vagotomy caused transient changes in blood pressure and breathing that stabilized after 10 minutes. Therefore the vagus nerve was transected 20-30 minutes (range) prior to administration of dichlorvos. Sham surgery was performed on all animals with

intact vagus nerves and consisted of the same neck dissection performed in the vagotomy surgery with the exception that the vagus nerve was not transected. The sham surgery was also followed by a 25-35 minute period before administration of dichlorvos.

Data Analysis

Data were continuously recorded and averaged into 15-second bins. Changes in oxygen saturation, respiratory rate, volume of inspired gas, minute ventilation, pulse rate and mean arterial pressure over time were calculated. Statistical significance of changes over time was determined using a repeated measure ANOVA. Mortality was analyzed using a chi-square test. Single comparisons of mean values between groups were analyzed using a Student's t-Test. Differences were considered significant for p-values <0.05.Results are presented as mean (+/- standard error of the mean (SEM)) unless otherwise stated.

3.4 RESULTS

Baseline Measurements

Baseline cardiovascular and respiratory values for all groups are listed in Table 3.2. Vagotomized animals (Group 1b & 2b) exhibited significantly lower baseline respiratory rate and minute ventilation, compared to the vagi intact animals (Group 1a & 2a). As expected, vagotomized animals demonstrated a larger volume of inspired gas. Vagotomized animals exhibited no significant change in

baseline blood pressure or pulse rate when compared to vagus intact animals, as reported previously in rats [213]. In summary, the baseline characteristics for each group are what would be expected from previous literature[214].

Group 1: Vagotomy was Associated with More Rapidly Progressive Hypoventilation and Circulatory Collapse (Figures 2-4)

Following dichlorvos injection, all animals exhibited a rapid decline in respiratory rate, and minute ventilation (Figure 3.2a,b). However, hypoventilation was more rapidly progressive in vagotomized animals. Figures 3.2a and 3.2b (from animals in Group 1a and 1b) show that the decline in respiratory rate and ventilation over the first 6 minutes following OP poisoning was more rapid in vagotomized animals compared to vagus intact animals (p=0.018 for respiratory rate, and p=0.023 for minute ventilation, repeated measure ANOVA). The beneficial effect of an intact vagus was modest. For example at 5 minutes, animals with intact vagi exhibited a 54% greater minute ventilation compared to vagotomized animals. Animals with intact vagi (Group 1a) developed central apnea an average of 5.47 min ($\pm$ 0.73 min) after sub-cutaneous injection of dichlorvos. Vagotomized animals exhibited central apnea an average of 4.4 min ($\pm$ 0.55 min) after poisoning. Therefore an intact vagus in rats poisoned with dichlorvos results in a significant reduction of the central hypoventilation associated with dichlorvos. The more severe hypoventilation preceding apnea seen in vagotomized animals corresponded to a trend toward more severe decrease in transcutaneous oxygen saturation compared to animals with intact

vagi (Figure 3.3, *p*=0.071, ANOVA) but the difference did not quite reach statistical significance.

Initial respiratory failure was followed by cardiovascular collapse and death in both vagi intact and vagotomized animals (Groups 1a and 1b) that did not receive mechanical ventilation. Animals in both groups showed an initial episode of hypertension before a gradual decline in mean arterial blood pressure (MAP) but the decline differed between vagi intact and vagotomized animals (Figure 3.4, p=0.001 ANOVA). The difference in MAP was greatest between groups at 10 min post dichlorvos (9% vs 110% of baseline) but the MAP was almost the same (0 vs 9.9% of baseline) at 40 minutes. Average time to 50% below baseline MAP was 6.83 min for vagotomized animals and 19.75 min for intact animals (students t-test, *p*=0.003).

Group 2: Lack of Effect of Vagotomy on Pulmonary Oxygenation and Circulation During Fixed Mechanical Ventilation-

Animals receiving mechanical ventilation at the point of apnea (Groups 2a and 2b) showed distinct differences before and after the initiation of mechanical ventilation. Figure 3.5 a-c shows the respiratory changes for animals that receive mechanical ventilation at the point of apnea. The data in these experiments confirmed the findings for the Group 1 experiments, i.e. that vagotomized animals have more profound hypoventilation than the vagi intact

animals. Respiratory rate and minute ventilation declined more rapidly in vagotomized animals (p,0.001 and p=0.004 respectively, ANOVA) but there was no significant change in volume of inspired gas (p=0.10, ANOVA) (Fig 3.5a,b,c). Once the animals were placed on a mechanical ventilator there was no difference (3.5 a,b,c, p<0.05, ANOVA). Similarly, the time to apnea between groups was not different (7:24 *vs*. 8:37, p=ns). Arterial blood gas measurements in Group 2 animals at baseline, apnea and post apnea are given in Table 3.3. At the point of apnea vagotomized animals (Group 2b) showed a significantly lower arterial PO_2 (75.0 *vs*. 38.9 mmHg, *p*=0.004) and increase in PCO_2 (45.1 *vs*. 63.0, *p*=0.045). The difference in arterial PO_2 was not due solely to changes in ventilation because the A-a gradient at the point of apnea was worse in vagotomized animals (46.4 (+/- 7.0) *vs*. 68.8 (+/- 5.2), *p*=0.045) but no difference was seen between groups at baseline (5.06 (+/- 0.85) *vs*. 7.2 (+/- 0.9), *p*=0.10) or post apnea (16.3 (+/-15.0) *vs*. 7.0 (+/-9.6), *p*=ns) (Figure 3.6, Table 3.3) despite similar ventilation (pCO2 48.9 (+/- 5.04) *vs*. 44.7 (+/- 4.53). Post apnea arterial blood gas samples were drawn at similar times from initiation of ventilation (10.42 min *vs*. 11.13 min). The range of oxygenation for vagus intact (31-194) and vagotomized animals (10-171) supports our previous findings of variability within the poisoning model[186] with some vagus intact animals catastrophically affected and others less so. In summary, vagotomy resulted in an initial deterioration of pulmonary function but there was no difference in pulmonary function post apnea between vagotomy and vagus intact animals. It is important

to note that these effects are distinct from the effects of vagotomy on OP-induced central apnea discussed previously.

Mechanical ventilation at the point of apnea prevented a complete cardiovascular collapse in most animals but vagotomized animals remained close to 100% of baseline MAP while vagus intact animals declined below 70%. However these trends were not statistically significant (Figure 3.7a, p=ns, ANOVA). Vagotomized animals showed a pulse rate greater then 70% of baseline throughout the experiment while vagus intact animals declined below 50% but again without statistical significance (Figure 3.7b, p=ns, ANOVA). An analysis of the mortality rates between groups receiving mechanical ventilation showed no difference between groups (15% vs 20%, p=ns, Chi-square). All of the animals that died despite mechanical ventilation showed tracheal secretions filling their tracheal tube at the time of death.

3.5 DISCUSSION

Our results suggest that vagal mechanisms have protective effects on respiratory function in a rat model of OP poisoning. In the early phase of poisoning, vagal mechanisms appear to blunt the progressive hypoventilation in spontaneously breathing animals. We infer this protective role of the vagus because vagotomized animals exhibit a more precipitous drop in ventilation, compared to

animals with intact vagi. However, despite vagal efferent connections to the glands and smooth muscle in the airways of the lung, when apneic animals are resuscitated by artificial ventilation, vagal mechanisms appear to have no effect on pulmonary gas exchange during poisoning, i.e. vagotomized, artificially ventilated animals have similar oxygenation compared to vagus intact animals.

Previous studies have described a role of vagal afferents in altering central respiratory activity, see reference [209] for a comprehensive review. Rapidly adapting mechanoreceptors and other small fiber afferents are activated by pulmonary “irritants” (e.g., smoke, histamine, capsaicin) that augment central inspiratory drive [215]. We found that vagotomized animals exhibited more profound hypoventilation following exposure to dichlorvos. OP agents cause bronchorrhea and bronchoconstriction and these airway effects could stimulate rapidly adapting irritant afferents, which in turn would enhance central neural inspiratory activity. The time course of dichlorvos induced pulmonary dysfunction (onset within 2 minutes) [51] is sufficient to support this hypothesis. Alternatively, the OP might act directly to activate irritant receptors. Further work is needed in reduced preparation using recordings of vagal afferents and phrenic nerve to distinguish these possibilities, or to suggest an alternative mechanism for vagal enhancement of respiratory rhythm during OP poisoning.

The cardiovascular effects of OP poisoning include hypotension, hypertension and cardiac arrest [48, 179, 216] with variable effects on pulse rate[217]

preceding cardiac arrest. Our previous work in the rodent animal model has shown that central apnea and pulmonary insufficiency are independent of the cardiovascular effects [186], notably the central apnea occurs early in the poisoning process, long before the development of systemic hypotension. It is not clear if the cardiovascular affects of OP poisoning are secondary to central or peripheral effects of the poisoning. Previous studies have demonstrated central mechanisms for cardiovascular changes via the vagus nerve [218] while others describe a direct effect of OP on the heart [219]. Our findings suggest that the heightened cardiovascular vulnerability in vagotomized animals can be explained at least in part by hypoxic inhibition of cardiovascular function [220]. In our study, animals with no mechanical ventilation (group 1) show increased cardiovascular collapse in vagotomized animals, but this difference is not seen in animals receiving mechanical ventilation (group 2). In short, vagotomized animals demonstrated earlier apnea and subsequently decreased tissue oxygenation that may have contributed to greater cardiovascular depression. We noted that, as a group more rapidly declining blood pressure was preceded by a steeper decline in transcutaneous oxygen saturation. However, one of the vagotomized animals showed a decrease in blood pressure prior to the development of arterial desaturation. Cardiovascular-depressant effects of OP have been described in the literature[217] but it is unclear to what degree a direct cardiac effect is responsible for the hypotension seen in our animal model. Further research is required to fully characterize the cardiac effects of acute dichlorvos poisoning.

Vagotomized animals showed an increased A-a gradient at the point of apnea, which cannot be explained by known vagal mechanisms. Vagal control of the airways and pulmonary vasculature is well established. Vagal stimulation has been shown to constrict pulmonary airways[221], and vagotomy abruptly dilates pulmonary airways [222]. In addition, stimulation of the vagus causes vasodilatation of the pulmonary vasculature [223]. Previously demonstrated pulmonary effects of acute OP poisoning suggest that ventilation-perfusion (V-Q) mismatch in poisoned animals is due at least in part to decreased ventilation from bronchoconstriction. If this were the sole mechanism then vagotomy would result in an improvement of pulmonary gas exchange, which our findings do not support. In our study, vagotomy-induced pulmonary bronchodilation or vasoconstriction or both could contribute to an increased V-Q mismatch and explain why the A-a gradient widened in vagotomized animals at the point of apnea.

Finally, we found in poisoned animals that vagotomy had no effect on pulmonary oxygenation during fixed mechanical ventilation. This result was unexpected. Previous studies have proposed a role of the vagus in acute OP poisoning [37] and “chemical vagotomy” with atropine is the main therapy for acute OP poisoning. One possible explanation for our findings involves the effects of vagal efferent signaling on pulmonary smooth muscle and glandular tissue. We noted an increased volume of expired gas at baseline in vagotomized animals receiving mechanical ventilation, which was expected. The associated increase in airway

caliber in vagotomized animals would be beneficial during OP-induced pulmonary airway constriction. Vagal control of pulmonary secretions is well established and would suggest a decrease in pulmonary secretions in vagotomized animals [211]. Our hypothesis that vagotomy would improve pulmonary oxygenation is not supported by our experiments. Furthermore, in artificially ventilated rats we found no difference between vagotomized and vagi intact animals in the number of animals who died with secretions filling the tracheal tube. This was unexpected as surgical vagotomy has been shown to decrease pulmonary secretions [212]. Vagal efferent signaling is not the only possible mechanism of OP induced pulmonary secretions as sectioning the vagus nerve does not remove the acetylcholine laden nerve terminals in the lung and direct application of OP to an isolated lung results in bronchorrhea [52]. However, we did not directly measure pulmonary secretions in this study therefore additional studies are required to quantify the pulmonary secretory changes attributable to OP effects on lung synapses versus cholinergic mechanisms resulting from bulbo-pulmonary vagal signaling mechanisms.

Our study suffered from some additional limitations. By cutting the vagi we simultaneously eliminated vagal efferent and afferent signaling. This prevented us from independently examining the effects of vagal efferent or afferent signaling in isolation. In addition, because we did not record vagal fiber activity in our model of OP poisoning, we are unable to test directly the effect of OP on vagal signaling. The present experiments provide evidence for a role for the

vagus nerve in an OP poisoning model, but future investigation will be needed to test more directly the separate role of afferent and efferent pathways.

Table 3.1 - Experimental Intervention for vagus intact and vagotomy groups

	Vagus Status	N	Mechanical Ventilation	FiO_2
Group 1a	Vagi Intact	20	None	100% O_2
Group 1b	Vagotomy	10	None	100% O_2
Group 2a	Vagi Intact	10	Initiated at onset of apnea	Titrated to achieve normoxia
Group 2b	Vagotomy	10	Initiated at onset of apnea	Titrated to achieve normoxia

FiO_2 = Fraction of inspired oxygen

N= number of animals in group

Table 3.2 -Baseline physiologic values for vagus intact and vagotomy groups

	MAP	HR	MV	Vi	RR
Group 1a	92.2 (2.3)	365.6 (7.0)	130.0 (7.5)	2.29 (0.10)	56 (2.2)
Group 1b	102.3 (8.71)	349.6 (7.66)	99.6 (9.57)*	3.0 (0.39)*	33.7 (3.0)*
Group 2a	84.1 (3.15)	369 (15.6)	136.1 (12.5)	2.16 (0.14)	62.7 (3.15)
Group 2b	93.3 (5.40)	349.2 (10.2)	104.0 (8.19)*	2.87(0.23)*	36.1 (1.14)*

MAP = mean arterial pressure (mmHg)

HR = heart rate (beats/min)

MV = minute ventilation (cc's/min)

Vi = Volume of inspired gas (cc's)

RR = respiratory rate (breaths/min)

- indicates statistical significance when compared between groups ($p<0.05$)

Results presented as average ($\pm$ standard error of mean). Baseline values represent point prior to poisoning but post surgical procedure.

Group 1a – Vagus intact, Spontaneously breathing throughout (n=20)

Group 1b – Vagotomy, Spontaneously breathing throughout (n=10)

Group 2a – Vagus intact, Mechanically ventilated (n=10)

Group 2b – Vagotomy, Mechanically ventilated (n=10)

Table 3.3 – Arterial blood gas measurements before and after exposure to dichlorvos

	Baseline			At Apnea			Post Apnea		
	pH	PaO2	PCO_2	pH	PaO2	PCO_2	pH	PaO2	PCO_2
Group 2a	7.30 (0.01)	115.5 (1.53)	44.2 (2.46)	7.23 (0.01)	75.0 (8.54)	45.1 (3.61)	7.18 (0.03)	104.9 (16.4)	48.9 (5.04)
Group 2b	7.25 (0.02)	115.9 (2.82)	41.3 (3.78)	7.18 (0.03)	38.9 (3.84)	63.0 (8.75)	7.21 (0.02)	117.0 (14.8)	44.7 (4.53)

Results presented as Average (SEM)

Group 2a – Vagus intact, Mechanically ventilated (n=10)

Group 2b – Vagotomy, Mechanically ventilated (n=10)

Figure 3.1 - Schematic of experimental interventions for vagus intact and vagotomy groups.

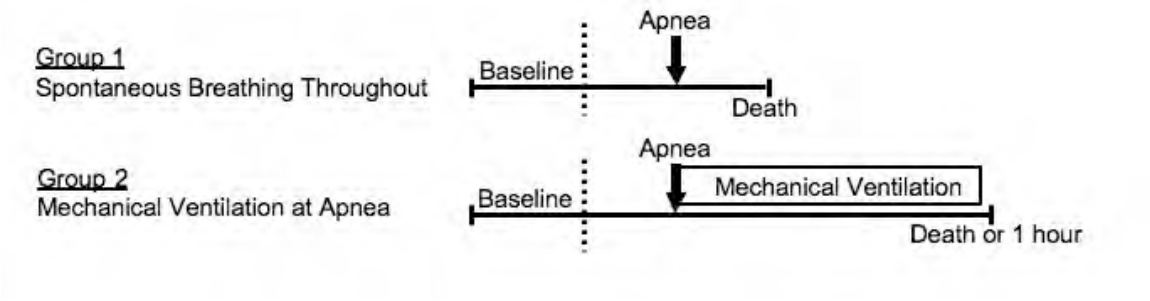

Dichlorvos (100mg/kg) was given at dotted line. The only difference between study groups is the initiation of mechanical ventilation at the point of apnea in Group 2.

Figure 3.2 A,B - Comparison of respiratory rate and minute ventilation between vagi intact and vagotomized animals (Group 1a and 1b) without mechanical ventilation.

Figure 3.2 A

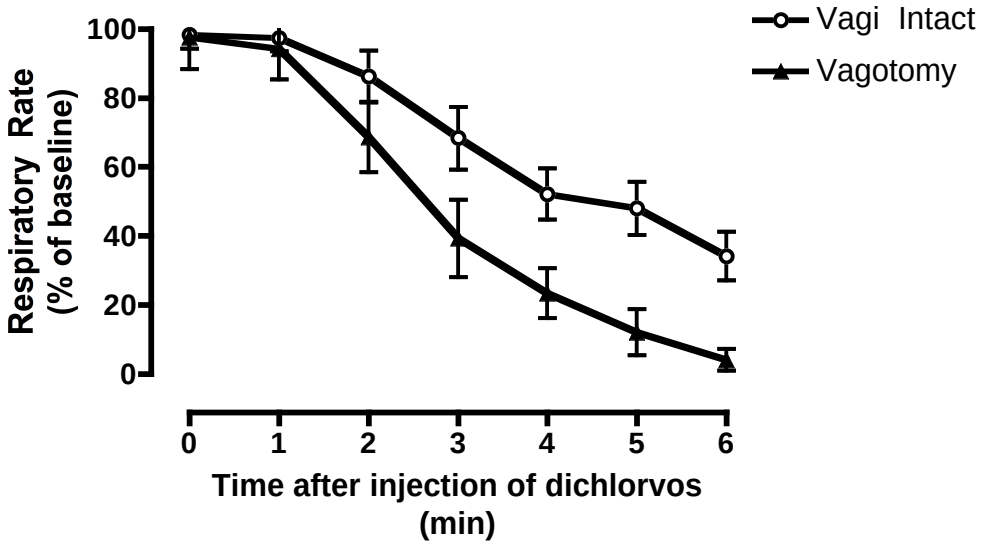

Figure 3.2 B

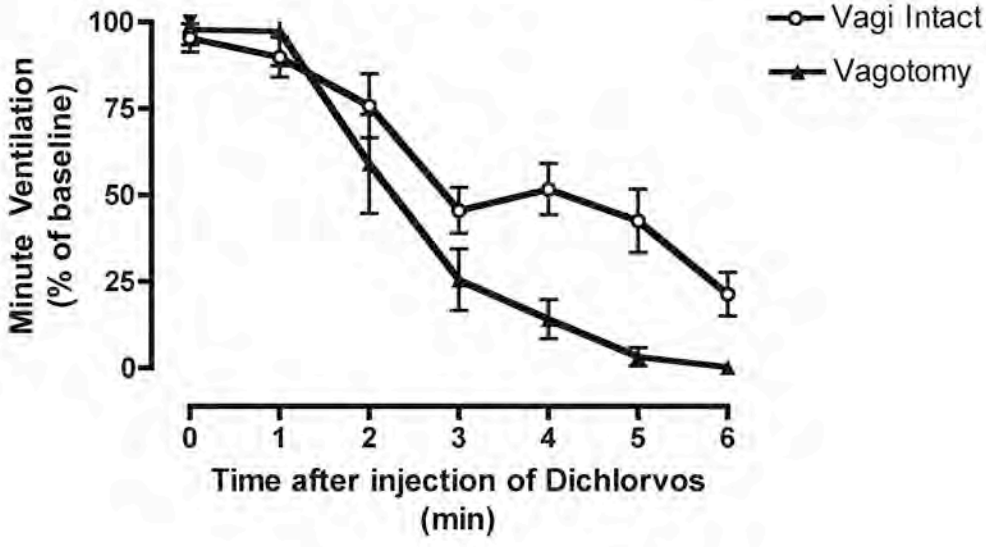

Results are shown as a percentage of baseline +/- standard error. There was no difference in time to apnea (p=ns, student's t-test) between vagotomized (n=20)

and vagi intact animals (n=10). Respiratory rate and minute ventilation were lower in vagotomized animals ($p<0.05$, ANOVA). For example, at 4 minutes respiratory rate (23 vs 52% of baseline) and minute ventilation (14 vs 52% of baseline) was less in vagotomized animals.

Figure 3.3 – Evolution of hypoxia after onset of apnea in vagi intact and vagotomized animals (Group 1a and 1b) without mechanical ventilation.

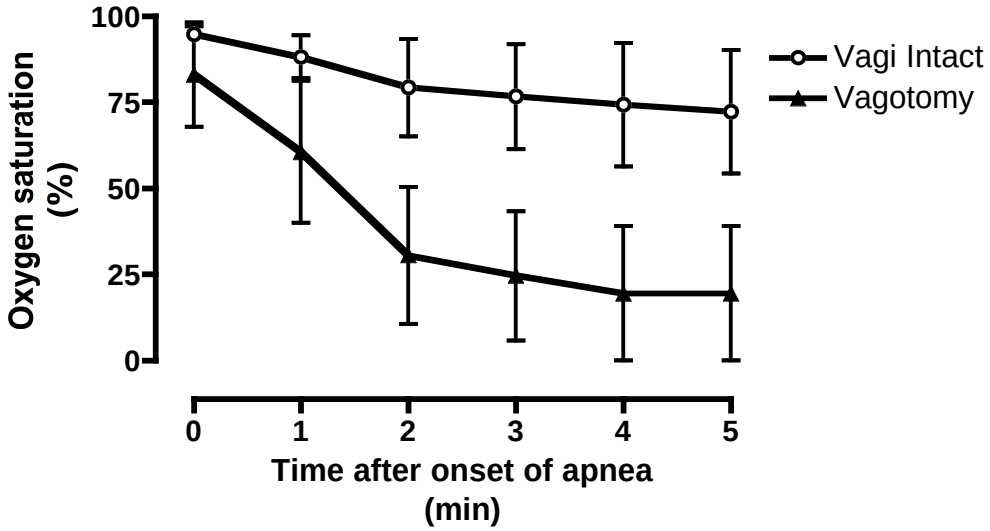

Oxygen saturation after the point of apnea was lower in vagotomized animals but it did not reach statistical significance (p=0.071, ANOVA). The greatest difference in oxygen saturation between groups was at 4 minutes (20 vs 74%, p=ns). Results are shown as mean values +/- standard error (n=5 each group).

Figure 3.4 – Changes in blood pressure of vagi intact and vagotomized animals without mechanical ventilation.

Figure 3.4

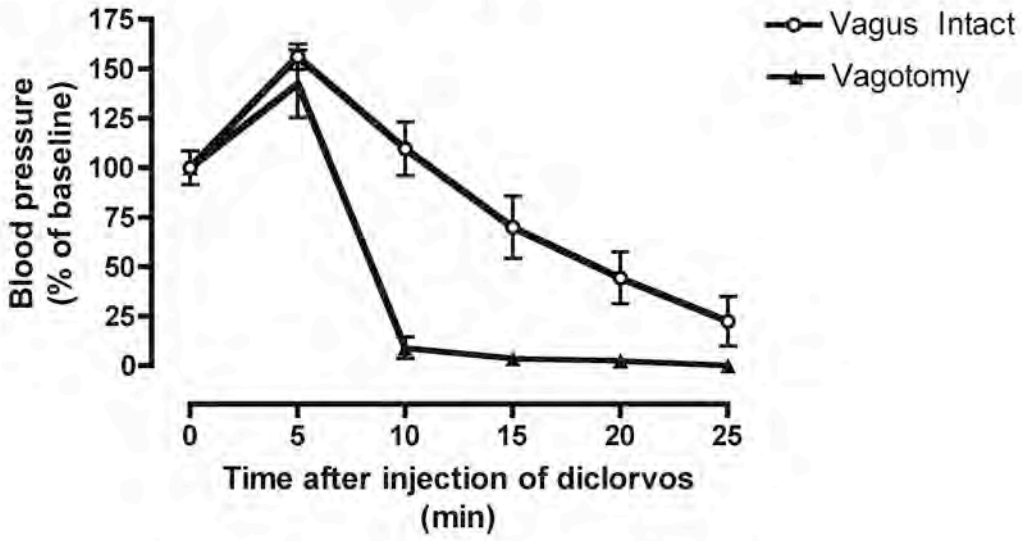

Grouped data sets show mean arterial pressure for animals following dichlorvos (Groups 1a and 1b). Vagotomized animals showed a significantly lower blood pressure following dichlorvos ($p<0.05$, repeated student's t-test after 5 minutes post poisoning. Data are shown from point of dichlorvos injection (time 0). Results are shown as percent of baseline mean arterial pressure +/- standard error (n=20 Group 1a, n=10 Group 1b)).

Figure 3.5 A,B, and C

Comparison of respiratory rate, volume of expired gas, and minute ventilation between vagi intact and vagotomized animals that received mechanical ventilation at the point of apnea (Group 2a and 2b).

Figure 3.5A

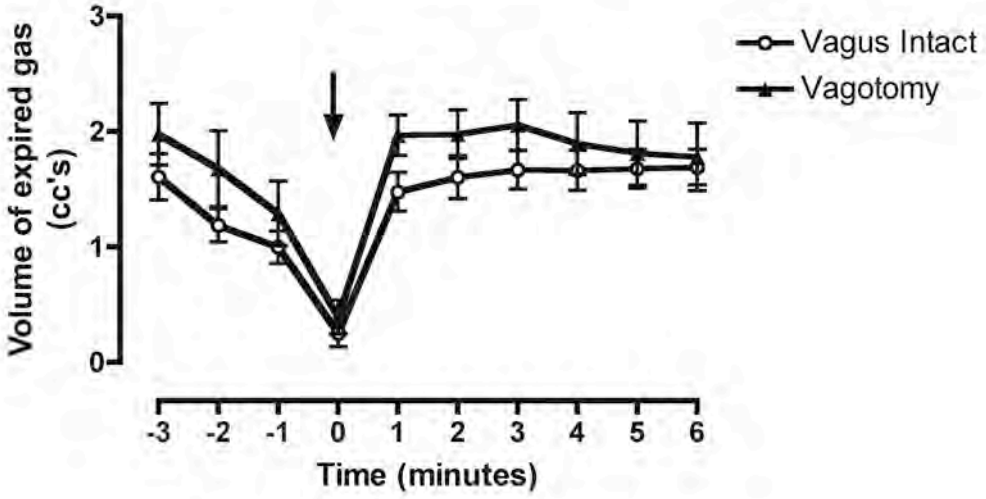

Figure 3.5B

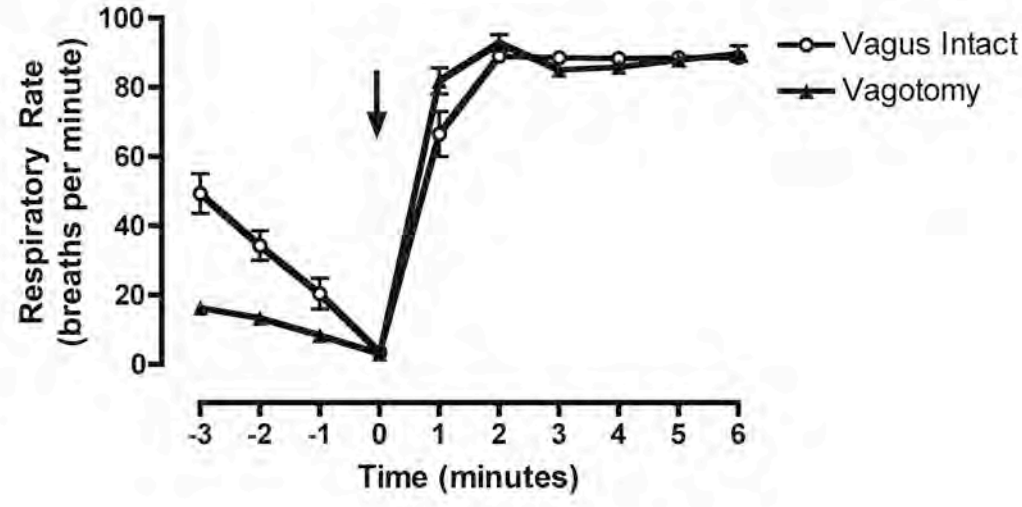

Figure 3.5C

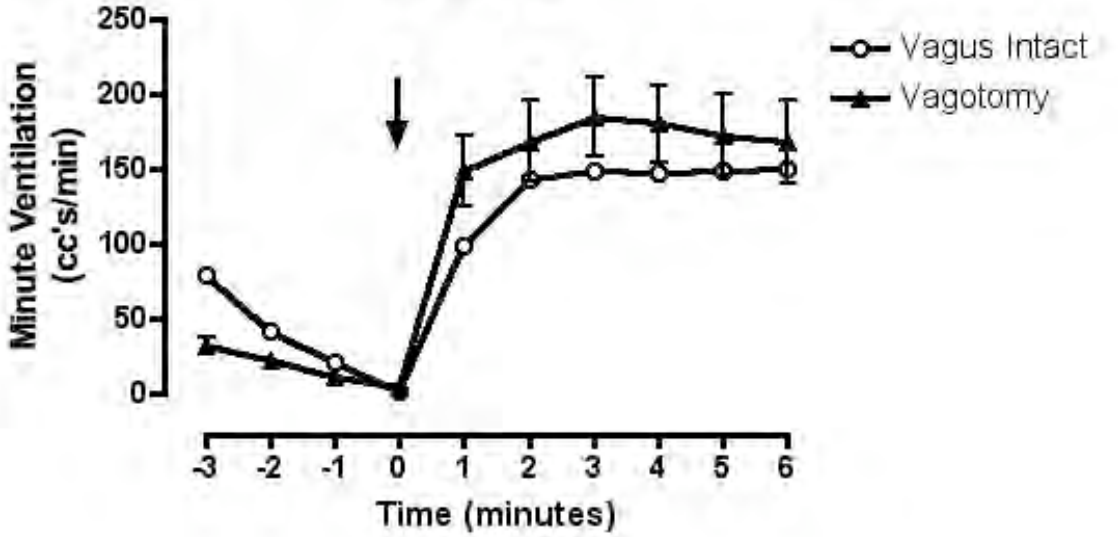

Results are shown as raw data synchronized at the point of apnea (black arrow). Animals are spontaneously breathing to the left of the arrow and mechanically ventilated to the right of the arrow. Prior to apnea respiratory rate was lower in vagotomized animals ($p<0.001$, ANOVA) but volume of expired gas was unchanged ($p=0.10$, ANOVA) resulting in a decrease in minute ventilation ($p=0.004$, ANOVA). Following apnea, there was no difference between vagotomized and vagus intact animals (p=ns, ANOVA). The greatest difference between groups for respiratory rate (66.5 ($\pm$20.4) vs 81.9 ($\pm$11.9) bpm), volume of expired gas (1.48 ($\pm$0.53)) vs 1.97 ($\pm$0.56) cc) and MV (98.3 ($\pm$10.9) vs 147.9 ($\pm$76.0) cc/min) post apnea was at 1 min.

Figure 3.6 – Oxygen saturation around the point of apnea in vagus intact and vagotomized animals.

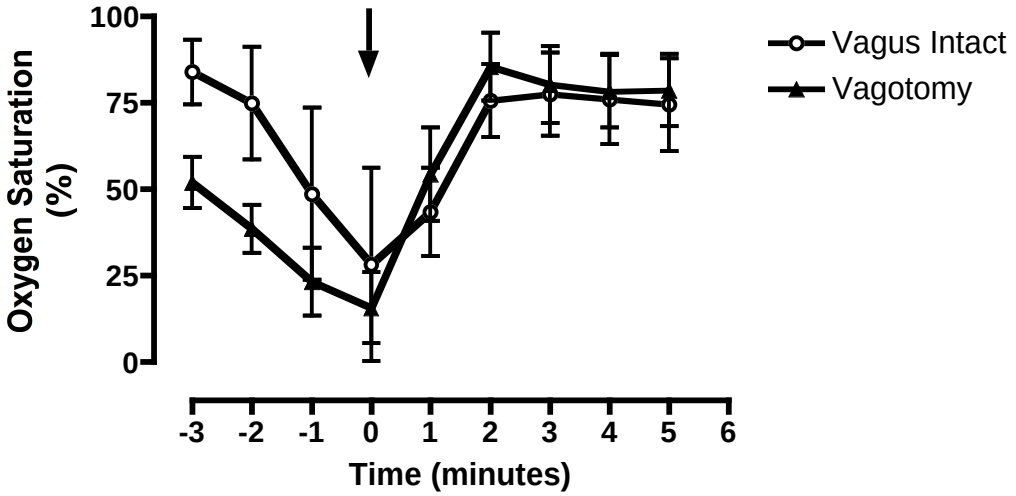

Grouped data sets show oxygen saturation for animals with dichlorvos and mechanical ventilation initiated at the point of apnea (Groups 2a and 2b). Oxygen saturation in vagotomized animals (n=10) was lower prior to the point of apnea (p=0.003, ANOVA) but there was no difference after the point of apnea (p=ns, ANOVA) when compare to vagus intact animals (n=10). At 5 min post apnea oxygen saturation was almost the same in both groups (74.5 (±40.5) vs 78.7 (±31.3)). Data are shown referenced to the point of apnea (indicated by black arrow). Results are shown as mean values +/- standard error (n=9 both groups).

Figure 3.7A, B – Changes in blood pressure and pulse rate of vagi intact and vagotomized animals with mechanical ventilation at apnea. (Groups 2a and 2b).

Figure 3.7A

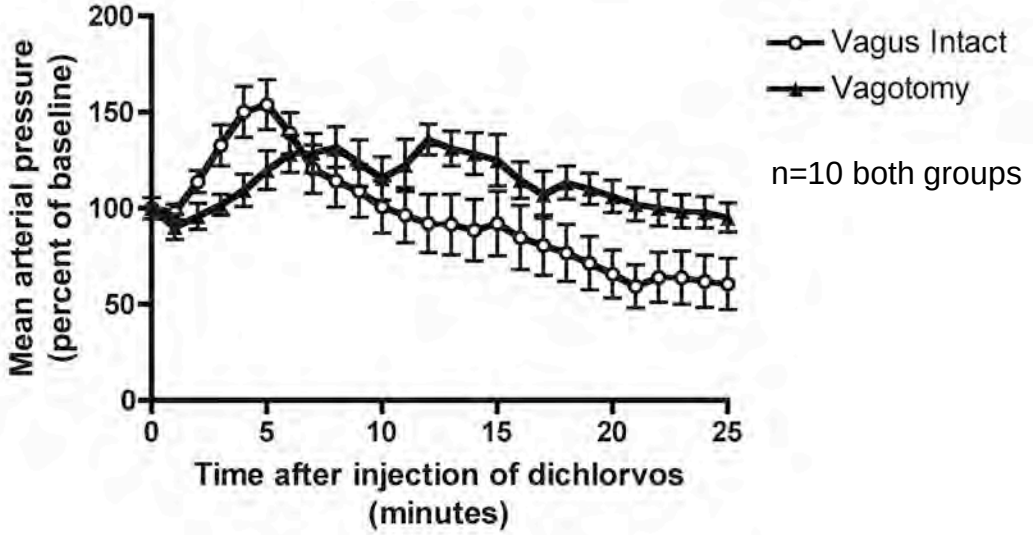

Figure 3.7B

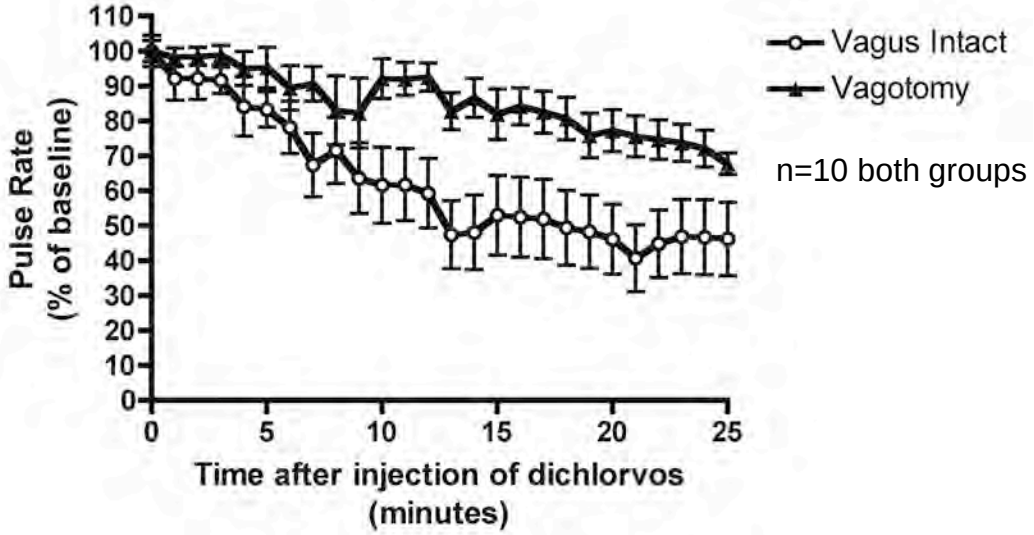

Dichlorvos was injected at time zero. Vagi intact animals showed a greater drop in blood pressure after the initiation of mechanical ventilation but the difference was not statistically significant (p=ns, ANOVA). MAP at 25 min was 62% (±43) of

baseline in vagi intact animals vs 98% (±26) in vagotomized animals. Vagi intact animals showed a greater drop in pulse rate after the initiation of mechanical ventilation (p=ns, ANOVA). Pulse rate at 25 min was 47% (±32) of baseline in vagi intact animals vs 72% (±16) in vagotomized animals. Results are shown as a percentage of baseline mean arterial pressure +/- standard error or baseline pulse rate +/- standard error (n=10 both groups).

Chapter 4 - Pulmonary changes in gas exchange following antimuscarinic therapy

4.1 Abstract

Atropine, an anti-muscarinic drug, is the primary therapy for acute OP poisoning. Cholinergic nerves that innervate pulmonary smooth muscle, glands and vasculature are active in regulating pulmonary gas exchange. It is unclear if atropine induces a ventilation-perfusion mismatch by altering cholinergic tone at matched airways and vasculature in the lung. We hypothesized that atropine causes alterations in pulmonary gas exchange. We conducted a prospective interventional study with detailed physiologic recordings in anesthetized, spontaneously breathing rats (n=8). Animals breathing a normoxic gas mixture were titrated to a partial arterial pressure of oxygen (PaO_2) of 110-120. An escalating dose of intravenous (IV) atropine (0.001, 0.01, 0.1, 5 and 20 mg/kg) was administered. Arterial blood gas measurements were recorded every 2 minutes (x5) at baseline and following each of the five doses of atropine. Between-group comparisons were made with Student t-tests.

Oxygenation decreased immediately following IV atropine despite a small increase in volume of inspired air and no change in respiratory rate and respiratory effort. Oxygen saturation decreased with increasing dose of atropine. Arterial blood gas analysis showed an increase in pulmonary dysfunction characterized by a widening of the A-a gradient ($p<0.003$ all groups except

lowest dose of atropine). The change in A-a gradient from baseline was 0.7, 21.4, 29.7, 30.2 and 30.3 at 0.001, 0.01, 0.1, 5 and 20 mg/kg respectively. Mean arterial pressure and pulse rate showed no changes with the lower doses of atropine but mean arterial pressure decreased significantly with the highest two doses. In conclusion, atropine decreases pulmonary gas exchange in this rat model, using doses that are comparable to the human therapeutic range.

4.2 Introduction

OP compounds have been used commercially for over 50 years yet there has been no significant advancement in the treatment of OP toxicity since the 1960's. The primary therapy for acute OP poisoning is atropine, an anti-cholinergic agent with central and peripheral actions. Atropine has a long clinical history but research into the pulmonary effects of atropine is incomplete. Atropine is rarely considered to have significant effects in the lung other then effects on pulmonary glandular tissue [162] and airway smooth muscle [43, 114, 224].

Acute OP toxicity results in profound changes in pulmonary physiology and severe poisonings clinically present with a difficulty maintaining adequate oxygenation and ventilation[7, 28]. Standard of care for OP toxicity includes treatment with atropine, sometimes in massive doses. Severe OP poisoning commonly results in the need for mechanical ventilation in addition to anti-cholinergic therapy. Hypoxia in mechanically ventilated, OP-poisoned patients is

multi-factorial involving bronchoconstriction, pulmonary secretions and/or pulmonary edema but the exact physiologic mechanism of the hypoxia is unknown.

Effective gas exchange in the lung is accomplished through matching ventilation and perfusion but the regulatory mechanisms that match ventilation and perfusion are not well understood. Cholinergic nerves that innervate pulmonary smooth muscle, glands and vasculature are active in regulating pulmonary gas exchange. Atropine has known effects on both the airways and pulmonary vasculature and it is unclear if these effects disrupt an existing regulatory process required for efficient exchange of gas from the airways to the vasculature. A single study on the pulmonary effects of atropine in humans found an impairment of gas exchange[35] but this effect was not completely characterized. Previous studies have shown that atropine dilates pulmonary arteries[225] and bronchial airways[224] but less attention has been paid to the effect on gas exchange. Dilatation of pulmonary arteries provides more blood to a region of the lung, resulting in a vascular shunt and a ventilation-perfusion mismatch if there is no matched increase in airflow. We hypothesize that intravenous atropine results in a ventilation-perfusion mismatch in a dose dependant manner.

4.3 Materials and Methods

The University of Massachusetts institutional animal use and care committee approved all procedures and protocols used in these experiments. The animal model used in this series of experiments was an adaptation of the one without mechanical ventilation described in chapter 2. However, in these experiments the amount of inspired oxygen (FiO2) was titrated prior to initiating the experiment to a partial arterial pressure (PaO2) of 110-120 mmHg. Eight adult male Wistar rats (300 gms) were anesthetized using isoflurane (Abbott Labs, North Chicago, IL) prior to tracheostomy and placement of arterial catheters. The animals spontaneously breathed a constant mixture of oxygen and anesthetic throughout the course of the experiment. Physiologic recordings were the same as those described in chapter 2 using an identical data acquisition system.

Baseline respiratory and cardiovascular parameters were recorded for at least 20 minutes prior to each animal receiving escalating doses of atropine at 0.001, 0.01, 0.1, 5 and 20 mg/kg intravenously in a volume of 0.2 ml of normal saline. Injections of 0.2 ml of normal saline (vehicle only) were performed between the highest two doses of atropine. An additional group of animals (n=3) received escalating doses of glycopyrrolate (peripheral anti-muscarinic) at 0.006, 0.06 and 0.6 mg/kg intravenously in a volume of 0.25m of normal saline. Sequential arterial blood gas analyses (Rapidlab 248, Bayer Healthcare East Walpole MA) were performed every 2 minutes (5 times) following the injection of each atropine or glycopyrollate dose. Volume of blood withdrawn for each blood gas analysis

was between 0.1 and 0.25 ml. The animal's respiratory and cardiovascular recordings were allowed to return to baseline values prior the next dose of atropine.

Statistical analysis of data was performed using a student's t-test or ANOVA where appropriate. Data is presented as mean $\pm$ standard deviation unless otherwise indicated. P values less then 0.05 are considered significant and p values less then 0.1 are indicated by p=ns.

4.4 Results

Escalating doses of atropine produced pulmonary effects in a dose-dependent manner. Minute ventilation (MV) increased at all doses except for the smallest (no effect) and largest (decreased MV) doses of atropine ($p<0.001$). This increase in MV was primarily related to an increase in the volume of inspired gas and not the respiratory rate (figure 4.1a-c). There was no statistical change in respiratory effort at any of the doses of atropine as measured by changes in esophageal pressure (figure 4.2, p=ns). Pulmonary gas exchange decreased as atropine dose increased with A-a gradient widening at all atropine doses greater then 0.001 mg/kg (figure 4.3, $p<0.0001$)). Oxygen saturation decreased over this same dose range (figure 4.4, $p<0.0005$)). Similar effects were seen after injection of glycopyrrolate with a peak A-a gradient of 21, 22, and 47 for

escalating doses of the drug. Injection of vehicle alone had no effect on oxygen saturation or arterial blood gas analysis.

The pulmonary effects of atropine peaked early after the dose was administered and diminished quickly. In all groups except the highest dose of atropine the oxygen saturation fell immediately after the atropine was administered but began improving within six minutes of atropine injection. (figure 4.5, $p<0.0001$ all groups) In the dose range that affects cardiac parameters in humans, the oxygen saturation reached baseline levels within 10 minutes of atropine injection. (figure 4.5b)

Some of the cardiovascular effects of atropine also showed a dose response. Blood pressure declined with escalating doses of atropine (figure 4.6, $p<0.0001$)) but pulse rate remained unchanged in all groups. These effects have been previously described in rats[226]. Not all animals survived the highest dose of atropine with 3 of the 8 animals showing cessation of cardiac activity soon after injection of the atropine.

4.5 Discussion

Atropine induced a dose dependant pulmonary dysfunction in spontaneously breathing, anesthetized rats with decreased gas exchange as evidenced by systemic hypoxia despite an increase in minute ventilation. This effect of atropine

is most likely secondary to anti-muscarinic effects as glycopyrrolate demonstrated a similar effect. The decrease in oxygen saturation is counterintuitive as atropine causes an increase in pulmonary ventilation and FiO2 does not change. There are two possible mechanisms to account for our findings; either there was a decrease in the ability of oxygen to diffuse across the alveolar-arteriole interface or pulmonary vascular changes resulted in vascular shunting. It is more likely that the findings are due to vascular dilatation as atropine is a vasodilator of the peripheral vasculature[227] and pulmonary arterials[225].

Atropine has well documented effects on bronchial smooth muscle tone with bronchodilation[224] lasting for hours following intravenous administration (half life 1-2 hours)[228]. To reconcile this fact with our finding that atropine decreases oxygenation requires either 1) segmental effects allowing decreased ventilation to areas of the lung with increased perfusion or 2) temporal effects with increased perfusion occurring prior to increased ventilation. Segmental pulmonary airway constriction (or lack of dilatation) is possible but unlikely as atropine induces an aggregate increase in airflow. The time course of the bronchodilatory effects of atropine supports a window of time when increased pulmonary blood flow is not matched by increased pulmonary airflow. This cascade of events would also explain the transient nature of the hypoxic effects of atropine if early vascular dilatation is followed closely by pulmonary airway dilatation.

The autonomic control of pulmonary vasculature has not been well characterized and it is not clear if the effects of atropine we describe are mediated centrally or peripherally. Studies in the 1980's demonstrated that vagal stimulation resulted in vasodilatation of bronchial arteries [74]. Studies in an isolated lung preparation have demonstrated peripherally mediated effects with vasodilatation from the direct application of atropine[225]. In both cases pulmonary artery dilatation occurred within 10 seconds of the stimulus (application of atropine or stimulation of the distal vagal trunk), consistent with the time course of the changes seen in our experiments[223]. To make things more complicated, it may be that autonomic control is not the sole physiologic mechanism for changing pulmonary vascular tone as increases in tracheobronchial blood flow during cold air hyperventilation are unaffected by either vagotomy or beta-blockade[229].

Results similar to ours have been described in one previously published human study. Healthy subjects exposed to a single dose of atropine (0.02 mg/kg) under mildly hypoxic conditions showed a small decrease in oxygenation despite no change in ventilation[35]. This study advances those findings by demonstrating that the hypoxia follows a dose-response relationship and is seen in normoxic conditions. We also were able to demonstrate that there was no clinical effect in airway resistance as respiratory effort and pleural pressure remained unchanged during the experiment.

It is unlikely that the cardiovascular effects of atropine contributed significantly to changes in pulmonary oxygen exchange. Blood pressure decreased between 10-75% with increasing levels of intravenous atropine however multiple lines of evidence support our contention that the hypotension was not the reason for the hypoxia. First we noted increasing hypotension over the first two minutes for the three highest doses of atropine but there was no corresponding decrease in oxygen saturation over the same time period. Second, in the two highest doses of atropine oxygen saturation failed to improve over time despite improving mean arterial pressure. Finally, a study looking at physiologic changes during hypotension and blood loss in rats showed the reverse of our findings, an increase in arterial oxygenation and a decrease in the alveolar-arteriole gradient[230].

Conclusion

The administration of intravenous atropine produces pulmonary effects in a dose dependent fashion with increasing doses of atropine resulting in greater levels of hypoxia due to increasing V-Q mismatch. We hypothesize that these effects are related to the effects of atropine on the pulmonary vasculature.

Figure 4.1 A,B,C - Respiratory rate, volume of inspired gas and minute ventilation following intravenous atropine

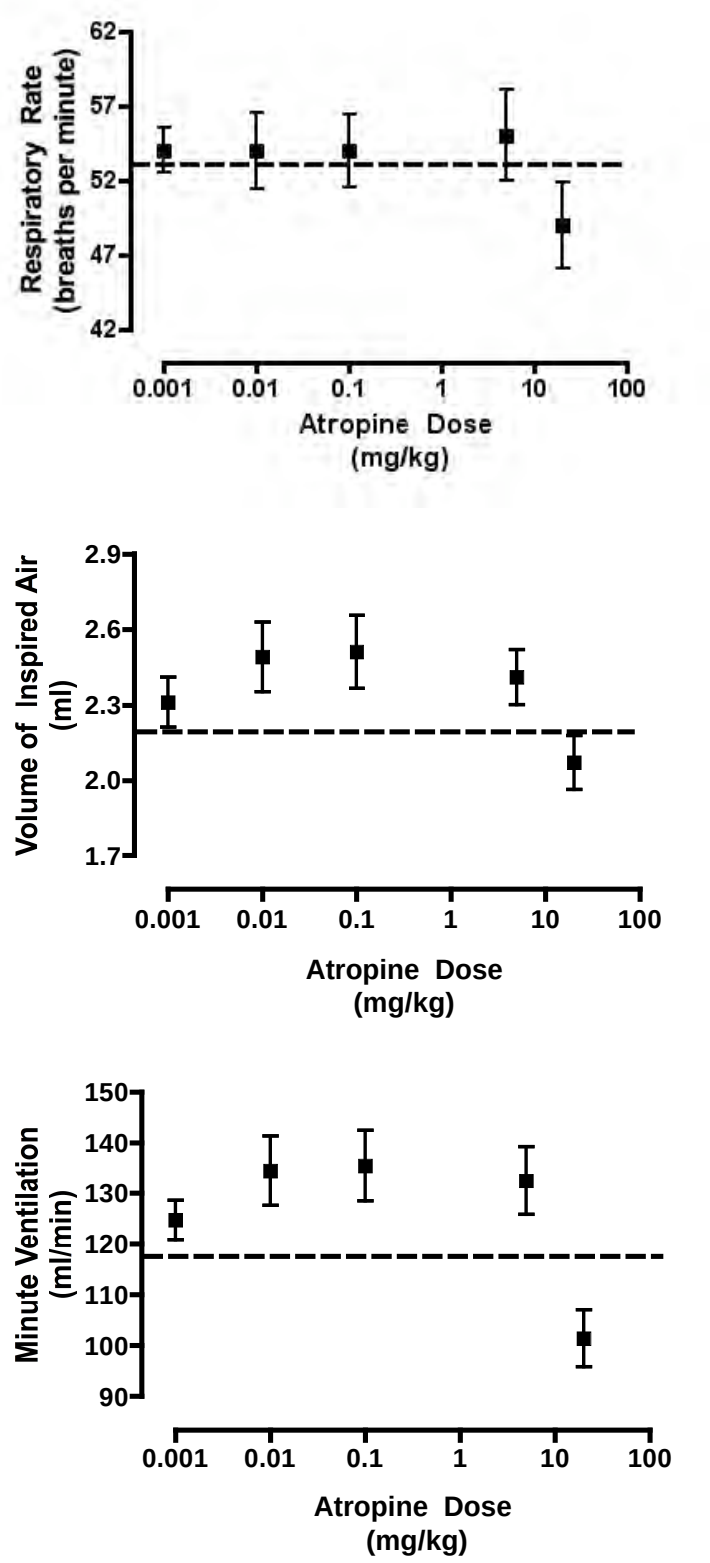

Grouped data sets (n=8) show respiratory rate, volume of inspired gas and minute ventilation from animals exposed to intravenous atropine in doses ranging from 0.001 to 20 mg/kg. There was no difference in respiratory rates between groups (p=ns). Volume of inspired gas was increased at 0.01 and 0.1 mg/kg and decreased at the highest dose ($p<0.01$). Minute ventilation increased at 0.01 (134.5 $\pm$ 19.5 cc/min), 0.1 (135.5 $\pm$ 19.7 cc/min) and 5 mg/kg (132.6 $\pm$ 19.1 cc/min) over baseline (120.4 $\pm$ 9.25 cc/min) but decreased at the highest dose (101.43 $\pm$ 15.8, $p<0.001$). Results are shown as mean +/- standard deviation.

Figure 4.2 – Respiratory effort following intravenous atropine

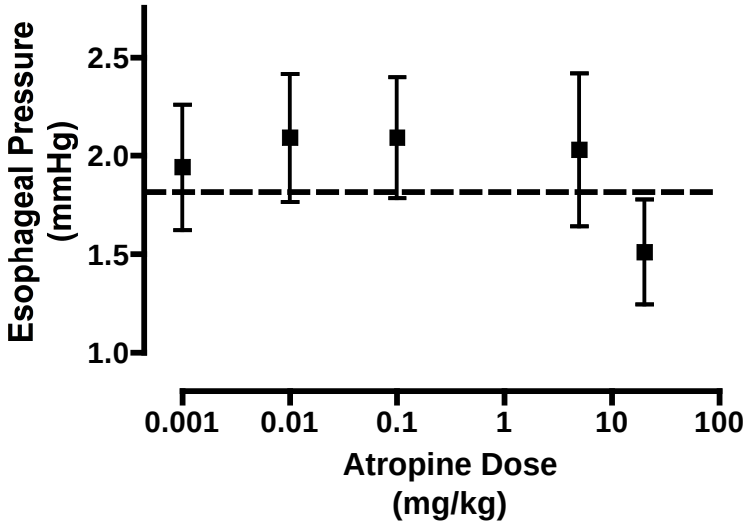

Grouped data sets (n=8) show esophageal pressure from animals exposed to intravenous atropine. Data consists of esophageal pressure over a dose range of atropine from 0.001 to 20 mg/kg. There was no change in respiratory effort across groups (p=ns). None of the esophageal pressure values (range 1.83-2.09 mmHg) differed statistically from baseline (1.83 $\pm$ 0.93 mmHg) except for the highest dose (1.5 $\pm$ 0.75 mmHg). Results are shown as mean +/- standard deviation.

Figure 4.3 – Alveolar-arteriole gradient following intravenous atropine

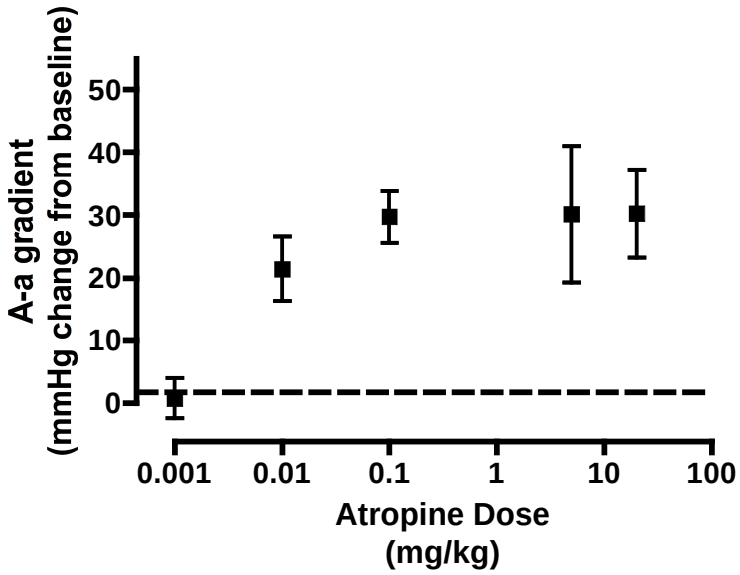

Grouped data sets show calculated A-a gradients from animals exposed to intravenous atropine. Data consists of arterial blood gas measurements performed immediately following intravenous atropine in doses ranging from 0.001 to 20 mg/kg. A-a gradients increased for all doses greater then 0.001 mg/kg ($p<0.0001$). A-a gradients were essentially unchanged at 0.1 mg/kg and greater (29.7, 30.1, 30.2 mmHg respectively). Results are shown as mean +/- standard deviation.

Figure 4.4 – Oxygen saturation two minutes following intravenous atropine

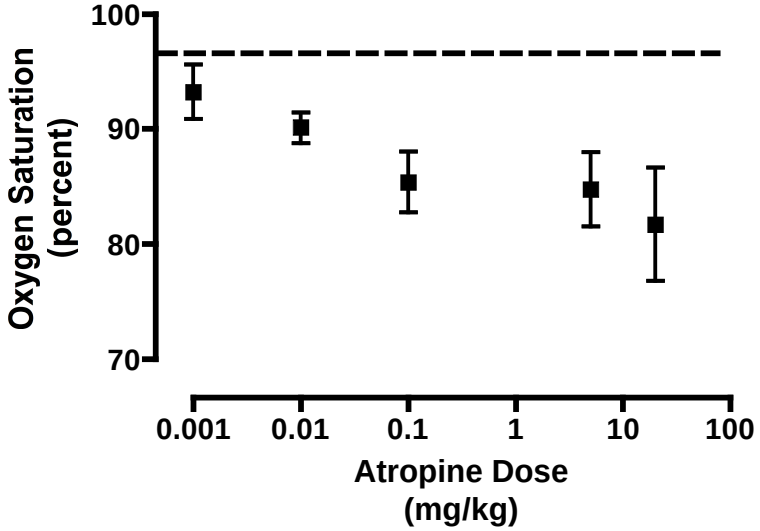

Grouped data sets (n=8) show oxygen saturation from animals exposed to intravenous atropine in doses ranging from 0.001 to 20 mg/kg. Oxygen saturation measurements performed 1 minute following intravenous atropine. Oxygen saturation decreased in all study groups except for the smallest dose ($p<0.0005$). As dose increased the oxygen saturation decreased from 96.7% ($\pm$1.4) to 81.7% ($\pm$13.9). Results are shown as mean +/- standard deviation.

Fig 4.5A – Oxygen saturation following intravenous atropine

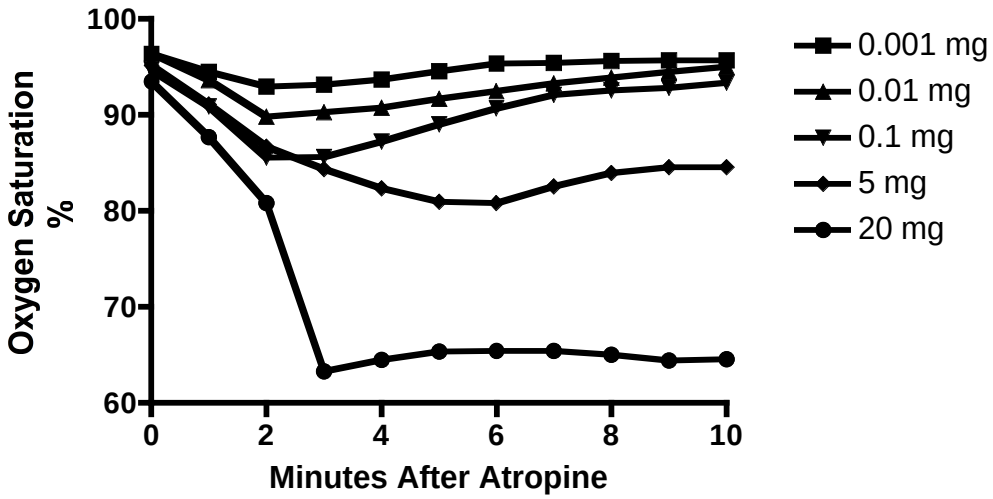

Grouped data sets show oxygen saturation from animals exposed to intravenous atropine in doses ranging from 0.001 to 20 mg/kg. Figure 4.5 includes all atropine doses and Figure 4.6 includes only atropine doses 0.001, 0.01 and 0.1 mg/kg. Increasing levels of atropine resulted in decreasing oxygen saturation ($p<0.0001$). Oxygen saturation decreased immediately after intravenous atropine but recovered within 10 minutes for all groups except the two largest doses. Data are shown from point of atropine injection (time 0). Results are shown as percent of baseline oxygen saturation.

Fig 4.5B – Oxygen saturation following clinically relevant doses of intravenous atropine that affect human cardiac function

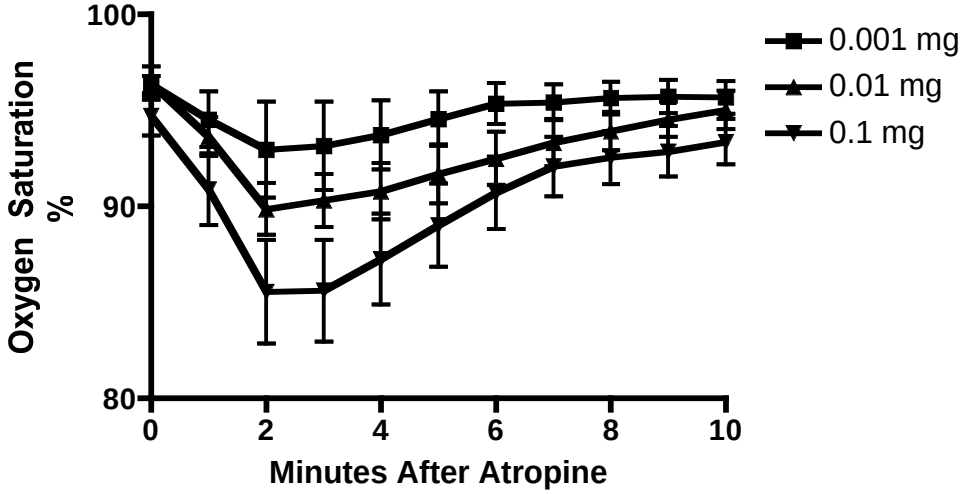

Grouped data sets show oxygen saturation from animals exposed to intravenous atropine in doses ranging from 0.001 to 0.1 mg/kg. Figure 4.5 includes all atropine doses and Figure 4.6 includes only atropine doses 0.001, 0.01 and 0.1 mg/kg. Increasing levels of atropine resulted in decreasing oxygen saturation ($p<0.0001$). Oxygen saturation decreased immediately after intravenous atropine but recovered within 10 minutes for all groups except the two largest doses. Maximal effect was seen at 2 min for all doses (92.9 ($\pm$6.5), 89.9 ($\pm$3.9), and 85.6 ($\pm$7.5) respectively). Data are shown from point of atropine injection (time 0). Results are shown as percent of baseline oxygen saturation +/- standard deviation.

Fig 4.6 A,B– Blood pressure following intravenous atropine

A.

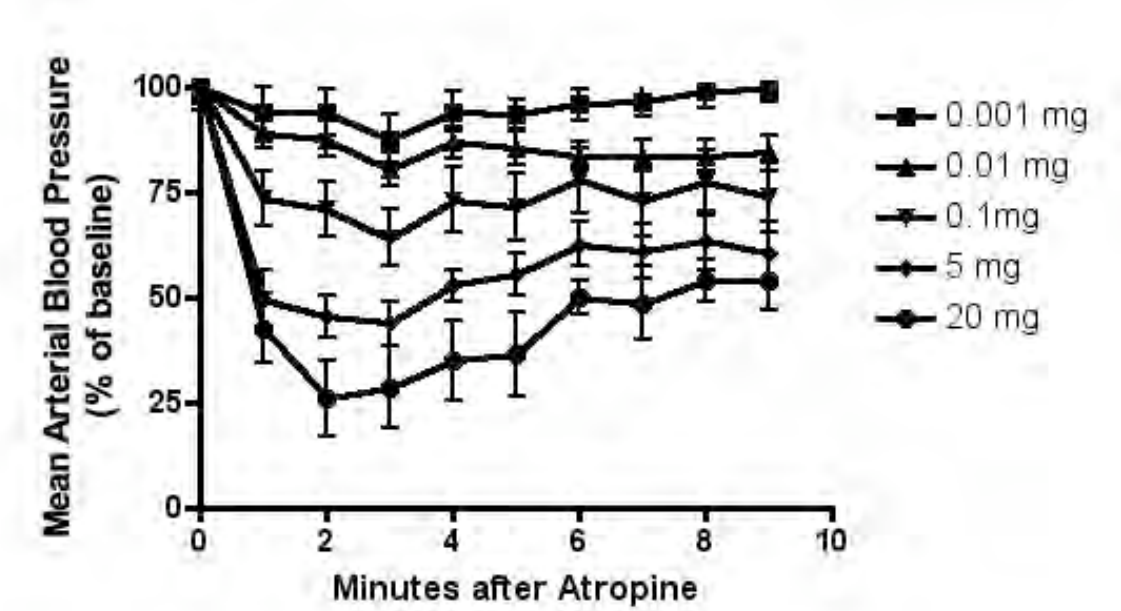

B.

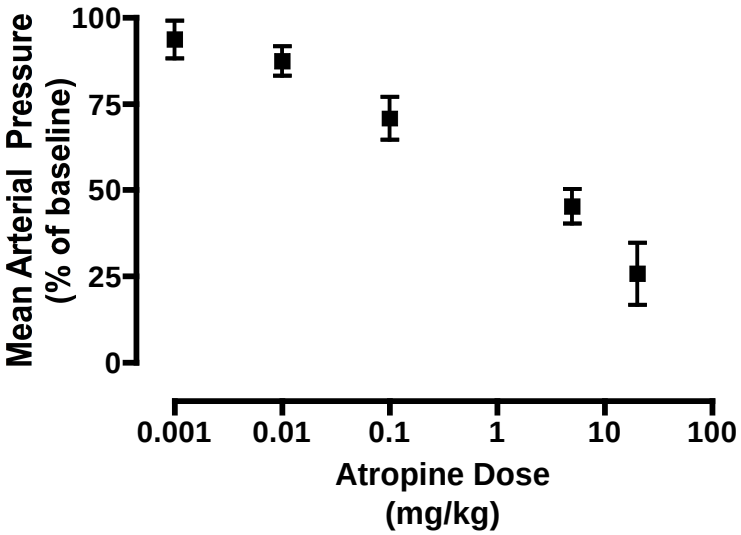

Grouped data sets (n=8) show mean arterial pressure from animals exposed to intravenous atropine in doses ranging from 0.001 to 20 mg/kg. Increasing levels of atropine resulted in decreasing mean arterial pressure ($p<0.0001$) that partially

recovered over the next 10 minutes. Data are shown from point of atropine injection (time 0). Maximal effect was seen at 2 minutes for all atropine doses (93.7, 87.5, 70.8, 45.2, 25.8 respectively). Figure 4.6b shows mean arterial pressure at 2 minutes. Results are shown as percent of baseline mean arterial pressure +/- standard deviation for both graphs.

Chapter V – Organophosphate-induced autoresuscitative breathing: The emergence of corrupted respiratory oscillator.

5.1 Abstract

It was noted anecdotally in earlier experiments that OP-induced apnea was not absolute. Animals regain respiratory activity over time if they survive. Here we show in a rat model of OP that breathing can resume spontaneously following prolonged central apnea. This autoresuscitative respiratory activity is suppressed by hypoxia, in contrast to the promoting effect of hypoxia on gasping. Analysis of phrenic nerve discharge activity reveals that peak inspiratory and post-inspiratory discharge activities are significantly reduced compared to eupneic breaths. In this animal model of OP, a form of autoresuscitative breathing emerges following prolonged central apnea that is physiologically distinct from both eupnea and gasping respiration.

5.2 Introduction

Acute OP causes progressive respiratory failure but we descried in chapter 2 that death could be prevented by artificial mechanical ventilation. We noticed that in some animals, respiratory rhythm spontaneously resumed following prolonged central apnea, suggesting a form of autoresuscitative breathing.

The return of autoresuscitative breathing in our animal model may represent a resumption of normal eupneic respiration or the emergence of a gasping respiration. Normal eupneic activity could return once the acetylcholinesterase inhibition by dichlorvos wanes. Alternatively, as hypoxia progresses to anoxia, breathing activity can resume in the form of gasping induced by anoxic excitation of brainstem circuits [231, 232]. This inspiratory excitatory effect of severe oxygen deprivation is a component of a neural 'autoresuscitative' response that has been shown to improve tissue oxygenation during cardiac arrest [233, 234], and may be an important survival mechanism in infants that are prone to life threatening cardiopulmonary disturbances during sleep[231].

Eupnea and gasping can be differentiated using the different characteristics of each respiratory activity. Eupnea is supported by oxygenation and gasping is supported by anoxia. In addition, eupneic breathing and gasping have different neural output patterns [235]. Phrenic inspiratory activity associated with gasping has a greater rate of rise, a higher peak level, and a longer inter-breath interval compared to the phrenic activity associated with eupneic breathing. The central neural circuits that generate these two distinct respiratory patterns may be anatomically distinct [236, 237], or may consist of a single or two overlapping circuits that are capable of switching functional states depending on the level of interstitial oxygen [238-240].

In the present study, we analyze OP associated autoresuscitative breathing by characterizing its response to oxygen levels and by comparing its phrenic nerve activity to that of eupneic breaths. We find that autoresuscitative respiratory activity is suppressed by hypoxia and is associated with a loss of the normal post-inspiratory discharge activity that is characteristic of eupneic breaths. Our findings suggest that in this animal model of OP, a form of autoresuscitative breathing emerges following prolonged central apnea that is physiologically distinct from both eupnea and gasping respiration.

5.3 MATERIALS AND METHODS

The University of Massachusetts Medical School Institutional Animal Care and Utilization Committee approved all experimental procedures and protocols.

General Preparation

The animal model and basic experimental methodology used in this study was described in chapter 2. Figure 5.1 is an example of some of the recordings. Inspiratory effort of the animal was monitored during mechanical ventilation through an analysis of the esophageal pressure. Inspiratory activity was visualized during positive pressure ventilation as negative deflections of the tracing (Figure 5.1). To confirm oxygenation levels, arterial blood gas analyses were performed on select animals during times of steady state (baseline and during mechanical ventilation).

Phrenic Nerve Isolation and Recording

The right phrenic nerve was isolated at the mid-cervical level using a dorsal approach. An incision was made dorso-lateral to the spine in the cervical region and the scapula was retracted laterally. The upper extremity on that side was retracted inferior-laterally and the muscles were bluntly dissected until the cervical nerve rootlets were identified exiting the paraspinal muscles. The phrenic nerve was identified branching from the superior cervical rootlets, diving ventral to the cervical rootlets and traveling parallel to the spine caudally. Recordings were performed on an uncut phrenic nerve draped over a bipolar electrode and covered with petroleum jelly. The signal was amplified (Molecular Devices, Sunnyvale, CA), filtered (lowpass and highpass cutoff 2000 Hz and 400 Hz respectively) and conditioned using a noise reduction device (HumBug noise eliminator, Quest Scientific, Vancouver Canada). Phrenic nerve activity was whole wave rectified and step-wise integrated over 50 ms intervals. The onset of the inspiratory phase of activity was defined when the integrated signal exceeded 3 standard deviations above the mean of the signal during the mid- to late-expiratory phase. In order to quantify the statistical properties of phrenic nerve activity for a full respiratory cycle during baseline and experimental conditions, we averaged integrated phrenic nerve activity with respect to time of inspiratory onset, i.e., event-triggered averaging.

Experimental Groups and Protocols

Following all surgical procedures, a baseline period of at least 20 minutes was recorded before the animals received Dichlorvos (Sigma-Aldrich, St Louis MO) 100mg/kg subcutaneously. Recordings were continued until blood pressure and pulse rate declined to the study endpoint (death or 1 hour, whichever came first). Animals were grouped into two cohorts that differed in terms of oxygenation. Animals in Group I (transient hypoxia post apnea) received oxygen supplementation that was titrated to achieve a P_aO_2 of ~110 mmHg during the baseline (pre-poisoning) period; once this level was achieved the fraction of inspired oxygen (F_iO_2) was kept at the same level throughout the experiment. Animals in Group II (no hypoxia) received 100% inspired oxygen throughout the experiment. Both groups received mechanical ventilation initiated at the point of apnea that continued until the study endpoint (death or 1 hour, whichever came first). Arterial blood was sampled for determination of P_aO_2 during the baseline period. Apnea was defined as no respiratory effort or airflow for 20 seconds.

Data Recording and Analyses

Data were recorded as described previously. Between-group comparisons were performed using an unpaired Student's *t*-test, repeated measure ANOVA or Fisher's Exact test where appropriate [176].

5.4 RESULTS

Autoresuscitative Breathing Following Organophosphate Poisoning

Animals in both groups demonstrated a central apnea with declining airflow and respiratory effort prior to the point of apnea (see table 5.1 for baseline characteristics). Apnea occurred an average of 4.53 min (±1.95) after poisoning, with no differences between groups (table 5.1, p=0.089). The majority of animals with mechanical ventilation at the point of apnea survived to the end of the study. Some animals did not survive (5 of 17) despite mechanical ventilation with no differences between groups (2 of 7 in Group I vs 3 of 10 in Group II, p=ns). Animals that did not survive despite mechanical ventilation had a large amount of secretions filling the tracheal tube and an inability to ventilate.

The different F_iO_2 between groups resulted in a difference in tissue oxygenation at baseline, at the point of apnea and post-poisoning (on ventilator), but a clinical difference in oxygen saturation between groups only occurred at the point of apnea (table 5.2). Animals receiving a normoxic gas mixture (Group I) demonstrated no hypoxia for the first five minutes but dropped their oxygen saturation to 24% by 10 minutes post poisoning before rebounding to close to 100% (fig 5.2a). Animals inspiring 100% oxygen (Group II) showed virtually no change in oxygen saturation despite the decreasing respiratory rate (fig 5.2b). Arterial blood gas analysis during steady state periods (baseline, during mechanical ventilation) confirmed the oxygen saturation data. The decreasing respiratory rate was unrelated to level of tissue oxygenation as respiratory rate decreased in both groups despite differing oxygenation levels (Figure 5.3).

There was a significant difference between the two groups in autoresuscitative breathing (Figure 5.4). No animals that survived to mechanical ventilation in Group I exhibited autoresuscitative breathing (0 of 7) whereas 4 out of 5 animals in Group II exhibited resumption of sustained (greater then 3 min) respiratory activity. The autoresuscitative breathing in these animals was characterized by an irregular, slow respiratory rate (8.6 bpm (4.2) lasting an average of 25.4 min (21.7). Respiratory effort during autoresuscitative breathing decreased 52% (40.6) from baseline. The difference in autoresuscitative breathing was not related to differences in MAP as the drop in blood pressure 30 minutes post dichlorvos did not differ significantly between groups (50% vs 56%, p= ns).

Characterization of Phrenic Nerve Activity

In order to characterize the neural inspiratory activities during autoresuscitative breathing following OP poisoning, we analyzed phrenic nerve activity in one of the animals receiving 100% oxygen. Figure 5.5 shows the event-triggered average of integrated phrenic nerve activity for 100 consecutive breaths recorded during the baseline period and for 100 consecutive autoresuscitative breaths that resumed 19.7 min after onset of apnea. Compared to the baseline breaths peak phrenic amplitude of autoresuscitative breaths decreased by 60%. Normalizing the peak amplitude allows a comparison of the morphology of integrated phrenic activity. There was no difference in the normalized phrenic activity during the inspiratory period. However, compared to the baseline phrenic activity, the

autoresuscitative breaths had reduced phrenic activity during the post-inspiratory period (repeated measure ANOVA , $p<0.004$).

5.5 DISCUSSION

Animals exposed to subcutaneous dichlorvos (100mg/kg) exhibit a rapidly progressive decline in respiratory activity culminating in apnea within minutes of exposure. OP-induced central apnea is not absolute as autoresuscitative breathing post apnea was seen in some animals oxygenated with mechanical ventilation, but only in animals that were not hypoxic at the point of apnea. Phrenic activity during the autoresuscitative breathing was distinct from both eupnea and gasping. Unlike eupneic respiration, phrenic peak inspiratory activity had a significantly longer inter-breath interval. Unlike gasping respiration, the peak inspiratory activity was significantly decreased from baseline. The phrenic neurogram had characteristics of eupneic breathing but without the normal post-inspiratory inspiratory activity and did not demonstrate the characteristics of gasping respiration.

The most important difference between groups is hypoxia at the point of apnea in Group I compared to the lack of any hypoxia in Group II. The episode of severe hypoxia in Group I resulted in post-hypoxic respiratory depression demonstrated by a loss of autoresuscitative breathing. It is well known that profound hypoxia causes respiratory depression in animals without intact carotid body afferent signaling[241]. Animals in this study had an intact glossopharyngeal nerve but

the OP poisoning may interfere with afferent signaling from the carotid body. Existing pontine neural mechanisms involved in post-hypoxic respiratory depression may be involved[242] but further study is needed. Severe hypoxia at the point of apnea in Group I may have also contributed to the acute loss of respiratory activity but the respiratory depressant effects of severe hypoxia are eliminated with increased oxygenation. Severe hypoxia cycled with oxygenation is a laboratory technique to reversibly suppress eupnea and elicit gasping[243]. The increased F_iO_2 (100% O_2) in Group II produced greater oxygen reserves that prevented hypoxia during apnea. This lack of hypoxia may have protected against respiratory depression by increasing oxygen dependent metabolism of dichlorvos.

There are potential differences in dichlorvos degradation between groups related to oxygen dependent metabolism but our understanding of how oxygen levels affect dichlorvos metabolism is incomplete. Dichlorvos is metabolized via two enzymatic pathways. The major pathway involves an “A”-type esterase and a minor pathway using glutathione-s-transferase[244]. Dichlorvos is rapidly degraded in tissue with a half-life of 19.9 minutes in rat whole blood[245] and none of the metabolites of dichlorvos inhibit acetylcholinesterase[246]. It is unknown if hypoxic conditions affect the rate of degradation of dichlorvos in the rat but this may have also contributed to the loss of autoresuscitative breathing in hypoxic animals.

Despite similar oxygen saturation, animals in Group II demonstrated significantly higher PaO_2 post-apnea (table 5.2) when autoresuscitative breathing occurs. It is possible that hyperoxia (Group II) during the autoresuscitative period stimulated autoresuscitative breathing over normoxia (Group I) but this seems less likely. Prolonged hyperoxia induces respiratory depression characterized by a larger drop in respiratory rate and a smaller increase in tidal volumes [247, 248]. Indirect evidence against a hyperoxia requirement for autoresuscitative breathing is that hyperoxia has no known beneficial CNS effects over normoxia[249-251].

Respiratory output during eupnea and gasping has been well described in the medical literature and OP-induced autoresuscitative breathing more closely resembles eupneic breathing. The response of OP-induced autoresuscitative breathing was the reverse of what is described for gasping respiration. Autoresuscitative breathing occurred during a period of hyperoxia but gasping respiratory activity is supported by hypoxia[252]. Additionally, respiratory effort during autoresuscitative breathing, as measured by both esophageal pressure and phrenic activity, was less then half of baseline effort. This is contrary to what occurs during gasping when respiratory effort is significantly increased. Finally, the phrenic discharge waveform during autoresuscitative breathing does not match classical gasping, i.e. rising rapidly during inspiration with a definite pause in the expiratory position and uniform in depth[236].

Whether phrenic discharge activity during OP-induced autoresuscitative breathing represents a corruption of the CRO is debatable but OP-induced autoresuscitative breathing lacks the normal post-inspiratory, inspiratory activity (PIIA) of eupneic respiration. PIIA represents inhibition of inspiratory neurons during early exhalation[253] and is characterized by a smaller decrescendo burst of activity during early exhalation. It could be argued that the loss of the PIIA is related to decreased chemical drive from excessive mechanical ventilation (i.e. hyperoxic hypocapnia). Hyperventilation decreases central respiratory activity[254, 255] and could theoretically decrease PIIA as well. This is an unlikely explanation, as previous experiments have demonstrated increased PIIA during hyperoxic hypocapnia[256], the opposite of what was seen in this study. A possible mechanism for the loss of PIIA is afferent feedback to the CRO secondary to OP exposure to the brainstem or lung. Mechanical stimulation of the airway with vagal feedback to the CRO results in a decrease in PIIA[256]. We speculate that OP exposure to the lung may provide a similar feedback.

In summary, apnea following acute OP poisoning is not absolute as respiratory activity resumes following a period of time post apnea. Post-hypoxic respiratory depression occurs in animals hypoxic at the point of apnea even when oxygenation was maintained post apnea. The resumption of respiratory activity represents an emergence of a respiratory oscillator distinct from eupnea and gasping and characterized by a loss of post-inspiratory inspiratory activity.

Our study design suffered from some limitations and did not allow us to independently control the oxygen saturation during the three time periods of the study (pre-apnea, at apnea, and post apnea). Further studies are needed to independently control oxygenation at those three time points and determine the effect (if any) on autoresuscitative breathing.

Table 5.1 – Characteristics of normoxic and hyperoxic study groups

	Group I (n=10)	Group II (n=6)	
Baseline			
Respiratory Rate (bpm)	58.6 (7.9)	54.2 (4.7)	P=ns
End Tidal CO2 (mmHg)	56.6 (5.2)	51.4 (1.1)	P=0.053
Mean Arterial Pressure (mmHg)	88.8 (10.3)	106.8 (14.5)	P=0.015
Oxygen Saturation (%)	97 (1.5)	98.5 (1.&)	P=ns
Respiratory Effort (mmHg)	- 3.54 (2.2)	- 4.04 (2.5)	P=ns
FiO2 for entire experiment	normoxic	hyperoxic	

Mean (SD) values are for the last 5-minutes of the baseline period, prior to injection of dichlorvos. Respiratory effort is the peak negative inspiratory pressure. There was no statistical difference between groups for any of the baseline variables except for mean arterial pressure.

Table 5.2 – F_iO_2, time to apnea, and oxygen saturation (O_2 sat) and partial pressure of oxygen in arterial blood (PaO_2) for normoxic and hyperoxic study groups.

	Group I	Group II	
F_iO_2	Normoxic	Hyperoxic	
Time to Apnea	3:38 (0:49)	5:39 (2:23)	P=0.086
Oxygen saturation (baseline)	96.8% (1.48)	98.5% (1.73)	P=ns
Oxygen saturation (apnea)	24.1% (39.1)	98.25% (2.36)	P=0.001
Oxygen saturation (post-apnea)	95.5% (3.37)	98% (2.83)	P=ns
PaO_2 (baseline)	115.6 (7.0)	238.0 (14.1)	P=0.0001
PaO_2 (post-apnea)	123.1 (22.3)	298 (22.6)	P=0.0002

Data are presented as mean (standard deviation). Baseline data represents an average of data from 3 minutes preceding dichlorvos injection. Apnea data represents a single point of data at the time point immediately prior to initiation of mechanical ventilation. Post apnea period represents an average of 3 minutes of data starting 5 minutes after the point of apnea. PaO2 was obtained using arterial blood gas analysis for a selection of animals in each group (n=5 Group I, n=2 Group II) and is presented in mmHg.

Figure 5.1 A,B – Physiologic tracings of single animals treated with dichlorvos poisoning and receiving mechanical ventilation initiated at the point of apnea.

A.

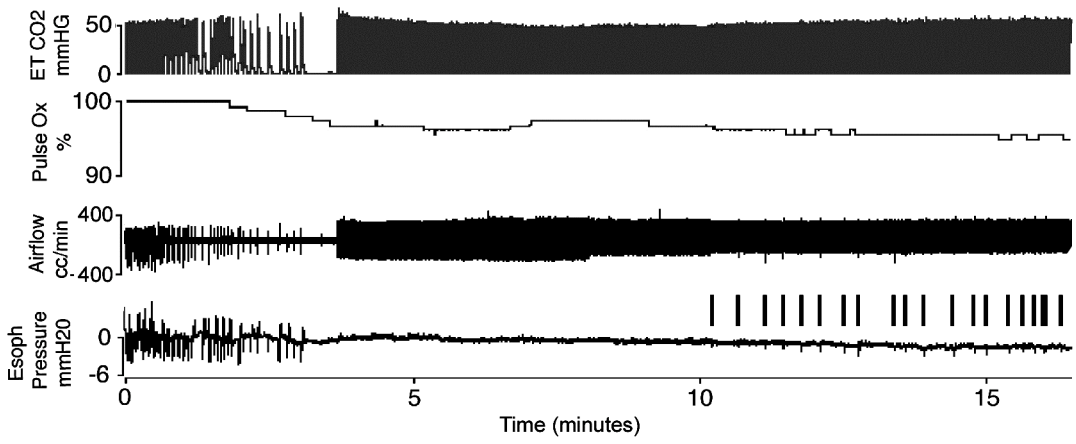

B.

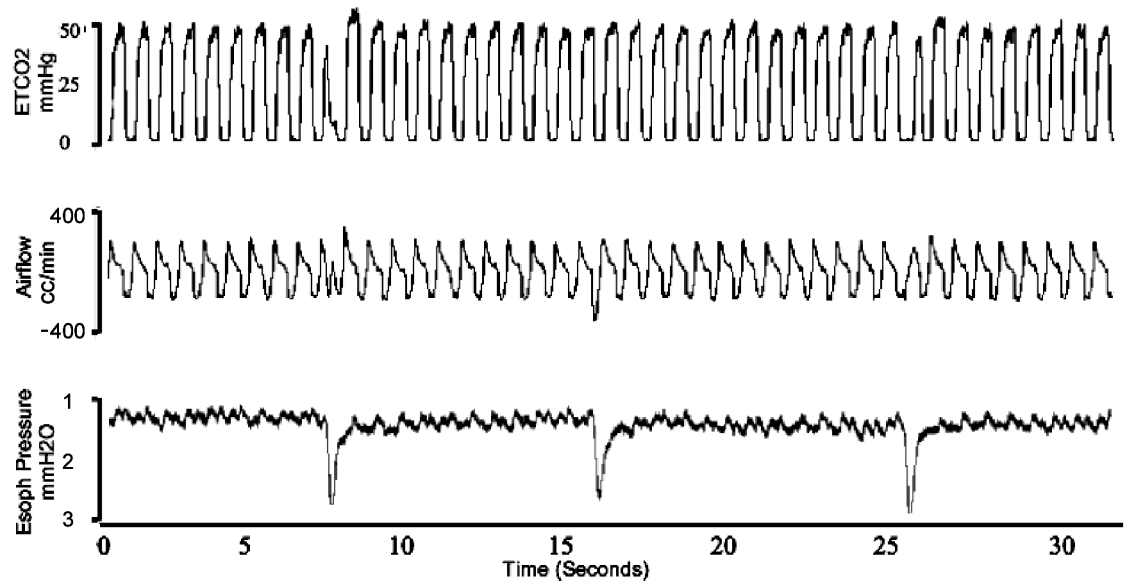

Data represent a single animal poisoned with dichlorvos at time zero (fig 5.1a) with apnea occurring around 3.5 minutes and mechanical ventilation initiated around 4 minutes. Note the negative deflections in the esophageal tracing (black bars) that represent respiratory effort despite mechanical ventilation. A magnified view of the tracings is provided in fig 5.1b.

Figure 5.2A,B – Oxygen saturation and respiratory rate following injection of dichlorvos in normoxic and hyperoxic rats with mechanical ventilation at the point of apnea.

Fig 5.2A

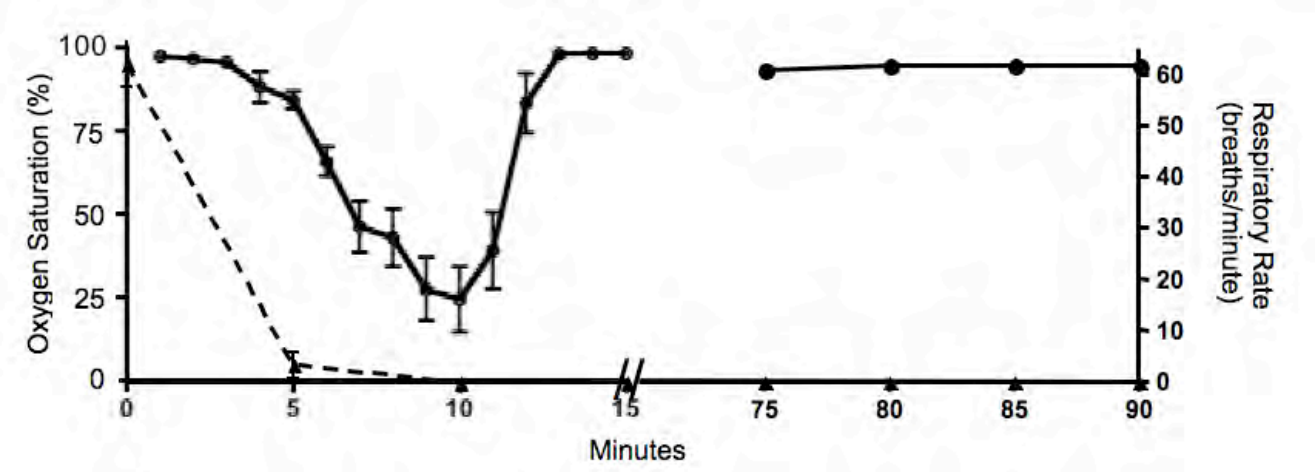

Fig 5.2B

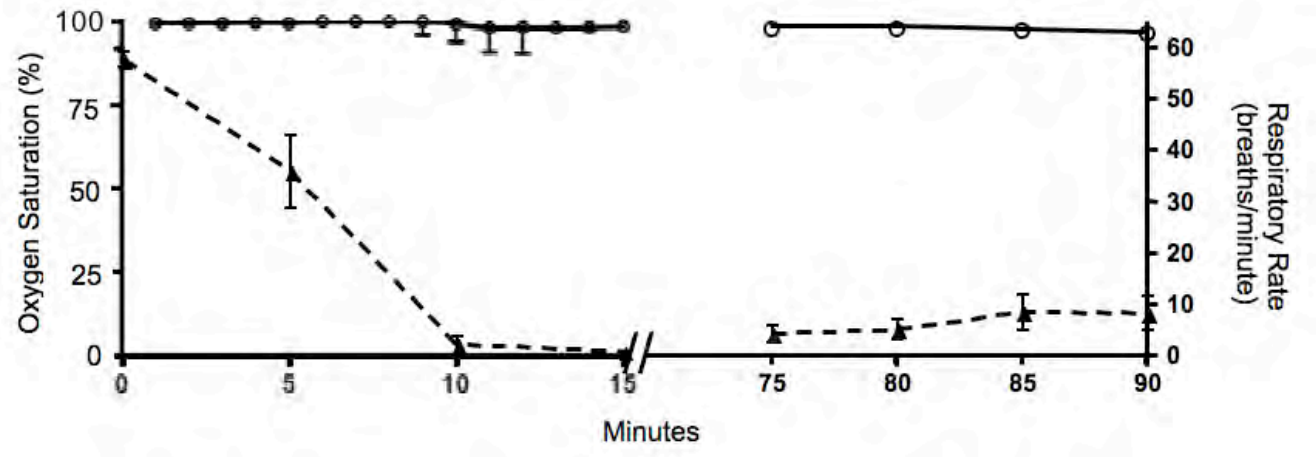

Grouped data set shows oxygen saturation and respiratory rate for spontaneously breathing animals with acute OP and oxygen titrated to a P_aO_2 of

roughly 110 mmHg (5.2a) and 100% oxygen (5.2b). Oxygen saturation reached a nadir at 10 min (24.1 ±39.2%) in Fig 5.2a compared to a nadir of 98.0 (±3.7%) at 13 minutes in Fig 5.2b. Respiratory rate is depicted with a dotted line and oxygen saturation is depicted with a solid line. Animals were placed on mechanical ventilation at the point of apnea. Dichlorvos was given at time zero. Results are shown as mean value +/- standard deviation.

Figure 5.3 – Correlation of respiratory rate and oxygen saturation.

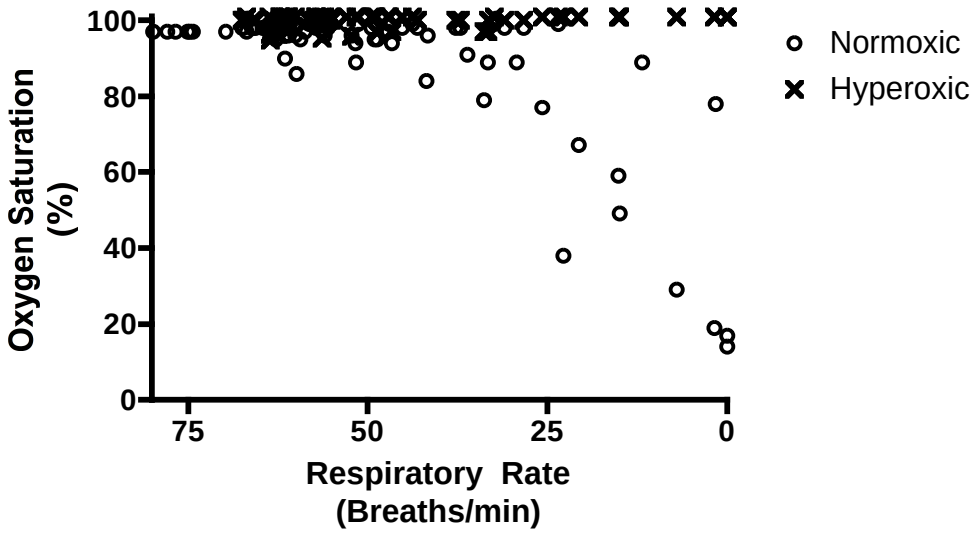

Data are plotted as a scatter plot of individual animal respiratory rate and oxygen saturation during the first 4 minutes after injection of dichlorvos. Data represent 15-second bins of data. Hyperoxic animals (crosses) demonstrate a range of respiratory rates at close to 100% oxygen saturation. Normoxic animals (circles) demonstrate a general trend of lower respiratory rates with lower oxygen saturation and a number of outliers that do not follow that pattern.

Figure 5.4 – Autoresuscitative breathing in animals with hyperoxia and normoxia.

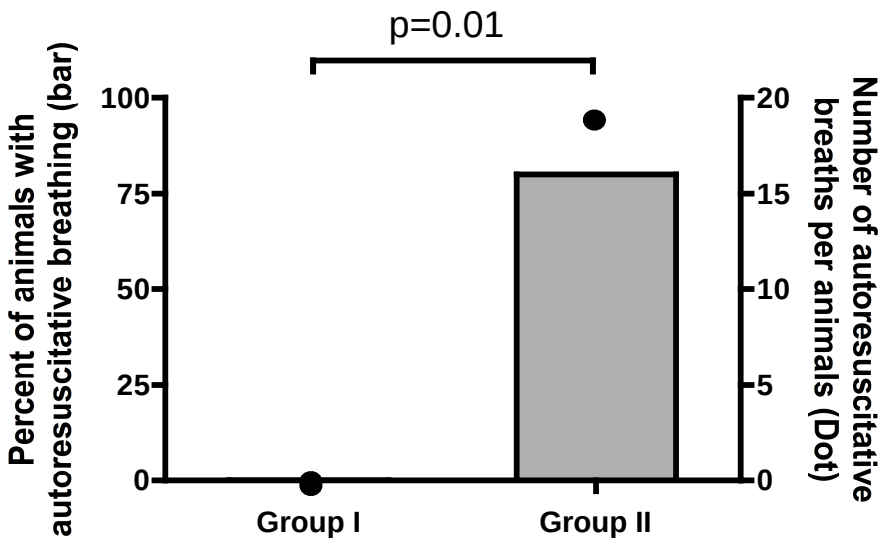

A comparison of autoresuscitative breathing between animals with 100% oxygen (Group II) and those with oxygen titrated to a PaO2 of around 110 mmHg (Group I). Animals with titrated oxygen (group I) experienced hypoxia at the point of apnea and animals with 100% oxygen did not. The percent of animals who demonstrated respiratory activity post-apnea is depicted as a bar and is referenced to the y axis on the right. The number of actual breaths post apnea (in all animals) is depicted as a dot and is referenced to the y axis on the left. The p-value corresponds to comparing the percent of animals in each group with respiratory activity post apnea.

Figure 5.5 A,B,C – Phrenic Nerve activity pre and post apnea

Fig 5.5A – Baseline phrenic activity

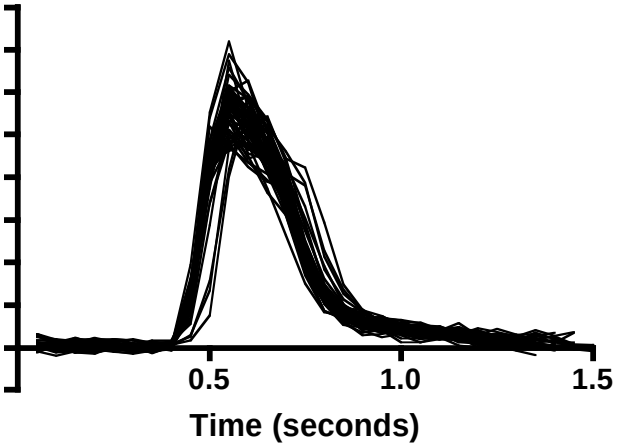

Fig 5.5B Autoresuscitative phrenic activity

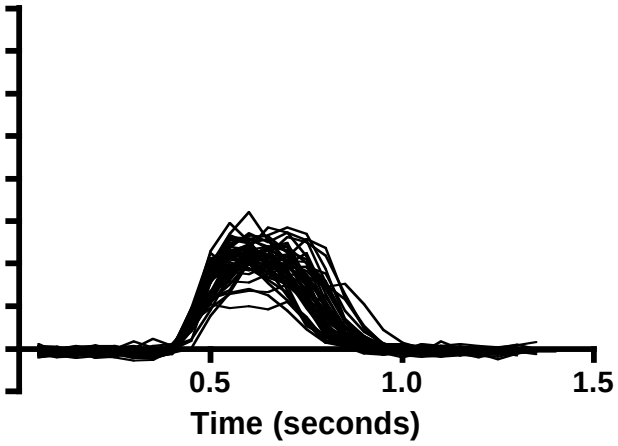

Fig 5.5C – Event triggered average of phrenic activity pre and post apnea

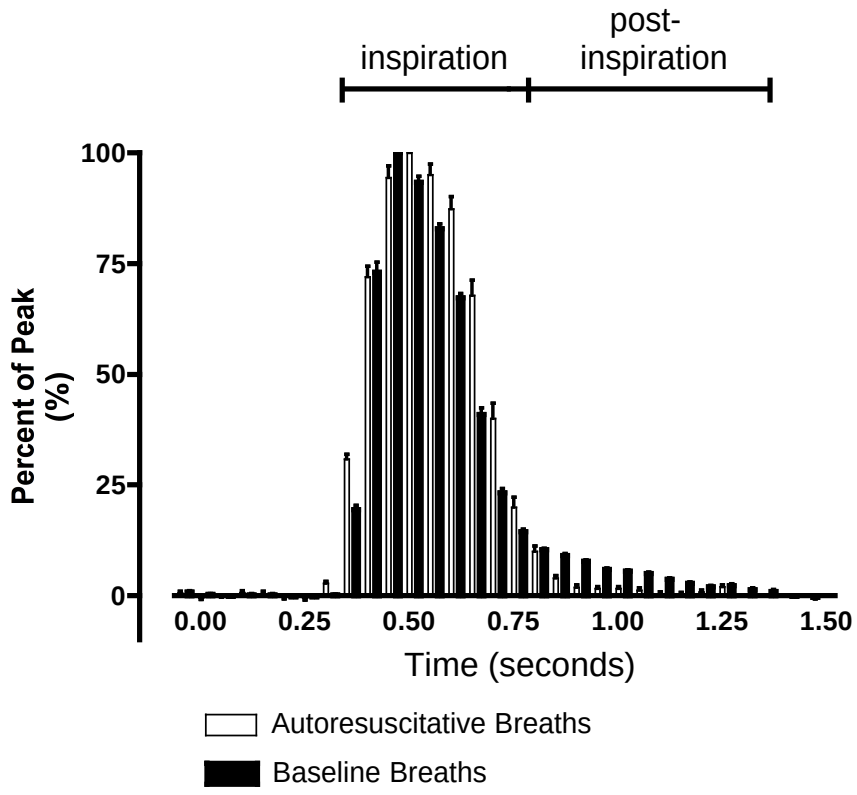

Figure 5.5 A and B shows individual tracings of integrated phrenic nerve activity for baseline (A) and post apnea (B). Activity is superimposed by synchronized at the initiation of phrenic activity. Y-axis for A and B are arbitrary (related to amplification settings) but units are in volt- seconds. Figure 5.5C shows an event triggered averaging of phrenic activity during the baseline period and post OP induced apnea (autoresuscitative breathing). Data are an average of 100 breaths for both the baseline period and post-apneic period. Average peak integrated phrenic activity over 0.05 msec time blocks are plotted over time and

synchronized to the onset of phrenic activity. Activity occurring during the inspiratory period and post-inspiratory period of the respiratory cycle are labeled with black bars at the top of the graph. The post-inspiratory activity was defined by the cessation of airflow (pneumotachometer). Note the loss of post-inspiratory inspiratory activity during autoresuscitative breathing.

Chapter VI - Location of action of Dichlorvos induced central apnea, effect of isolated exposure of the brainstem and pre-Botzinger complex.

6.1 Abstract

We demonstrated previously that OP poisoning causes a central apnea but the mechanism involved and location of action of the OP are not well understood. Respiratory control is located in the brainstem and involves a number of sites within the medulla and pons. The primary site of respiratory rhythm generation is in the medulla and is thought to be the pre-Botzinger complex which is a primary candidate for the CNS substrate both necessary and sufficient for OP-induced apnea due to it's central role in respiratory rhythm generation and its known cholinergic inputs. We performed a series of experiments exposing first the entire brainstem and then the pre-Botzinger complex alone to an OP. Exposure of the brainstem to an OP resulted in a central apnea similar to apnea seen in the intact animal. However, exposure of the pre-Botzinger complex did not have a similar effect. Exposure of bilateral pre-Botzinger complex to dichlorvos resulted in some respiratory depression but only 27% of the animals became apneic. In summary, exposure of the brainstem to OP was sufficient to induce a central apnea but exposure of the pre-Botzinger complex alone was not sufficient.

6.2 Introduction

Central apnea following acute OP exposure was described and characterized in chapter 2 but the location of action of the OP is unknown. A number of brainstem sites have been implicated in OP-induced apnea. Exposure of the ventral surface of the medulla to cholinergic agonists results in a decrease in respiratory rate and tidal volume [48]. Injection of a small volume (10-60nl) of a cholinergic agonist into the medial portion of the rostral pons (near the pontine reticular formation involved in REM sleep) results in respiratory depression [49]. Exposure of the pre-Botzinger complex in the medulla to elevated levels of acetylcholine modulates respiratory activity[50, 257].

The pre-Botzinger complex in the medulla is considered by many to be the kernel of the central respiratory oscillator (CRO) responsible for generating inspiratory activity[88] and critical for eupneic respiration[237]. It is not clear if OP exposure to the pre-Botzinger complex is needed for OP-induced apnea as elevated acetylcholine levels in different areas of the brainstem result in respiratory depression[48, 50, 258] and elevated levels of acetylcholine in the pre-Botzinger complex increases respiratory activity[188]. The pre-Botzinger complex contains both muscarinic and nicotinic receptors that modulate respiratory activity[50, 187, 188] but previous studies have used medullary slice preparations without the intact neural circuitry of a whole animal. In this section, we hypothesize that exposure of the pre-Botzinger complex to an OP is sufficient for OP-induced central apnea.

6.3 Methods

Working Heart Brainstem Preparation

The methodology used in the working heart brainstem has been previously published in detail[259]. Wistar rats (85-120 grams) were acquired and cared for in accordance with NIH published guidelines. The institutional Animal Care and Use Committee of the University of Massachusetts approved this study protocol. Animals were housed in pairs and maintained on a 12-hour light dark cycle with food and water provided *ad libitum*.

Rats were exposed to anesthetic gas (isoflurane, Sigma Aldrich, St Louis MO) in an anesthetic chamber until there was no withdrawal to foot pinch and respiratory activity was depressed. The animals were removed from the anesthetic chamber, hemi-sected immediately below the diaphragm and the head, neck and thorax were immersed in iced artificial cerebrospinal fluid (125Mm NaCl, 5mM KCl, 1.25 mM $MgSO_4$, 24 mM $NaHCO_3$, 1.25 mM KH_2PO_4, 2.5 mM CaCl and 10mM *D*-glucose). The skull bone overlying the cerebral hemispheres and cerebellum was removed and the animal was decerebrated at the precollicular level, removing all brain tissue rostral to this transection with suction. The diaphragm was dissected from its attachments to the ribs and spine and the anterior portion of the rib cage and sternum were removed, exposing the thoracic cavity. The left phrenic nerve was identified and isolated from its surrounding connective tissue. The lungs were removed and the animal was transferred to a

recording chamber where the descending aorta was cannulated with a double lumen catheter. The animal was then artificially perfused through the catheter with warmed artificial CSF plus 1.25% ficol (Sigma Aldrich, St Louis MO) equilibrated with a 5% CO2/95% O2 gas mixture. The second lumen of the catheter was connected to a pressure transducer to monitor arterial pressure.

Perfusion pressure was provided by a peristaltic pump (Watson Marlow, Falmouth, Cornwall) circulating artificial perfusate in a circuit from a reservoir, through the animal back to the reservoir. The perfusate was warmed by passing through a heated water jacket (Neslab Instruments, Portsmouth NH) and filtered by passing through a bubble trap and filter paper (Millipore, Billerica MA). Perfusate seeped out of the open surgical sites of the animal before being collected in the basin of the recording chamber and pumped back to the reservoir of artificial CSF. The reservoir was continuously bubbled with a 5%CO2/95%O2 gas mixture. A diagram of this technique is in figure 6.1.

Sustained phrenic nerve activity was obtained after achieving appropriate perfusion pressure and temperature. Increasing pump speed gradually over time increased perfusion pressure from 0 mmHg to a target perfusion pressure between 40 to 60 mmHg. Once perfusion pressure reached the target range, temperature was increased by elevating the temperature in the water jacket to a target temperature of 29^{o}C at the aortic catheter. This temperature has been previously validated as the optimum temperature to support sustained respiratory

activity. The phrenic nerve was draped over a bipolar electrode and encased in petroleum jelly.

Artificial perfusion pressure was held in a constant range by increasing or decreasing pump speed during the experiment. Data were recorded on a data acquisition system (Powerlab, ADI instruments) and displayed in real-time during the experiment (Chart, ADI instruments). Fictive respiratory rate and tidal volume (calculated from phrenic nerve activity) were monitored and recorded for changes in respiratory output.

Microdialysis into pre-Botzinger complex

Seven adult male Wistar rats were induced with 2.2% isoflurane (Abbott Labs, North Chicago, IL) and subsequently titrated to maintain an adequate respiratory rate (40-60 bpm) with sufficient anesthesia (monitored via foot pinch). Animals underwent a tracheostomy but were allowed to breath 100% oxygen spontaneously at all times. During a baseline period the animals were anesthetized with a constant amount of isoflurane (range 1.6-1.8%) that was not changed once the experiment began. Physiologic recordings included respiratory (airflow, respiratory rate, end tidal CO2, oxygen saturation) and cardiovascular (blood pressure, pulse rate) parameters. All animals served as their own control with comparisons made between baseline and post dichlorvos. Data were recorded using an A-D converter and PC data acquisition system (ADI instruments, Colorado Springs CO).

Animals were placed prone in a stereotactic apparatus with ear bars and bite block (Kopf Instruments, Tugunga California) and the skin overlying the skull was incised and retracted from midline. Bilateral 2mm trephination holes were drilled in the skull over the location of the pre-Botzinger complex using stereotactic coordinates (-3.3 intra-aural, 2 mm lateral). A microdialysis guide cannula (CMA Microdialysis, North Chelmsford MA) was introduced into the holes to a depth of 6mm. A 2 mm long, 100 kDa cut-off microdialysis probe was inserted into the guide cannula. If needed, the animal was allowed to return to baseline prior to proceeding. The animal was maintained at a baseline level for at least 20 minutes prior to initiating the experimental procedure. All experimental protocols were approved by our institutional animal care utilization committee.

Organophosphate Exposure and Controls

Working heart brainstem preparation

Respiratory rate and perfusion pressure were allowed to equilibrate for 10 minutes prior to initiating the experiment. Each animal served as its own control with 1 cc of vehicle (35% isopropyl alcohol) introduced into the artificial perfusate reservoir. Ten minutes following the vehicle control, dichlorvos (50 mg in 1cc of 35% isopropyl alcohol) was introduced into the artificial perfusate reservoir.

Microdialysis

In the microdialysis experiments the dichlorvos and control solutions were microdialyzed directly into bilateral pre-Botzinger complex. Dialysis catheters placed in bilateral guide cannula were attached to a syringe pump filled with a dialysis solution. The dialysis solution contained 12.5 mg/cc of dichlorvos mixed from a stock solution of 25 mg of dichlorvos solubolized in 1 cc of 35% isopropyl alcohol and 1cc of CNS perfusion fluid (CMA Microdialysis, North Chelmsford, MA). Each animal served as its own control and vehicle alone (1:1 mixture of 35% isopropyl alcohol and CNS perfusion fluid) was dialyzed for 12 minutes at 5 µl per minute. Animals were allowed to return to baseline for 10 minutes prior to exposure to dichlorvos. The dichlorvos solution was dialyzed at 5 µl per minute for a total of 12 minutes for a cumulative dose of 750 µg.

Confirmation of probe placement was accomplished using $KMnO_4$ to mark the center of the microdialysis probe membrane. Following the termination of the experiment, the dialysis probes were removed from the guide cannula. The bilateral guide cannula remained attached to stereotactic arms, and were not moved during the removal of the microdialysis catheter. Needles extending just beyond the tip of the guide cannula were connected via tubing to a syringe pump (CMA Microdialysis, North Chelmsford, MA) and inserted into the guide cannula. $KMnO_4$ (40mg/cc) was micro-injected at 8.3 µl/min for 5 min resulting in a direct oxidation of cells at the tip of the needle and a precipitation of manganese dioxide visible to the naked eye. Animals were immediately perfused with 4%

paraformaldehyde and the brain was removed for sectioning and identification of probe tip location.

Measurement of dichlorvos tissue level

To assure adequate exposure of the pre-Botzinger complex following microdialysis, brain samples were sent for a determination of tissue dichlorvos levels. An additional animal underwent dialysis of dichlorvos into the pre-Botzinger complex as described above but was decapitated immediately after dialysis. The brainstem was removed and frozen at -20^{o}C, sectioned into 2mm slices, cut into 1mm by 1mm square sections, weighed and refrozen at -20^{o}C. All samples of the brainstem, as well samples of a similar size from the forebrain, were sent for a determination of dichlorvos level using gas chromatography mass spectrometry (GCMS). Barbra Evans at the UMMS Proteomic & Mass Spectrometry Core Facility analyzed samples. As a control, samples of forebrain tissue from a naive animal (no intervention), and additional samples of forebrain tissue from a naive animal with dichlorvos added to the tissue sample post harvesting were also sent for a determination of dichlorvos level.

Tissue samples were stored at -80 ^{o}C prior to extraction. Dichlorvos was extracted from the brain samples with ethyl acetate containing d_6-dichlorvos internal standard and the extract directly analyzed by selected ion monitoring electron impact GCMS using a modification of the method described by Ma et al[260]. Brain samples were extracted by maceration and 5 min sonication in a

bath sonicator in 100 µl of ethyl acetate containing 7.5 ng of d_6- dichlorvos internal standard. The extract was cleared by centrifugation for 5 min and the clear supernatant transferred to autosampler vials for GCMS analysis. One µl of each sample was injected (splitless mode) onto a 30 mm X 0.25 mm ID DB5-MS capillary column that was connected directly to the ion source of a Waters Quattro-II triple quadrupole mass spectrometer. Helium was used as the carrier gas at a constant flow of 1 ml/min and the column temperature was programmed from 75^o C to 130^o C at 30^o C/min and held at 130^o for 3.7 min. Electron impact ionization (EI) was used at 70 eV with the source at 225^o C. Selected ion monitoring of m/z 108.9 (dwell 0.3 sec) for dichlorvos and m/z 114.9 (dwell 0.03 sec) for the internal standard. External calibration standards containing 0.25, 0.5 and 1.0 µg/ml of dichlorvos and 0.5 µg/ml internal standard were also analyzed before and after each 10 samples. The calculation of dichlorvos in each tissue sample was calculated from the ratio of the dichlorvos peak area to that of the internal standard multiplied times 7.5 ng.

Data Analysis

Data were obtained using a data acquisition system (ADI Instruments, Colorado Springs, CO) and recorded using Chart software. The primary endpoint was time to apnea. Secondary endpoints included changes of respiratory and cardiovascular parameters from baseline. Apnea was defined as a cessation of airflow through the pneumotachometer (or cessation of phrenic activity) for more

than 20 seconds. Previous studies in our lab indicate that this definition reliably predicts an extended loss of respiratory effort.

Raw phrenic signals were amplified (Cyberamp 320, Molecular Devices, Sunnyvale CA) and filtered (Humbug Noise Eliminator, Vancouver BC) prior to display. Phrenic nerve activity greater then 3 standard deviations from baseline were rectified and step-wise integrated (time constant 50 ms). Fictive tidal volume was calculated as a percentage of baseline, with 100% defined as the peak phrenic activity and 0% as zero. Data are presented as mean (+/- SD) unless otherwise noted. Comparison between groups is performed using student's T-test where appropriate.

6.4 Results

Working brainstem spinal cord preparation

Respiratory activity started after reaching an average perfusion pressure of 44.6mm Hg and stabilized at a respiratory rate of 17.8 bpm during the baseline period prior to initiating the experiment. There was no statistical change in fictive respiratory rate or fictive tidal volume with the exposure to vehicle alone. Respiratory activity began falling around 2 minutes after dichlorvos was introduced into the reservoir (figure 6.2). Nine of 10 animals demonstrated a steady decline in respiratory rate and eventual apnea an average of 3 minutes 43 seconds (+/- 2:47) post dichlorvos exposure. Respiratory rate and fictive tidal

volume decreased in all animals over 50% and 75% respectively within two minutes of poisoning.

Respiratory activity resumed post apnea in 8 of the 9 animals that demonstrated apnea. Respiratory activity resumed an average of 11 minutes 2 seconds (+/- 11:57) after the point of apnea with some animals demonstrating a sustained respiratory activity (n=5) and others with a short burst of respiratory activity followed by a resumption of apnea (n=3). Animals that demonstrated sustained post-apneic respiratory activity had phrenic bursts at a regular rate of 12.78 (+/- 4.28) breaths per minute. The resumption of respiratory activity started regular but slow and increased gradually over time until the termination of the experiment 1 hour post dichlorvos exposure.

Perfusion pressure increased post dichlorvos exposure despite no change in pump speed. Perfusion pressure increased 34% over baseline in all animals (10 of 10), peaking 1.72 min (±0.28 min) post exposure. This reaction was so reliable that it is now used as an indicator of dichlorvos exposure in this model.

Microdialysis into pre-Botzinger complex

Microdialysis of dichlorvos into the pre-Botzinger complex resulted in a progressive decrease in respiratory rate, volume of expired gas and minute ventilation but no change in mean arterial pressure or pulse rate (Figures 6.3 and 6.4). Apnea was seen in 28.6 percent of the animals (2 of 7) an average of 9.87

min after the initiation of dialysis. Average respiratory rate, volume of expired gas and minute ventilation each declined 60% by the end of the study. Microdialysis of vehicle alone (35% isopropyl alcohol in artificial CNS fluid) had a minor effect on minute ventilation and tidal volume but did not cause apnea. Animals in this group showed no change in volume of expired gas but they did show an average 20% decrease in respiratory rate and minute ventilation.

To determine the location of the microdialysis probes, $KMnO_4$ was injected to mark the center of the 2mm microdialysis membrane. $KMnO_4$ injection successfully marked the location of the microdialysis catheter in 72% of animals. In some cases injection of the $KMnO_4$ failed due to obstruction within the guide cannula. Location of the microdialysis catheters is depicted in Figure 6.6. A scatter plot of time to apnea vs distance from pre-Botzinger complex (figure 6.7) shows no correlation between the two data sets. $KMnO_4$ caused cellular coagulation and cell death resulting in apnea in 83% of the animals that were spontaneously breathing prior to the injection of $KMnO_4$ (Figure 6.8). In animals that were spontaneously breathing prior to the $KMnO_4$, apnea occurred an average of 1:34 post initiation of injection with three of the animals becoming apneic within 6 seconds of initiating the $KMnO_4$ injection.

Dichlorvos levels in the brainstem are depicted in figure 6.9. The areas of the brainstem closest to the dialysis catheter showed elevated levels of dichlorvos (1-2 µg/gm). The two negative control samples from naïve animals showed

levels of dichlorvos of 0.00 and 0.02 µg/g. The small amount of dichlorvos in one of the negative controls was most likely due to cross contamination from the cutting surface during tissue harvesting.

6.5 Discussion

The working-brainstem preparation consists of the brainstem and spinal cord and retains the connections within the brainstem but lacks any afferent input from the cerebral hemispheres (decerebration) or feedback from the lungs (bilateral pneumonectomy). Exposure of the brainstem to dichlorvos resulted in a cessation of respiratory activity on a time scale similar to our previously published whole animals model[186]. Exposure of the pre-Botzinger complex alone did not have the same effect. Dichlorvos exposure to the pre-Botzinger complex resulted in respiratory depression but only 28.6% demonstrated apnea. Exposure of the pre-Botzinger complex to dichlorvos is insufficient for OP-induced apnea.

Dichlorvos exposure of the brainstem was sufficient for OP-induced central respiratory apnea. Central respiratory control involves a network of interconnected neurons in the medulla and pons, and it is logical that exposure of this area is required for OP-induced central apnea. At the heart of the central respiratory drive is the central respiratory oscillator responsible for the generation of rhythmic neural impulses resulting in inspiration. The pre-Botzinger complex is

considered by many to be the kernel of the CRO, has a central role in generating respiratory activity[261] and contains cholinergic receptors[50] that may be stimulated during acute OP intoxication.

The lack of apnea following exposure of bilateral pre-Botzinger complex indicates that exposure of the pre-Botzinger complex alone is insufficient for OP-induced apnea. Previous studies with OP exposure to the pre-Botzinger complex have shown similar results with respiratory depression but not apnea[50]. The brainstem contains many sites involved in respiratory control and a number of these sites are potentially involved in OP-induced central apnea but further research is needed.

It is unlikely that insufficient dichlorvos exposure to the pre-Botzinger complex was responsible for the lack of effect. Although placement of the microdialysis catheter showed slight variability, histological confirmation of the catheter tip showed that most catheter tips were within 2.0mm of the pre-Botzinger complex and there was no association between distance from the pre-Botzinger complex and respiratory depression. The response to $KMnO_4$ injection provides indirect evidence for accurate catheter placement in the area of central respiratory control and matches previously published studies on lesioning the pre-Botzinger complex[261]. Cell ablation at the tip of the catheter with $KMnO_4$ caused apnea within 1.57 min, with 3 of the animals demonstrating apnea within 3 seconds of the initiation of the microinjection. Most importantly, measured levels of

dichlorvos at the pre-Botzinger complex were sufficient to induce apnea. Dichlorvos levels at the pre-Botzinger complex were greater then previously published levels following lethal IV exposure. Lethal IV dichlorvos (10mg/kg) generates a tissue level in the brain of 0.2-0.3 µg/g[245] and levels at the pre-Botzinger complex in this study were greater then 1 µg/g.

The kinetics of dichlorvos degradation may have played a minor role in the lack of respiratory effects following microdialysis. The bio-effects of a single bolus of dichlorvos decrease over time as dichlorvos is rapidly degraded by two enzymatic pathways in the rat with the predominant pathway involving hydrolysis by an A-esterase present in the rat plasma and liver[262]. Introducing the dichlorvos over a protracted period during microdialysis of time should effectively decrease the peak exposure levels due to the increased time available for degradation. The half-life of dichlorvos in rat plasma is less then 15 min but this may be decreased with microdialysis. Regardless of the kinetics of degradation, levels of dichlorvos at the pre-Botzinger complex were substantial as measured post-dialysis.

In summary, dichlorvos exposure of the rat brainstem is sufficient for OP-induced central apnea. Although the pre-Botzinger complex may be involved in OP-induced apnea, dichlorvos exposure to the pre-Botzinger complex alone is insufficient.

Future Directions

There are alternative sites in the brainstem that could be involved in OP-induced central apnea, but the few studies exploring these areas show mixed results. Cholinergic neurons are involved in the modulation of respiratory activity during sleep[263] and cause respiratory depression when stimulated[49]. Acetylcholine applied iontophoretically to individual respiratory related neurons in the ventral respiratory group produce changes in membrane potentials but have no effect on fictive respiratory rate or tidal volume[193, 195]. Cholinergic stimulation of the ventral medullary surface involved in chemosensitivity augments respiration[194]. Other cholinergic sites in the brainstem involved in respiratory control have not been rigorously studied.

Limitations

The working brainstem-spinal cord preparation produces a respiratory rate that is much lower then the native respiratory rate, implying changes at the neural level that may limit the generalizability of the findings in this model to the intact animal. In addition, the working brainstem-spinal cord model involves hypothermia and artificial perfusion that may introduce changes in the brainstem respiratory center unrelated to the dichlorvos exposure.

Figure 6.1 - Diagram of Working Brainstem-Spinal Cord Preparation

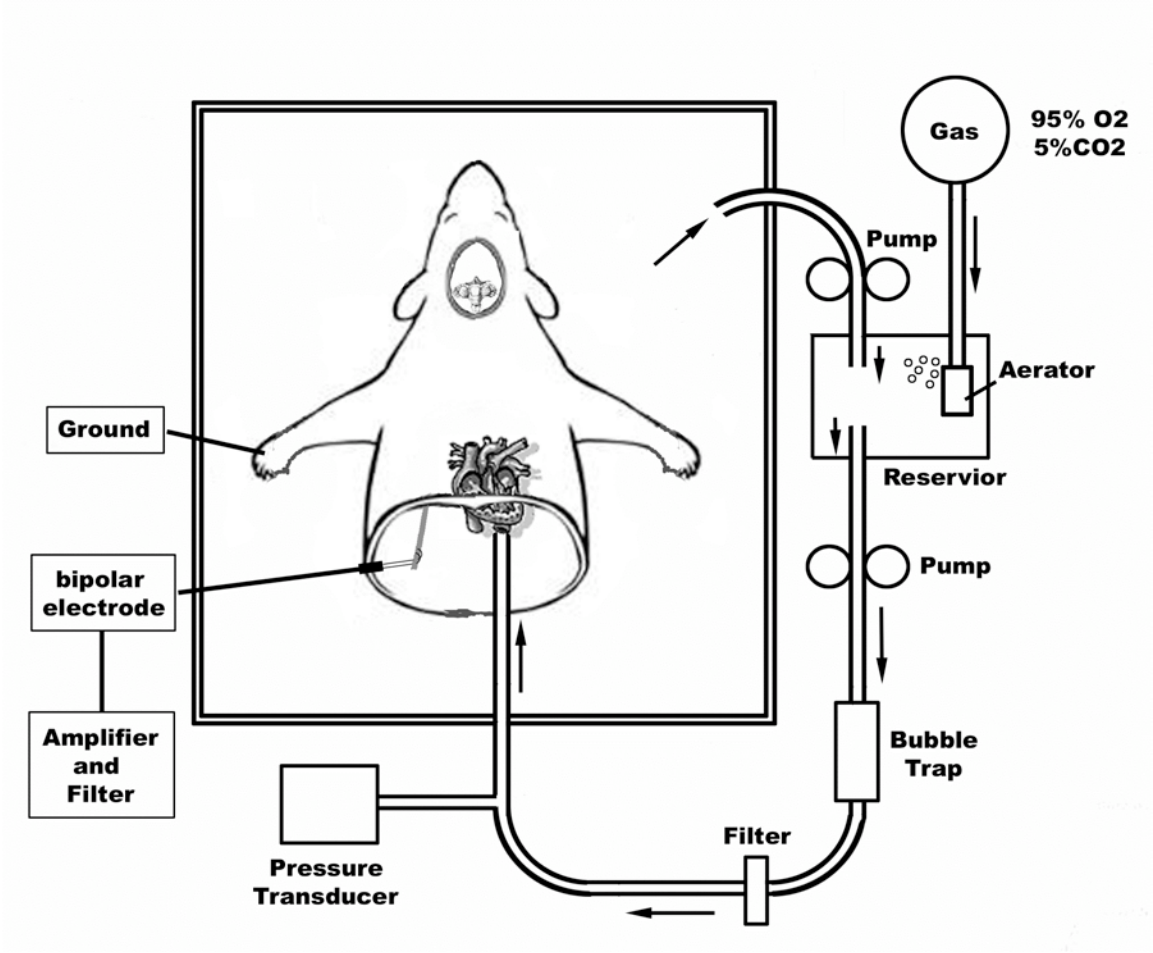

Artificial perfusate is pumped from a reservoir through a warming jacket, bubble trap and filter. The decerebrate, hemi-sected animal lies in an open basin and is perfused through its aorta. Perfusate leaks out of the surgical sites and pools in the basin before returning to the reservoir that is continuously bubbled with a 5% CO_2/95% O_2 gas mixture.

Figure 6.2 A,B – Fictive respiratory activity post dichlorvos in the working brainstem spinal cord preparation

A.

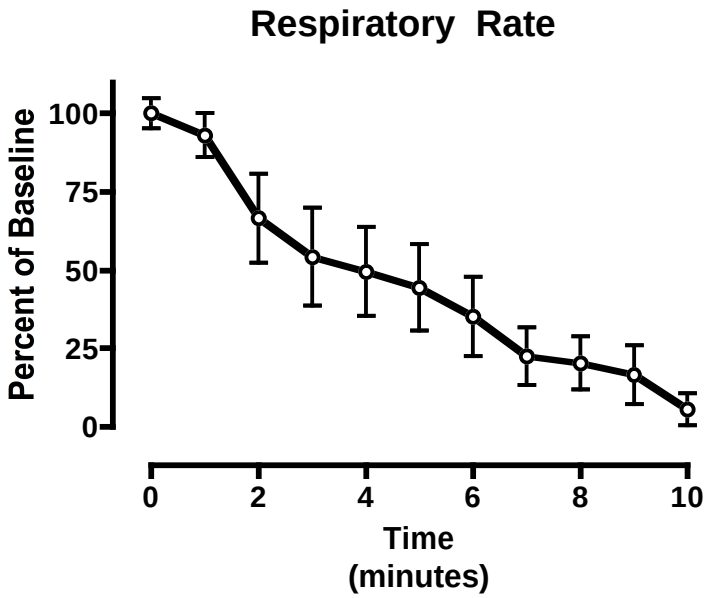

B.

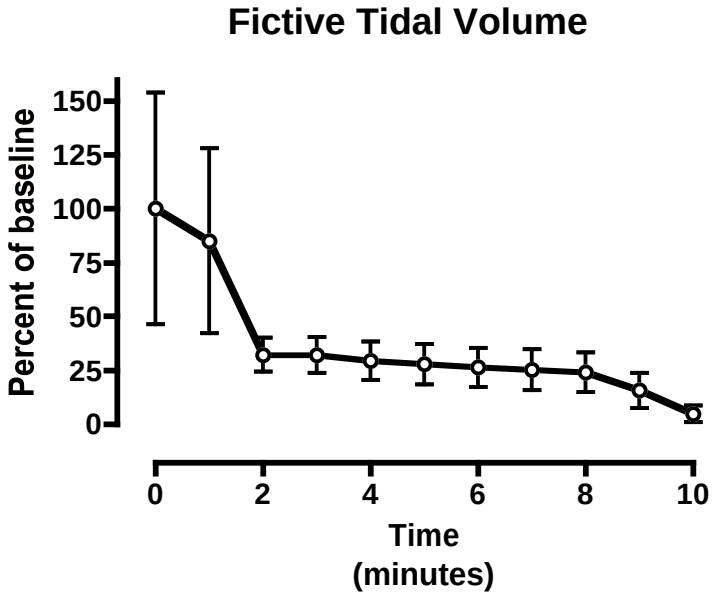

Fictive respiratory rate and tidal volume were calculated from an analysis of phrenic nerve activity. Dichlorvos was introduced into the reservoir at time zero. Values are presented at a percentage of baseline activity with 100% equal to peak phrenic discharge (tidal volume) or rate of phrenic discharge (respiratory rate) during baseline period.

Figure 6.3 A,B,C – Respiratory rate, volume of expired gas and minute ventilation post dialysis of dichlorvos into the pre-Botzinger complex

A.

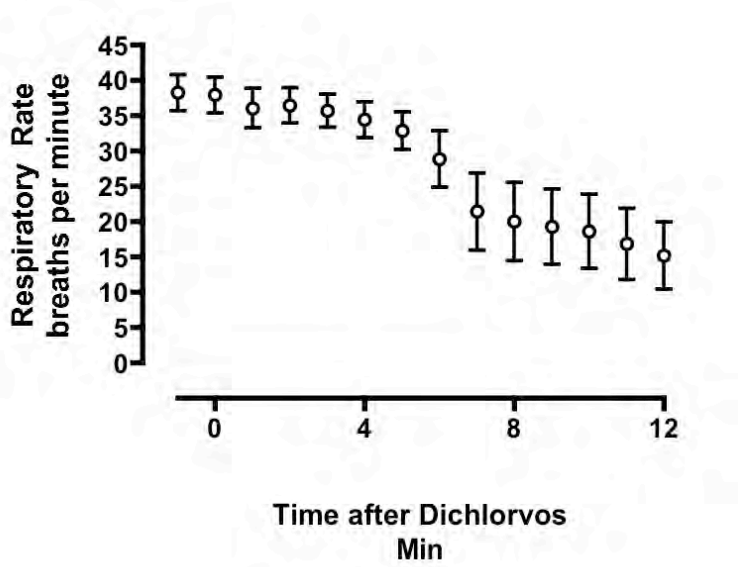

B.

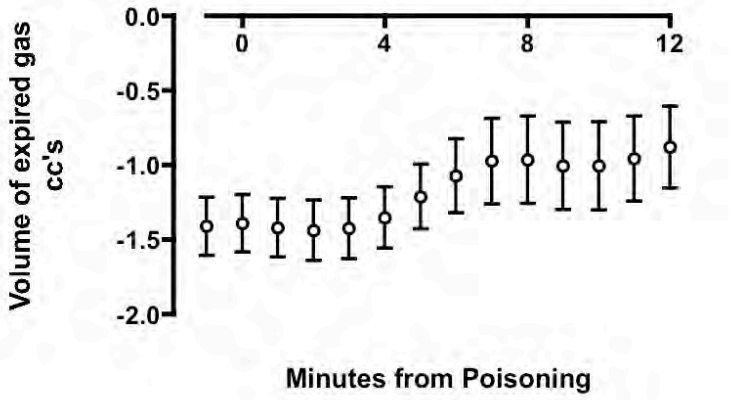

C.

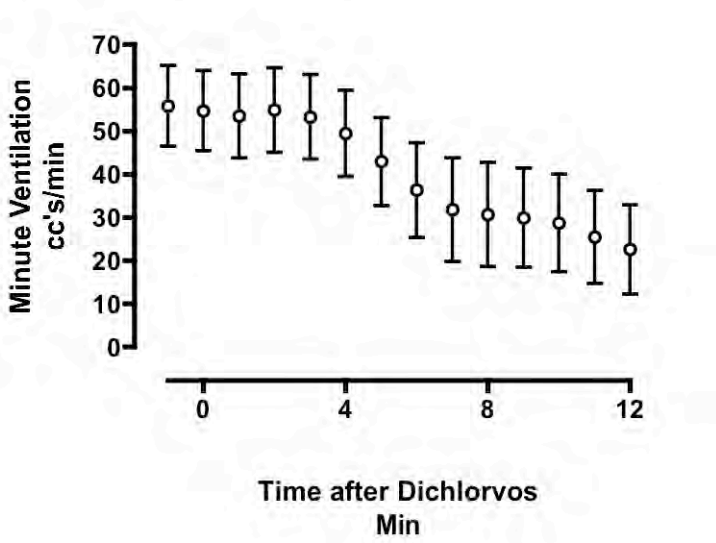

Microdialysis of dichlorvos into the pre-Botzinger complex was initiated at time zero. Data represent an average of all animals.

Figure 6.4 A,B – Pulse rate and mean arterial pressure post dialysis of dichlorvos into the pre-Botzinger complex

A.

B.

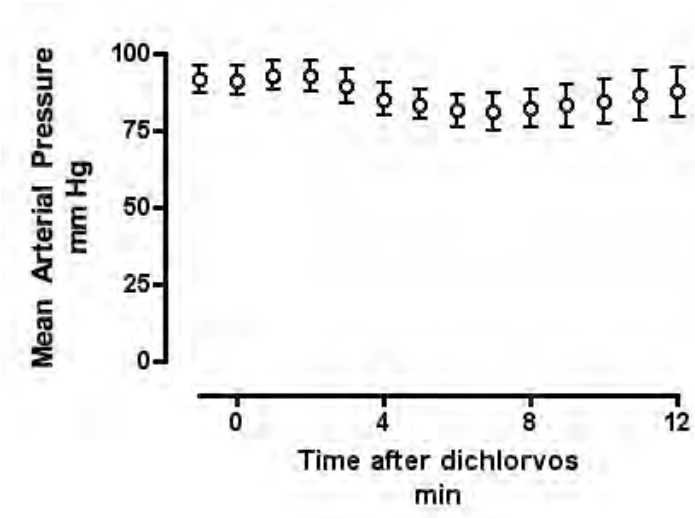

Microdialysis of dichlorvos into the pre-Botzinger complex was initiated at time zero. Data represent an average of all animals.

Figure 6.5 – Microdialysis probe locations

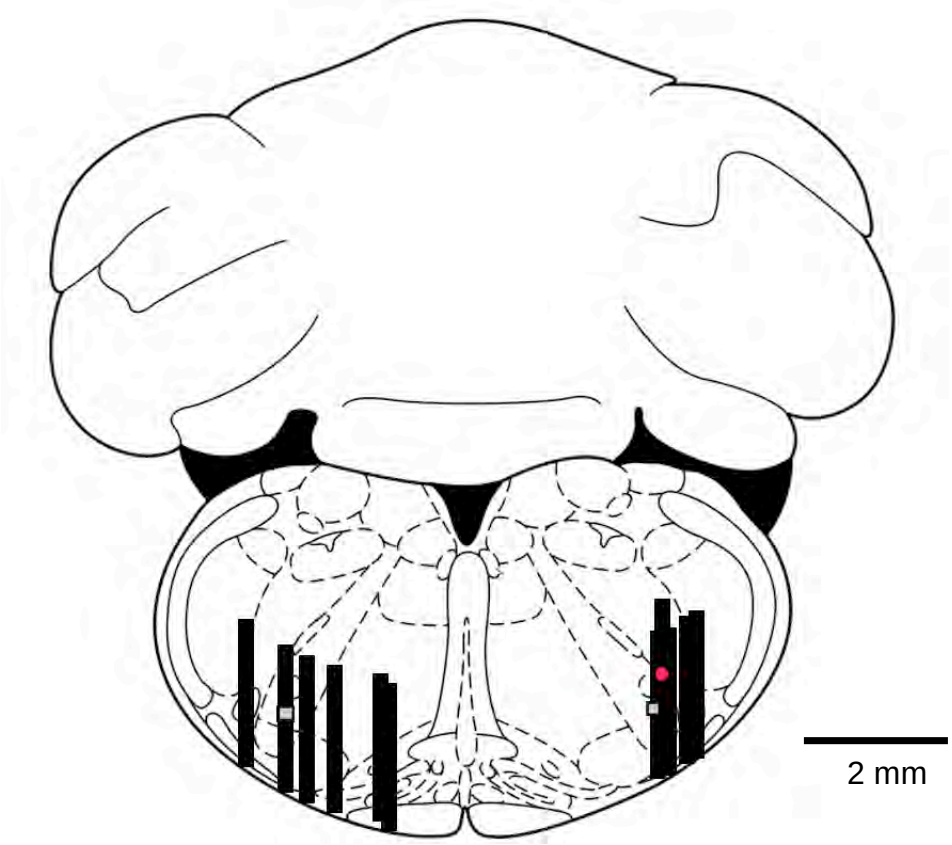

Dialysis probe location were marked using microinjection of $KMnO_4$ at the midpoint of the 2mm x 0.4mm dialysis membrane. The grey squares represent the pre-Botzinger complex. Black rectangles represent the 2mm dialysis membrane. The red circle represents an injection site 2mm cephalad to the pre-Botzinger complex. Animals with inadequate $KMnO_4$ injection resulting in an insufficient lesion on the histological specimen were not included.

Figure 6.6 – Relationship of changes in minute ventilation and average distance from pre-Botzinger complex.

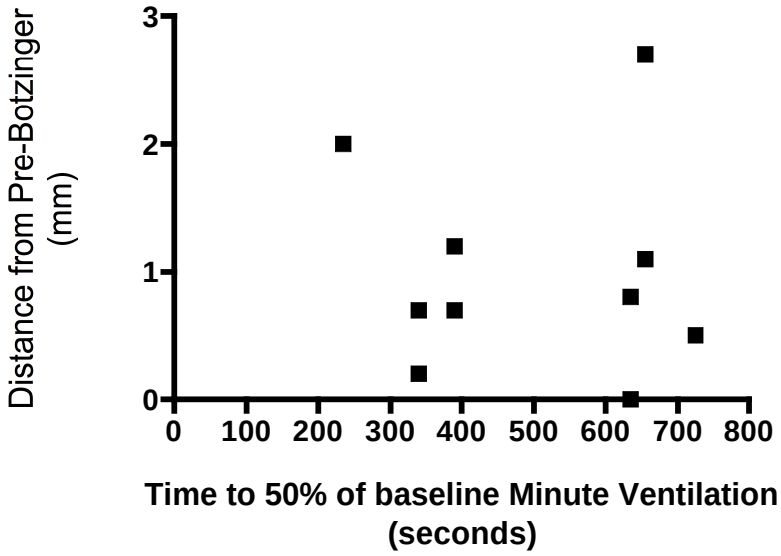

The distance of the probe location from the pre-Botzinger complex was measured in three dimensions and plotted against time to 50% of baseline minute ventilation. Each dot represents an average of both sites for a single animal. Animals with inadequate $KMnO_4$ injection resulting in an insufficient lesion on the histological specimen were not included.

Figure 6.7 A,B,C – Respiratory rate, volume of expired gas and minute ventilation post injection of KMnO4 into the pre-Botzinger complex

A.

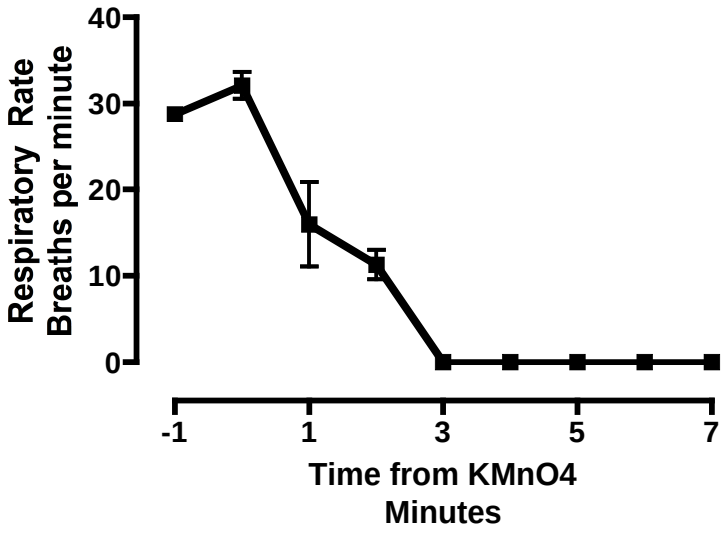

B.

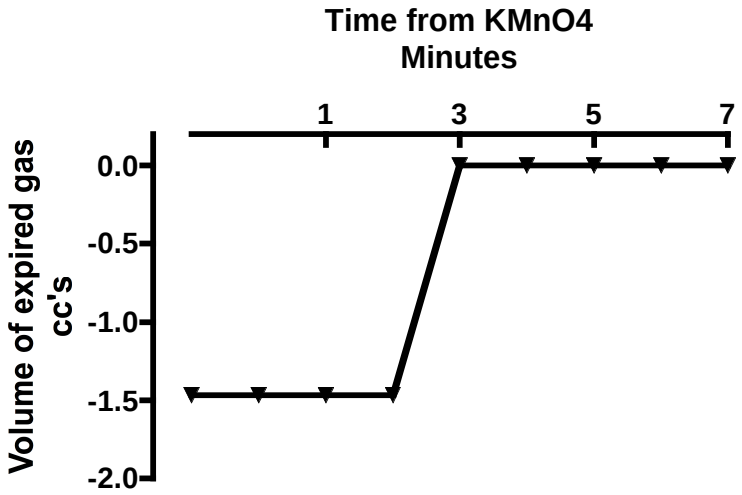

C.

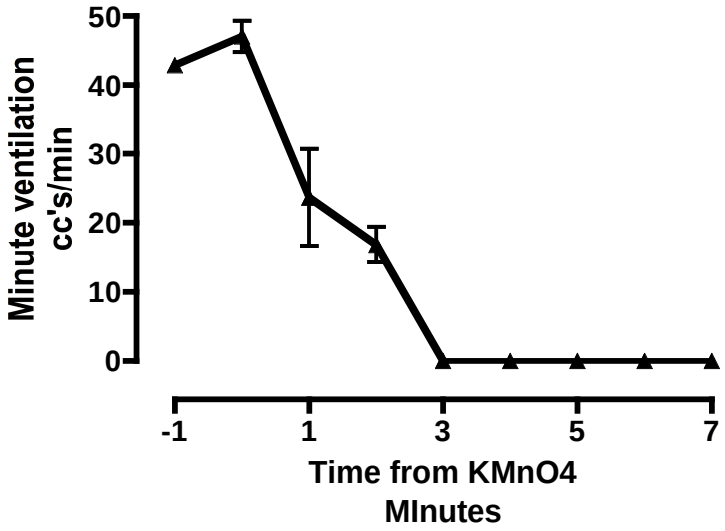

Microinjection of $KMnO_4$ into the pre-Botzinger complex was initiated at time zero. Data represents an average for control (2 of 2) and experimental (3 of 4) animals that were breathing at the end of the experiment. Animals that were not breathing at the beginning of the $KMnO_4$ injection were not included in this data set.

Figure 6.8 - Level of dichlorvos in brainstem following microdialysis of dichlorvos into bilateral pre-Botzinger complex.

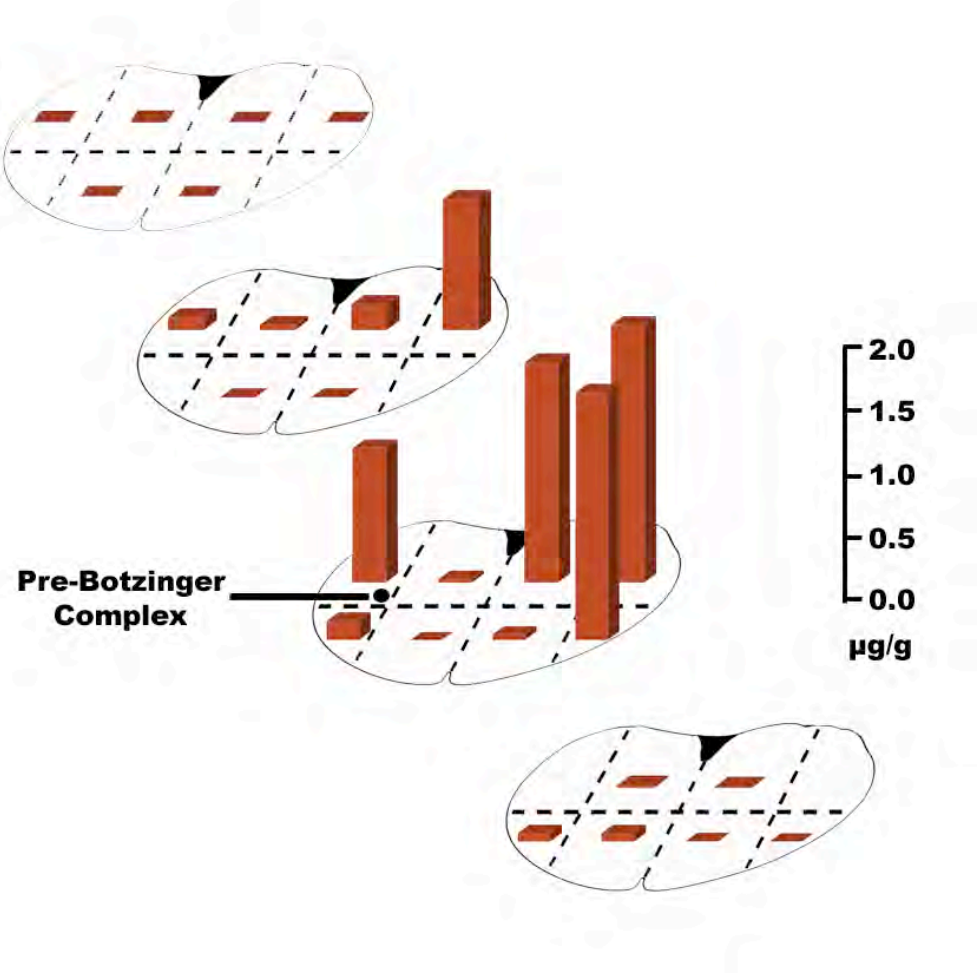

Microdialysis of dichlorvos (750 µg over 12 minutes) into bilateral pre-Botzinger complex was performed prior to sectioning the brainstem along dotted lines. The dichlorvos in each sample (1mm x 1mm x 2mm) was extracted and measured via gas chromatography-mass spectrometer. The results are presented as µg of dichlorvos per gram of brain tissue. A level greater then 3µg/g corresponds to a lethal level. The pre-Botzinger complex location is depicted by a black circle.

Chapter VII – Summary

7.1 Study findings

Respiratory failure following acute dichlorvos poisoning involves an initial central apnea that occurs rapidly and is followed by a pulmonary dysfunction. The central apnea occurs within minutes of poisoning and is characterized by decreasing respiratory effort, tidal volume and rate. Vagal afferent feedback to the brainstem has a minor contribution to the central apnea but is not the driving mechanism of central respiratory failure. Cerebral feed-forward input to the brainstem respiratory centers is not necessary for OP-induced central apnea. Exposure of the brainstem is sufficient for OP-induced central apnea but exposure of the pre-Botzinger complex alone (the central respiratory oscillator) is not sufficient for apnea.

Respiratory failure following acute OP exposure is not permanent. Animals supported with mechanical ventilation demonstrate a gradual re-emergence of respiratory activity following a period of apnea. This re-emergence is characterized by an alteration of the phrenic output of the central respiratory oscillator that is distinct from normal eupneic respiration and gasping.

Pulmonary dysfunction following acute OP exposure is not uniform. Roughly 20% of animals demonstrate a catastrophic increase in pulmonary secretions that fill the lung and trachea. These animals die quickly despite mechanical

intervention. The rest of the poisoned animals demonstrate a variability of dysfunction that is relatively short lived. Studies with anti-cholinergic therapy indicate that transient dysfunction of the pulmonary vasculature is a component of the pulmonary dysfunction.

7.2 Impact on Clinical Therapy

The central apnea following acute OP poisoning occurs rapidly but is a greater concern for first responders, paramedics, fire and rescue personnel, and battlefield medics then physicians in a hospital setting. The rapidity and uniformly lethal nature of the OP-induced central apnea prevents most untreated patients with OP-induced apnea from surviving to reach definitive care. In addition, mass casualty triage in situations with OP exposures may require rapid endotracheal intubation and transport for those patients showing signs of apnea. In a battlefield situation, rapidly treating apneic patients without pulmonary dysfunction and transporting them to an inpatient facility would greatly increase their chances of survival without requiring significant additional resources.

Unrecognized central apnea could cause problems clinically if the apnea was prolonged following exposure. There are almost 900 different OP agents with subtlety different characteristics in fat solubility, tissue clearance and time course of effects. Prolonged clinical effects would impact ventilated patients as well. Using pulmonary secretions to guide atropine therapy is a common clinical

strategy, but in mechanically ventilated patients this could result in failure to transition the patient off of the ventilator due to under-treatment of the central apnea. Individuals with relatively smaller pulmonary effects but prolonged central apnea would receive little to no atropine. Dosing atropine to inspiratory effort could provide a better strategy for those patients with little pulmonary dysfunction.

Atropine is an effective therapy for severe OP poisoning but the effect of atropine on pulmonary vasculature has not been previously considered. OP-poisoned patients can receive tremendous amounts of atropine, commonly in response to pulmonary dysfunction. A common strategy for mechanically vented OP patients is dosing atropine with the clinical goal of “drying pulmonary secretions” to prevent hypoxia. Unrecognized disruption in pulmonary gas exchange from high doses of atropine could be attributed to OP-induced pulmonary dysfunction, triggering more atropine. Discerning between the hypoxic effects of pulmonary secretions and atropine-induced ventilation-perfusion mismatch requires recognition of the effects of atropine on pulmonary vasculature.

The emergence of a distinct respiratory pattern post OP-induced apnea raises questions about the central respiratory oscillator and how it reconfigures when disrupted. Previous authors have described respiratory activity post OP-induced apnea that is unaffected by repeated exposure to the same agent despite increased acetylcholine levels[166]. This combined with our findings implies a

fundamental change in the central respiratory oscillator. Relatively little attention has been paid to characterizing reconfigured respiratory oscillators. With wild speculation, it is possible to imagine inducing temporary changes in central respiratory control to stimulate sustained respiratory activity during a period of profound hypoxia, such as during cardiac arrest. A compound that could induce neural respiratory activity during cardiac arrest would eliminate the need for cardiopulmonary resuscitation as we know it. It is less speculative to imagine pre-treating soldiers with a compound that renders them immune to the apneic effects of nerve agents.

7.2 Conclusions

OP respiratory failure involves a combination of central apnea and pulmonary dysfunction. OP-induced central apnea is rapid but transient and relates to direct exposure of the OP to the brainstem but exposure of the pre-Botzinger complex alone is insufficient. OP-induced pulmonary dysfunction is variable and involves prominent pulmonary secretions and pulmonary vascular changes resulting in profound hypoxia.

Bibliography

1. Minette, PA and PJ Barnes, Muscarinic receptor subtypes in lung. Clinical implications. Am Rev Respir Dis 1990; **141**(3 Pt 2): p. S162-5.
2. Canning, BJ and A Fischer, Neural regulation of airway smooth muscle tone. Respir Physiol 2001; **125**(1-2): p. 113-27.
3. Racke, K and S Matthiesen, The airway cholinergic system: physiology and pharmacology. Pulm Pharmacol Ther 2004; **17**(4): p. 181-98.
4. Chang, FC, RE Foster, ET Beers, DL Rickett, and MG Filbert, Neurophysiological concomitants of soman-induced respiratory depression in awake, behaving guinea pigs. Toxicol Appl Pharmacol 1990; **102**(2): p. 233-50.
5. Bird, SB, RJ Gaspari, and EW Dickson, Early death due to severe organophosphate poisoning is a centrally mediated process. Acad Emerg Med 2003; **10**(4): p. 295-8.
6. Sungur, M and M Guven, Intensive care management of organophosphate insecticide poisoning. Crit Care 2001; **5**(4): p. 211-5.
7. Goswamy, R, A Chaudhuri, and AA Mahashur, Study of respiratory failure in organophosphate and carbamate poisoning. Heart Lung 1994; **23**(6): p. 466-72.
8. Tsao, TC, YC Juang, RS Lan, WB Shieh, and CH Lee, Respiratory failure of acute organophosphate and carbamate poisoning. Chest 1990; **98**(3): p. 631-6.

9. Binns JH, BC, Bloom F et al, *Gulf War Illness and the Health of Gulf War Veterans. Scientific Findings and Recommendations* 2008, Veteran's Affairs: Washington DC. p. 1-465.

10. Page, WF, Long-term health effects of exposure to sarin and other anticholinesterase chemical warfare agents. Mil Med 2003; **168**(3): p. 239-45.

11. Crouzier, D, VB Le Crom, E Four, G Lallement, and G Testylier, Disruption of mice sleep stages induced by low doses of organophosphorus compound soman. Toxicology 2004; **199**(1): p. 59-71.

12. Icenogle, LM, NC Christopher, WP Blackwelder, DP Caldwell, D Qiao, FJ Seidler, TA Slotkin, and ED Levin, Behavioral alterations in adolescent and adult rats caused by a brief subtoxic exposure to chlorpyrifos during neurulation. Neurotoxicol Teratol 2004; **26**(1): p. 95-101.

13. Jamal, GA, Neurological syndromes of organophosphorus compounds. Adverse Drug React Toxicol Rev 1997; **16**(3): p. 133-70.

14. Eyer, P, Neuropsychopathological changes by organophosphorus compounds--a review. Hum Exp Toxicol 1995; **14**(11): p. 857-64.

15. Singh, S and N Sharma, Neurological syndromes following organophosphate poisoning. Neurol India 2000; **48**(4): p. 308-13.

16. Damodaran, TV, ST Greenfield, AG Patel, HK Dressman, SK Lin, and MB Abou-Donia, Toxicogenomic studies of the rat brain at an early time point following acute sarin exposure. Neurochem Res 2006; **31**(3): p. 367-81.

17. Jortner, BS, SK Hancock, J Hinckley, L Flory, L Tobias, L Williams, and M Ehrich, Neuropathological studies of rats following multiple exposure to tri-ortho-tolyl phosphate, chlorpyrifos and stress. Toxicol Pathol 2005; **33**(3): p. 378-85.

18. Joosen, MJ, E Jousma, TM van den Boom, WC Kuijpers, AB Smit, PJ Lucassen, and HP van Helden, Long-term cognitive deficits accompanied by reduced neurogenesis after soman poisoning. Neurotoxicology 2009; **30**(1): p. 72-80.

19. Muggleton, NG, AJ Smith, EA Scott, SJ Wilson, and PC Pearce, A long-term study of the effects of diazinon on sleep, the electrocorticogram and cognitive behaviour in common marmosets. J Psychopharmacol 2005; **19**(5): p. 455-66.

20. Zhu, H, W Zhou, XR Li, T Ma, IK Ho, and RW Rockhold, Methyl parathion increases neuronal activities in the rat locus coeruleus. J Biomed Sci 2004; **11**(6): p. 732-8.

21. Bushnell, PJ, KL Kelly, and TR Ward, Repeated inhibition of cholinesterase by chlorpyrifos in rats: behavioral, neurochemical and pharmacological indices of tolerance. J Pharmacol Exp Ther 1994; **270**(1): p. 15-25.

22. Choudhary, S, G Raheja, V Gupta, and KD Gill, Possible involvement of dopaminergic neurotransmitter system in dichlorvos induced delayed neurotoxicity. J Biochem Mol Biol Biophys 2002; **6**(1): p. 29-36.

23. Gause, EM, RJ Hartmann, BZ Leal, and I Geller, Neurobehavioral effects of repeated sublethal soman in primates. Pharmacol Biochem Behav 1985; **23**(6): p. 1003-12.

24. Carpentier, P, A Foquin, G Rondouin, M Lerner-Natoli, DM de Groot, and G Lallement, Effects of atropine sulphate on seizure activity and brain damage produced by soman in guinea-pigs: ECoG correlates of neuropathology. Neurotoxicology 2000; **21**(4): p. 521-40.

25. Eddleston, M, NA Buckley, P Eyer, and AH Dawson, Management of acute organophosphorus pesticide poisoning. Lancet 2008; **371**(9612): p. 597-607.

26. Buckley, NA, L Karalliedde, A Dawson, N Senanayake, and M Eddleston, Where is the evidence for treatments used in pesticide poisoning? Is clinical toxicology fiddling while the developing world burns? J Toxicol Clin Toxicol 2004; **42**(1): p. 113-6.

27. Buckley, NA, M Eddleston, and AH Dawson, The need for translational research on antidotes for pesticide poisoning. Clin Exp Pharmacol Physiol 2005; **32**(11): p. 999-1005.

28. Munidasa, UA, IB Gawarammana, SA Kularatne, PV Kumarasiri, and CD Goonasekera, Survival pattern in patients with acute organophosphate poisoning receiving intensive care. J Toxicol Clin Toxicol 2004; **42**(4): p. 343-7.

29. Emerson, GM, NM Gray, GA Jelinek, D Mountain, and HJ Mead, Organophosphate poisoning in Perth, Western Australia, 1987-1996. J Emerg Med 1999; **17**(2): p. 273-7.

30. Bardin, PG, SF van Eeden, and JR Joubert, Intensive care management of acute organophosphate poisoning. A 7-year experience in the western Cape. S Afr Med J 1987; **72**(9): p. 593-7.

31. Lee, P and DY Tai, Clinical features of patients with acute organophosphate poisoning requiring intensive care. Intensive Care Med 2001; **27**(4): p. 694-9.

32. Tsai, JR, CC Sheu, MH Cheng, JY Hung, CS Wang, IW Chong, MS Huang, and JJ Hwang, Organophosphate poisoning: 10 years of experience in southern Taiwan. Kaohsiung J Med Sci 2007; **23**(3): p. 112-9.

33. Murali, R, A Bhalla, D Singh, and S Singh, Acute pesticide poisoning: 15 years experience of a large North-West Indian hospital. Clin Toxicol (Phila) 2009; **47**(1): p. 35-8.

34. Heiser, JF and JC Gillin, The reversal of anticholinergic drug-induced delirium and coma with physostigmine. Am J Psychiatry 1971; **127**(8): p. 1050-4.

35. Ito, S, H Sasano, N Sasano, J Hayano, JA Fisher, and H Katsuya, Vagal nerve activity contributes to improve the efficiency of pulmonary gas exchange in hypoxic humans. Exp Physiol 2006; **91**(5): p. 935-41.

36. Marx, J, ed. *Rosen's Emergency Medicine: Concepts and Clinical Practice*. 6th ed., ed. J. Marx. Vol. 3. 2006, Mosby: St Louis MO.

37. Fryer, AD, PJ Lein, AS Howard, BL Yost, RA Beckles, and DA Jett, Mechanisms of organophosphate insecticide-induced airway hyperreactivity. Am J Physiol Lung Cell Mol Physiol 2004; **286**(5): p. L963-9.

38. Gralewicz, S, [Possible consequences of AChE inhibition in organophosphate poisoning. A new approach to an old problem]. Med Pr 1997; **48**(4): p. 469-72.

39. DOD. *Countermeasures against chemical threats (CounterACT) advanced development cooperative agreements.* 2007 [cited; Available from: grants.nih.gov/grants/rfa-files/RFA-NS-08-003.html.

40. Wadia, RS, S Chitra, RB Amin, RS Kiwalkar, and HV Sardesai, Electrophysiological studies in acute organophosphate poisoning. J Neurol Neurosurg Psychiatry 1987; **50**(11): p. 1442-8.

41. Gupta, RC and WD Dettbarn, Potential of memantine, D-tubocurarine, and atropine in preventing acute toxic myopathy induced by organophosphate nerve agents: soman, sarin, tabun and VX. Neurotoxicology 1992; **13**(3): p. 649-61.

42. Maselli, RA and BC Soliven, Analysis of the organophosphate-induced electromyographic response to repetitive nerve stimulation: paradoxical response to edrophonium and D-tubocurarine. Muscle Nerve 1991; **14**(12): p. 1182-8.

43. Abbrecht, PH, RR Kyle, and HJ Bryant, Pulmonary mechanical responses to cholinesterase inhibitor. Fundam Appl Toxicol 1989; **13**(3): p. 593-604.

44. Thompson, JW and RM Stocks, Brief bilateral vocal cord paralysis after insecticide poisoning. A new variant of toxicity syndrome. Arch Otolaryngol Head Neck Surg 1997; **123**(1): p. 93-6.

45. Fleming, NW, TR Henderson, and KL Dretchen, Mechanisms of respiratory failure produced by neostigmine and diisopropyl fluorophosphate. Eur J Pharmacol 1991; **195**(1): p. 85-91.

46. Rickett, DL, JF Glenn, and ET Beers, Central respiratory effects versus neuromuscular actions of nerve agents. Neurotoxicology 1986; **7**(1): p. 225-36.

47. Sahin, G, T Oruc, G Simsek, and I Guner, The effect of central and peripheral administration of acetylcholine and epinephrine on respiration. Indian J Physiol Pharmacol 1998; **42**(1): p. 20-4.

48. Gillis, RA, DP Walton, JA Quest, IJ Namath, P Hamosh, and KL Dretchen, Cardiorespiratory effects produced by activation of cholinergic muscarinic receptors on the ventral surface of the medulla. J Pharmacol Exp Ther 1988; **247**(2): p. 765-73.

49. Fung, ML and WM St John, Pontine cholinergic respiratory depression in neonatal and young rats. Life Sci 1998; **62**(24): p. 2249-56.

50. Shao, XM and JL Feldman, Cholinergic neurotransmission in the preBotzinger Complex modulates excitability of inspiratory neurons and regulates respiratory rhythm. Neuroscience 2005; **130**(4): p. 1069-81.

51. Bakima, M, HM Baudet, P Lekeux, and F Lomba, Respiratory and pulmonary haemodynamic changes during experimental organophosphate poisoning in goats. Vet Res Commun 1989; **13**(2): p. 127-33.

52. Segura, P, J Chavez, LM Montano, MH Vargas, A Delaunois, V Carbajal, and P Gustin, Identification of mechanisms involved in the acute airway toxicity induced by parathion. Naunyn Schmiedebergs Arch Pharmacol 1999; **360**(6): p. 699-710.

53. Delaunois, A, P Gustin, and M Ansay, Altered capillary filtration coefficient in parathion- and paraoxon-induced edema in isolated and perfused rabbit lungs. Toxicol Appl Pharmacol 1992; **116**(2): p. 161-9.

54. Bonham, AC and DR McCrimmon, Neurones in a discrete region of the nucleus tractus solitarius are required for the Breuer-Hering reflex in rat. J Physiol 1990; **427**: p. 261-80.

55. Hsieh, JH, YC Chang, CK Su, JC Hwang, CT Yen, and CY Chai, A single minute lesion around the ventral respiratory group in medulla produces fatal apnea in cats. J Auton Nerv Syst 1998; **73**(1): p. 7-18.

56. St John, WM and SC Wang, Integration of chemoreceptor stimuli by caudal pontile and rostral medullary sites. J Appl Physiol 1976; **41**(5 Pt. 1): p. 612-22.

57. Burton, MD and H Kazemi, Neurotransmitters in central respiratory control. Respir Physiol 2000; **122**(2-3): p. 111-21.

58. Mellen, NM, M Roham, and JL Feldman, Afferent modulation of neonatal rat respiratory rhythm in vitro: cellular and synaptic mechanisms. J Physiol 2004; **556**(Pt 3): p. 859-74.

59. Paintal, AS, The nature and effects of sensory inputs into the respiratory centers. Fed Proc 1977; **36**(10): p. 2428-32.

60. Coleridge, JC and HM Coleridge, Afferent vagal C fibre innervation of the lungs and airways and its functional significance. Rev Physiol Biochem Pharmacol 1984; **99**: p. 1-110.

61. Gaultier, C and JP Mortola, Hering-Breuer inflation reflex in young and adult mammals. Can J Physiol Pharmacol 1981; **59**(9): p. 1017-21.

62. Widdicombe, JG, Pulmonary and respiratory tract receptors. J Exp Biol 1982; **100**: p. 41-57.

63. Sant'Ambrogio, G, Afferent pathways for the cough reflex. Bull Eur Physiopathol Respir 1987; **23 Suppl 10**: p. 19s-23s.

64. Paydarfar, D, FL Eldridge, PG Wagner, and RT Dowell, Neural respiratory responses to cortically induced seizures in cats. Respir Physiol 1992; **89**(2): p. 225-37.

65. Jammes, Y, B Buchler, S Delpierre, A Rasidakis, C Grimaud, and C Roussos, Phrenic afferents and their role in inspiratory control. J Appl Physiol 1986; **60**(3): p. 854-60.

66. Yu, J and M Younes, Powerful respiratory stimulation by thin muscle afferents. Respir Physiol 1999; **117**(1): p. 1-12.

67. Orani, GP, JW Anderson, G Sant'Ambrogio, and FB Sant'Ambrogio, Upper airway cooling and l-menthol reduce ventilation in the guinea pig. J Appl Physiol 1991; **70**(5): p. 2080-6.

68. Shannon, R, Intercostal and abdominal muscle afferent influence on medullary dorsal respiratory group neurons. Respir Physiol 1980; **39**(1): p. 73-94.

69. Saponjic, J, M Radulovacki, and DW Carley, Modulation of respiratory pattern and upper airway muscle activity by the pedunculopontine tegmentum: role of NMDA receptors. Sleep Breath 2006; **10**(4): p. 195-202.

70. Bradley, DJ, JP Pascoe, JF Paton, and KM Spyer, Cardiovascular and respiratory responses evoked from the posterior cerebellar cortex and fastigial nucleus in the cat. J Physiol 1987; **393**: p. 107-21.

71. Roda, F, C Gestreau, and AL Bianchi, Discharge patterns of hypoglossal motoneurons during fictive breathing, coughing, and swallowing. J Neurophysiol 2002; **87**(4): p. 1703-11.

72. Li, PC, SC Li, YJ Lin, JT Liang, CT Chien, and CF Shaw, Thoracic vagal efferent nerve stimulation evokes substance p-induced early airway bronchonstriction and late proinflammatory and oxidative injury in the rat respiratory tract. J Biomed Sci 2005; **12**(4): p. 671-81.

73. Matran, R, K Alving, CR Martling, JS Lacroix, and JM Lundberg, Vagally mediated vasodilatation by motor and sensory nerves in the tracheal and bronchial circulation of the pig. Acta Physiol Scand 1989; **135**(1): p. 29-37.

74. Nandiwada, PA, AL Hyman, and PJ Kadowitz, Pulmonary vasodilator responses to vagal stimulation and acetylcholine in the cat. Circ Res 1983; **53**(1): p. 86-95.

75. Phipps, RJ and PS Richardson, The effects of irritation at various levels of the airway upon tracheal mucus secretion in the cat. J Physiol 1976; **261**(3): p. 563-81.

76. Schultz, HD, AM Roberts, C Bratcher, HM Coleridge, JC Coleridge, and B Davis, Pulmonary C-fibers reflexly increase secretion by tracheal submucosal glands in dogs. J Appl Physiol 1985; **58**(3): p. 907-10.

77. Krolo, M, EA Stuth, M Tonkovic-Capin, FA Hopp, DR McCrimmon, and EJ Zuperku, Relative magnitude of tonic and phasic synaptic excitation of medullary inspiratory neurons in dogs. Am J Physiol Regul Integr Comp Physiol 2000; **279**(2): p. R639-49.

78. Jordan, D, Central nervous pathways and control of the airways. Respir Physiol 2001; **125**(1-2): p. 67-81.

79. Haxhiu, MA, BO Erokwu, and NS Cherniack, The brainstem network involved in coordination of inspiratory activity and cholinergic outflow to the airways. J Auton Nerv Syst 1996; **61**(2): p. 155-61.

80. Douglas, CL, GJ Demarco, HA Baghdoyan, and R Lydic, Pontine and basal forebrain cholinergic interaction: implications for sleep and breathing. Respir Physiol Neurobiol 2004; **143**(2-3): p. 251-62.

81. Kubin, L and V Fenik, Pontine cholinergic mechanisms and their impact on respiratory regulation. Respir Physiol Neurobiol 2004; **143**(2-3): p. 235-49.

82. Dutschmann, M and H Herbert, Pontine cholinergic mechanisms enhance trigeminally evoked respiratory suppression in the anesthetized rat. J Appl Physiol 1999; **87**(3): p. 1059-65.

83. Yamada, KA, P Hamosh, and RA Gillis, Respiratory depression produced by activation of GABA receptors in hindbrain of cat. J Appl Physiol 1981; **51**(5): p. 1278-86.

84. Schmid, K, G Bohmer, and K Gebauer, Glycine receptor-mediated fast synaptic inhibition in the brainstem respiratory system. Respir Physiol 1991; **84**(3): p. 351-61.

85. Hayashi, F and J Lipski, The role of inhibitory amino acids in control of respiratory motor output in an arterially perfused rat. Respir Physiol 1992; **89**(1): p. 47-63.

86. Anderson, MK and DF Speck, Differential effects of excitatory amino acid receptor antagonism in the ventral respiratory group. Brain Res 1999; **829**(1-2): p. 69-76.

87. Onimaru, H and I Homma, Point:Counterpoint: The parafacial respiratory group (pFRG)/pre-Botzinger complex (preBotC) is the primary site of respiratory rhythm generation in the mammal. Point: the PFRG is the primary site of respiratory rhythm generation in the mammal. J Appl Physiol 2006; **100**(6): p. 2094-5.

88. Feldman, JL and WA Janczewski, Point:Counterpoint: The parafacial respiratory group (pFRG)/pre-Botzinger complex (preBotC) is the primary site of respiratory rhythm generation in the mammal. Counterpoint: the

preBotC is the primary site of respiratory rhythm generation in the mammal. J Appl Physiol 2006; **100**(6): p. 2096-7; discussion 2097-9, 2103-8.

89. Smith, JC, HH Ellenberger, K Ballanyi, DW Richter, and JL Feldman, Pre-Botzinger complex: a brainstem region that may generate respiratory rhythm in mammals. Science 1991; **254**(5032): p. 726-9.

90. Mulkey, DK, RL Stornetta, MC Weston, JR Simmons, A Parker, DA Bayliss, and PG Guyenet, Respiratory control by ventral surface chemoreceptor neurons in rats. Nat Neurosci 2004; **7**(12): p. 1360-9.

91. Hori, T, GI Roth, and WS Yamamoto, Respiratory sensitivity of rat brain-stem surface to chemical stimuli. J Appl Physiol 1970; **28**(6): p. 721-4.

92. Putnam, RW, JA Filosa, and NA Ritucci, Cellular mechanisms involved in CO(2) and acid signaling in chemosensitive neurons. Am J Physiol Cell Physiol 2004; **287**(6): p. C1493-526.

93. Bruce, EN and NS Cherniack, Central chemoreceptors. J Appl Physiol 1987; **62**(2): p. 389-402.

94. Nattie, EE and A Li, Central chemoreception in the region of the ventral respiratory group in the rat. J Appl Physiol 1996; **81**(5): p. 1987-95.

95. Mitchell, RL, HH. Massion, WH. Severinghaus JW, Respiratory responses mediated through superficial chemosensitive areas on the medulla. J Appl Physiol 1963; **18**: p. 523-533.

96. Nattie, EE and AH Li, Ventral medulla sites of muscarinic receptor subtypes involved in cardiorespiratory control. J Appl Physiol 1990; **69**(1): p. 33-41.

97. Burton, MD, DC Johnson, and H Kazemi, CSF acidosis augments ventilation through cholinergic mechanisms. J Appl Physiol 1989; **66**(6): p. 2565-72.

98. Iturriaga, R, Carotid body chemoreception: the importance of CO2-HCO3- and carbonic anhydrase. (review). Biol Res 1993; **26**(3): p. 319-29.

99. Lopez-Barneo, J, P Ortega-Saenz, R Pardal, A Pascual, and JI Piruat, Carotid body oxygen sensing. Eur Respir J 2008; **32**(5): p. 1386-98.

100. Haji, A, R Takeda, and M Okazaki, Neuropharmacology of control of respiratory rhythm and pattern in mature mammals. Pharmacol Ther 2000; **86**(3): p. 277-304.

101. Mizusawa, A, H Ogawa, Y Kikuchi, W Hida, H Kurosawa, S Okabe, T Takishima, and K Shirato, In vivo release of glutamate in nucleus tractus solitarii of the rat during hypoxia. J Physiol 1994; **478 (Pt 1)**: p. 55-66.

102. Orem, J, A Netick, and WC Dement, Breathing during sleep and wakefulness in the cat. Respir Physiol 1977; **30**(3): p. 265-89.

103. Orem, J and CA Anderson, Diaphragmatic activity during REM sleep in the adult cat. J Appl Physiol 1996; **81**(2): p. 751-60.

104. Steriade, M, S Datta, D Pare, G Oakson, and RC Curro Dossi, Neuronal activities in brain-stem cholinergic nuclei related to tonic activation processes in thalamocortical systems. J Neurosci 1990; **10**(8): p. 2541-59.

105. Kayama, Y, M Ohta, and E Jodo, Firing of 'possibly' cholinergic neurons in the rat laterodorsal tegmental nucleus during sleep and wakefulness. Brain Res 1992; **569**(2): p. 210-20.

106. Kayama, Y and Y Koyama, Brainstem neural mechanisms of sleep and wakefulness. Eur Urol 1998; **33 Suppl 3**: p. 12-5.

107. Rukhadze, I and L Kubin, Mesopontine cholinergic projections to the hypoglossal motor nucleus. Neurosci Lett 2007; **413**(2): p. 121-5.

108. Steininger, TL, DB Rye, and BH Wainer, Afferent projections to the cholinergic pedunculopontine tegmental nucleus and adjacent midbrain extrapyramidal area in the albino rat. I. Retrograde tracing studies. J Comp Neurol 1992; **321**(4): p. 515-43.

109. Taguchi, O, L Kubin, and AI Pack, Evocation of postural atonia and respiratory depression by pontine carbachol in the decerebrate rat. Brain Res 1992; **595**(1): p. 107-15.

110. Langhorst, P, B Schulz, G Schulz, and M Lambertz, Reticular formation of the lower brainstem. A common system for cardiorespiratory and somatomotor functions: discharge patterns of neighboring neurons influenced by cardiovascular and respiratory afferents. J Auton Nerv Syst 1983; **9**(2-3): p. 411-32.

111. Rogers, DF, Motor control of airway goblet cells and glands. Respir Physiol 2001; **125**(1-2): p. 129-44.

112. Altiere, RJ, DC Travis, J Roberts, and DC Thompson, Pharmacological characterization of muscarinic receptors mediating acetylcholine-induced

contraction and relaxation in rabbit intrapulmonary arteries. J Pharmacol Exp Ther 1994; **270**(1): p. 269-76.

113. Sada, K, M Shirai, and I Ninomiya, Vagally and acetylcholine-mediated constriction in small pulmonary vessels of rabbits. J Appl Physiol 1987; **63**(4): p. 1601-9.

114. Holtzman, MJ, MP McNamara, D Sheppard, LM Fabbri, HL Hahn, PD Graf, and JA Nadel, Intravenous versus inhaled atropine for inhibiting bronchoconstrictor responses in dogs. J Appl Physiol 1983; **54**(1): p. 134-9.

115. Fisher, JT, SG Vincent, J Gomeza, M Yamada, and J Wess, Loss of vagally mediated bradycardia and bronchoconstriction in mice lacking M2 or M3 muscarinic acetylcholine receptors. Faseb J 2004; **18**(6): p. 711-3.

116. Fernandes, LB, AD Fryer, and CA Hirshman, M2 muscarinic receptors inhibit isoproterenol-induced relaxation of canine airway smooth muscle. J Pharmacol Exp Ther 1992; **262**(1): p. 119-26.

117. Reinheimer, T, T Mohlig, S Zimmermann, KD Hohle, and I Wessler, Muscarinic control of histamine release from airways. Inhibitory M1-receptors in human bronchi but absence in rat trachea. Am J Respir Crit Care Med 2000; **162**(2 Pt 1): p. 534-8.

118. Moffatt, JD, TM Cocks, and CP Page, Role of the epithelium and acetylcholine in mediating the contraction to 5-hydroxytryptamine in the mouse isolated trachea. Br J Pharmacol 2004; **141**(7): p. 1159-66.

119. Shioya, T, J Solway, NM Munoz, M Mack, and AR Leff, Distribution of airway contractile responses within the major diameter bronchi during exogenous bronchoconstriction. Am Rev Respir Dis 1987; **135**(5): p. 1105-11.

120. Levitzky, MG, *Pulmonary Physiology*. Lange Physiology Series, ed. M.G. Levitzky. 2003, Philadelphia, PA: McGraw-Hill Professional.

121. Ming, Z and DX Wang, Sympathetic innervation of pulmonary circulation and its role in hypoxic pulmonary vasoconstriction. J Tongji Med Univ 1989; **9**(3): p. 153-9.

122. Conzen, P, A Goetz, W Oettinger, and W Brendel, Hypoxic pulmonary vasoconstriction and endogenous prostaglandin (PG) and thromboxane (TX) release in anesthetized pigs. Biomed Biochim Acta 1984; **43**(8-9): p. S265-8.

123. Lindenschmidt, RC, CE Patterson, RB Forney, and RA Rhoades, Selective action of prostaglandin F2 alpha during paraquat-induced pulmonary edema in the perfused lung. Toxicol Appl Pharmacol 1983; **70**(1): p. 105-14.

124. Feddersen, CO, MM Mathias, IF McMurtry, and NF Voelkel, Acetylcholine induces vasodilation and prostacyclin synthesis in rat lungs. Prostaglandins 1986; **31**(5): p. 973-87.

125. van der Velden, VH and AR Hulsmann, Autonomic innervation of human airways: structure, function, and pathophysiology in asthma. Neuroimmunomodulation 1999; **6**(3): p. 145-59.

126. Ide, H, H Nakano, T Ogasa, S Osanai, K Kikuchi, and J Iwamoto, Regulation of pulmonary circulation by alveolar oxygen tension via airway nitric oxide. J Appl Physiol 1999; **87**(5): p. 1629-36.

127. Wagerle, LC and DW Busija, Cholinergic mechanisms in the cerebral circulation of the newborn piglet: effect of inhibitors of arachidonic acid metabolism. Circ Res 1989; **64**(5): p. 1030-6.

128. Wadsworth, RM, Vasoconstrictor and vasodilator effects of hypoxia. Trends Pharmacol Sci 1994; **15**(2): p. 47-53.

129. Peatfield, AC and PS Richardson, The action of dust in the airways on secretion into the trachea of the cat. J Physiol 1983; **342**: p. 327-34.

130. Haxhiu, MA, B Haxhiu-Poskurica, V Moracic, WA Carlo, and RJ Martin, Reflex and chemical responses of tracheal submucosal glands in piglets. Respir Physiol 1990; **82**(3): p. 267-77.

131. Racke, K, UR Juergens, and S Matthiesen, Control by cholinergic mechanisms. Eur J Pharmacol 2006; **533**(1-3): p. 57-68.

132. Koyama, S, SI Rennard, and RA Robbins, Acetylcholine stimulates bronchial epithelial cells to release neutrophil and monocyte chemotactic activity. Am J Physiol 1992; **262**(4 Pt 1): p. L466-71.

133. Brunn, G, I Wessler, and K Racke, Mucosa-dependent muscarinic liberation of prostaglandins from rat isolated trachea. Br J Pharmacol 1995; **116**(3): p. 1991-8.

134. Freitag, A, I Wessler, and K Racke, Adrenoceptor- and cholinoceptor-mediated mechanisms in the regulation of 5-hydroxytryptamine release

from isolated tracheae of newborn rabbits. Br J Pharmacol 1996; **119**(1): p. 91-8.

135. Sato, E, S Koyama, Y Okubo, K Kubo, and M Sekiguchi, Acetylcholine stimulates alveolar macrophages to release inflammatory cell chemotactic activity. Am J Physiol 1998; **274**(6 Pt 1): p. L970-9.

136. Borovikova, LV, S Ivanova, M Zhang, H Yang, GI Botchkina, LR Watkins, H Wang, N Abumrad, JW Eaton, and KJ Tracey, Vagus nerve stimulation attenuates the systemic inflammatory response to endotoxin. Nature 2000; **405**(6785): p. 458-62.

137. Blanchet, MR, E Israel-Assayag, and Y Cormier, Inhibitory effect of nicotine on experimental hypersensitivity pneumonitis in vivo and in vitro. Am J Respir Crit Care Med 2004; **169**(8): p. 903-9.

138. Lee, LY and TE Pisarri, Afferent properties and reflex functions of bronchopulmonary C-fibers. Respir Physiol 2001; **125**(1-2): p. 47-65.

139. Martin, MA and HJ Silverman, Gram-negative sepsis and the adult respiratory distress syndrome. Clin Infect Dis 1992; **14**(6): p. 1213-28.

140. Nagase, T, N Uozumi, S Ishii, K Kume, T Izumi, Y Ouchi, and T Shimizu, Acute lung injury by sepsis and acid aspiration: a key role for cytosolic phospholipase A2. Nat Immunol 2000; **1**(1): p. 42-6.

141. Melton, SM, KA Davis, CB Moomey, Jr., TC Fabian, and KG Proctor, Mediator-dependent secondary injury after unilateral blunt thoracic trauma. Shock 1999; **11**(6): p. 396-402.

142. Roberts, AM, J Bhattacharya, HD Schultz, HM Coleridge, and JC Coleridge, Stimulation of pulmonary vagal afferent C-fibers by lung edema in dogs. Circ Res 1986; **58**(4): p. 512-22.

143. Widdicombe, JG, Neural control of airway vasculature and edema. Am Rev Respir Dis 1991; **143**(3 Pt 2): p. S18-21.

144. Sant'Ambrogio, G, Afferent nerves in reflex bronchoconstriction. Bull Eur Physiopathol Respir 1987; **23 Suppl 10**: p. 81s-88s.

145. Stavinoha, WB, AT Modak, and ST Weintraub, Rate of accumulation of acetylcholine in discrete regions of the rat brain after dichlorvos treatment. J Neurochem 1976; **27**(6): p. 1375-8.

146. Jarvie, EM, S Cellek, and GJ Sanger, Potentiation by cholinesterase inhibitors of cholinergic activity in rat isolated stomach and colon. Pharmacol Res 2008; **58**(5-6): p. 297-301.

147. Bian, XC, JC Bornstein, and PP Bertrand, Nicotinic transmission at functionally distinct synapses in descending reflex pathways of the rat colon. Neurogastroenterol Motil 2003; **15**(2): p. 161-71.

148. Hubel, KA, Intestinal nerves and ion transport: stimuli, reflexes, and responses. Am J Physiol 1985; **248**(3 Pt 1): p. G261-71.

149. Buckley, N and G Burnstock, Autoradiographic localisation of muscarinic receptors in guinea-pig intestine: distribution of high and low affinity agonist binding sites. Brain Res 1984; **294**(1): p. 15-22.

150. Wang, P, GR Luthin, and MR Ruggieri, Muscarinic acetylcholine receptor subtypes mediating urinary bladder contractility and coupling to GTP binding proteins. J Pharmacol Exp Ther 1995; **273**(2): p. 959-66.

151. Hegde, SS, A Choppin, D Bonhaus, S Briaud, M Loeb, TM Moy, D Loury, and RM Eglen, Functional role of M2 and M3 muscarinic receptors in the urinary bladder of rats in vitro and in vivo. Br J Pharmacol 1997; **120**(8): p. 1409-18.

152. Fuder, H, Functional consequences of prejunctional receptor activation or blockade in the iris. J Ocul Pharmacol 1994; **10**(1): p. 109-23.

153. Chiba, S, T Kimura, and K Hashimoto, Muscarinic suppression of the nicotinic action of acetylcholine on the isolated, blood-perfused atrium of the dog. Naunyn Schmiedebergs Arch Pharmacol 1975; **289**(3): p. 315-25.

154. Criscione, L, DJ Reis, and WT Talman, Cholinergic mechanisms in the nucleus tractus solitarii and cardiovascular regulation in the rat. Eur J Pharmacol 1983; **88**(1): p. 47-55.

155. Brezenoff, HE, Cardiovascular regulation by brain acetylcholine. Fed Proc 1984; **43**(1): p. 17-20.

156. Krstic, MK and D Djurkovic, Cardiovascular response to intracerebroventricular administration of acetylcholine in rats. Neuropharmacology 1978; **17**(6): p. 341-7.

157. Haxhiu, MA, P Kc, CT Moore, SS Acquah, CG Wilson, SI Zaidi, VJ Massari, and DG Ferguson, Brain stem excitatory and inhibitory signaling

pathways regulating bronchoconstrictive responses. J Appl Physiol 2005; **98**(6): p. 1961-82.

158. Roth, SH, B Schofield, and JC Yates, Effects of atropine on secretion and motility in isolated gastric mucosa and attached muscularis externa from ferret and cat. J Physiol 1979; **292**: p. 351-61.

159. Katschinski, M, C Steinicke, M Reinshagen, G Dahmen, C Beglinger, R Arnold, and G Adler, Gastrointestinal motor and secretory responses to cholinergic stimulation in humans. Differential modulation by muscarinic and cholecystokinin receptor blockade. Eur J Clin Invest 1995; **25**(2): p. 113-22.

160. Pedigo, NW, Jr. and KR Brizzee, Muscarinic cholinergic receptors in area postrema and brainstem areas regulating emesis. Brain Res Bull 1985; **14**(2): p. 169-77.

161. Nakamura, M, Y Tada, T Akaishi, and K Nakata, M3 muscarinic receptor mediates regulation of protein secretion in rabbit lacrimal gland. Curr Eye Res 1997; **16**(6): p. 614-9.

162. Lung, MA, Autonomic nervous control of myoepithelial cells and secretion in submandibular gland of anaesthetized dogs. J Physiol 2003; **546**(Pt 3): p. 837-50.

163. Vreugdenhil, AP, GL de Lange, AV Nieuw Amerongen, and PA Roukema, Morphological changes in the salivary glands upon stimulation by receptor-selective agonists. II. Submandibular glands of the mouse. J Biol Buccale 1980; **8**(1): p. 73-86.

164. Vreugdenhil, AP, GL de Lange, AV Nieuw Amerongen, and PA Roukema, Morphological changes in the salivary glands upon stimulation by receptor-selective agonists. III. Sublingual glands of the mouse. J Biol Buccale 1980; **8**(1): p. 87-98.

165. Gupta, RC, GT Patterson, and WD Dettbarn, Mechanisms of toxicity and tolerance to diisopropylphosphorofluoridate at the neuromuscular junction of the rat. Toxicol Appl Pharmacol 1986; **84**(3): p. 541-50.

166. Adams, GK, 3rd, HI Yamamura, and JF O'Leary, Recovery of central respiratory function following anticholinesterase intoxication. Eur J Pharmacol 1976; **38**(1): p. 101-12.

167. Tuovinen, K, Organophosphate-induced convulsions and prevention of neuropathological damages. Toxicology 2004; **196**(1-2): p. 31-9.

168. Takahashi, H, T Kojima, T Ikeda, S Tsuda, and Y Shirasu, Differences in the mode of lethality produced through intravenous and oral administration of organophosphorus insecticides in rats. Fundam Appl Toxicol 1991; **16**(3): p. 459-68.

169. Dettbarn, WD, Pesticide induced muscle necrosis: mechanisms and prevention. Fundam Appl Toxicol 1984; **4**(2 Pt 2): p. S18-26.

170. Okudera, H, Clinical features on nerve gas terrorism in Matsumoto. J Clin Neurosci 2002; **9**(1): p. 17-21.

171. Tafuri, J and J Roberts, Organophosphate poisoning. Ann Emerg Med 1987; **16**(2): p. 193-202.

172. Hayes, W and E Laws, *Handbook of Pesticide Toxicology*, ed. W. Hayes and E. Laws. 1991, San Diego, CA: Academic Press.

173. Burton, MD, M Nouri, and H Kazemi, Acetylcholine and central respiratory control: perturbations of acetylcholine synthesis in the isolated brainstem of the neonatal rat. Brain Res 1995; **670**(1): p. 39-47.

174. Anzueto, A, GG Berdine, GT Moore, C Gleiser, D Johnson, CD White, and WG Johanson, Jr., Pathophysiology of soman intoxication in primates. Toxicol Appl Pharmacol 1986; **86**(1): p. 56-68.

175. Davis, GM, AL Coates, D Dalle, and MA Bureau, Measurement of pulmonary mechanics in the newborn lamb: a comparison of three techniques. J Appl Physiol 1988; **64**(3): p. 972-81.

176. Armitage, P and G Berry, *Statistical Methods in Medical Research*. Second ed. 2001, Boston, MA: Blackwell Scientific. 832.

177. Perkin, RM and DB Resnik, The agony of agonal respiration: is the last gasp necessary? J Med Ethics 2002; **28**(3): p. 164-9.

178. Sanocka, UM, DF Donnelly, and GG Haddad, Autoresuscitation: a survival mechanism in piglets. J Appl Physiol 1992; **73**(2): p. 749-53.

179. Asari, Y, Y Kamijyo, and K Soma, Changes in the hemodynamic state of patients with acute lethal organophosphate poisoning. Vet Hum Toxicol 2004; **46**(1): p. 5-9.

180. St John, WM and KV Knuth, A characterization of the respiratory pattern of gasping. J Appl Physiol 1981; **50**(5): p. 984-93.

181. Stockton, JM, NJ Birdsall, AS Burgen, and EC Hulme, Modification of the binding properties of muscarinic receptors by gallamine. Mol Pharmacol 1983; **23**(3): p. 551-7.

182. Lazareno, S, A Popham, and NJ Birdsall, Allosteric interactions of staurosporine and other indolocarbazoles with N-[methyl-(3)H]scopolamine and acetylcholine at muscarinic receptor subtypes: identification of a second allosteric site. Mol Pharmacol 2000; **58**(1): p. 194-207.

183. Lai, J, XM Shao, RW Pan, E Dy, CH Huang, and JL Feldman, RT-PCR reveals muscarinic acetylcholine receptor mRNA in the pre-Botzinger complex. Am J Physiol Lung Cell Mol Physiol 2001; **281**(6): p. L1420-4.

184. Morin-Surun, MP, J Champagnat, M Denavit-Saubie, and S Moyanova, The effects of acetylcholine on bulbar respiratory related neurones. Consequences of anaesthesia by pentobarbital. Naunyn Schmiedebergs Arch Pharmacol 1984; **325**(3): p. 205-8.

185. Fryer, AD and J Maclagan, Pancuronium and gallamine are antagonists for pre- and post-junctional muscarinic receptors in the guinea-pig lung. Naunyn Schmiedebergs Arch Pharmacol 1987; **335**(4): p. 367-71.

186. Gaspari, RJ and D Paydarfar, Pathophysiology of respiratory failure following acute dichlorvos poisoning in a rodent model. Neurotoxicology 2007; **28**(3): p. 664-71.

187. Shao, XM and JL Feldman, Pharmacology of nicotinic receptors in preBotzinger complex that mediate modulation of respiratory pattern. J Neurophysiol 2002; **88**(4): p. 1851-8.

188. Shao, XM and JL Feldman, Acetylcholine modulates respiratory pattern: effects mediated by M3-like receptors in preBotzinger complex inspiratory neurons. J Neurophysiol 2000; **83**(3): p. 1243-52.

189. Endoh, T, Muscarinic M2 receptor inhibition of calcium current in rat nucleus tractus solitarius. Neuroreport 2007; **18**(11): p. 1141-5.

190. Chamberlin, NL, CM Bocchiaro, RW Greene, and JL Feldman, Nicotinic excitation of rat hypoglossal motoneurons. Neuroscience 2002; **115**(3): p. 861-70.

191. Eugenin, J and JG Nicholls, Chemosensory and cholinergic stimulation of fictive respiration in isolated CNS of neonatal opossum. J Physiol 1997; **501 (Pt 2)**: p. 425-37.

192. Woch, G, H Ogawa, RO Davies, and L Kubin, Behavior of hypoglossal inspiratory premotor neurons during the carbachol-induced, REM sleep-like suppression of upper airway motoneurons. Exp Brain Res 2000; **130**(4): p. 508-20.

193. Haji, A, S Furuichi, and R Takeda, Effects on iontophoretically applied acetylcholine on membrane potential and synaptic activity of bulbar respiratory neurones in decerebrate cats. Neuropharmacology 1996; **35**(2): p. 195-203.

194. Nattie, EE, J Wood, A Mega, and W Goritski, Rostral ventrolateral medulla muscarinic receptor involvement in central ventilatory chemosensitivity. J Appl Physiol 1989; **66**(3): p. 1462-70.

195. Jordan, D and KM Spyer, Effects of acetylcholine on respiratory neurones in the nucleus ambiguus-retroambigualis complex of the cat. J Physiol 1981; **320**: p. 103-11.

196. Delaunois, A, P Gustin, and M Ansay, Multiple muscarinic receptor subtypes mediating pulmonary oedema in the rabbit. Pulm Pharmacol 1994; **7**(3): p. 185-93.

197. Haberberger, RV, M Bodenbenner, and W Kummer, Expression of the cholinergic gene locus in pulmonary arterial endothelial cells. Histochem Cell Biol 2000; **113**(5): p. 379-87.

198. Gosens, R, J Zaagsma, M Grootte Bromhaar, A Nelemans, and H Meurs, Acetylcholine: a novel regulator of airway smooth muscle remodelling? Eur J Pharmacol 2004; **500**(1-3): p. 193-201.

199. Reinheimer, T, P Bernedo, H Klapproth, H Oelert, B Zeiske, K Racke, and I Wessler, Acetylcholine in isolated airways of rat, guinea pig, and human: species differences in role of airway mucosa. Am J Physiol 1996; **270**(5 Pt 1): p. L722-8.

200. Taylor, P, *ANTICHOLINESTERASE AGENTS* 11th ed. Goodman & Gilman's The Pharmacological Basis of Therapeutics, ed. L.L. Brunton. 2006, New York: McGraw-Hill.

201. el-Kashef, H and JD Catravas, The nature of muscarinic receptor subtypes mediating pulmonary vasoconstriction in the rabbit. Pulm Pharmacol 1991; **4**(1): p. 8-19.

202. De Michele, M, C Cavallotti, and F Amenta, Autoradiographic localization of muscarinic acetylcholine receptors in the rat pulmonary vascular tree. Eur J Pharmacol 1991; **192**(1): p. 71-8.

203. Leff, AR, NM Munoz, J Tallet, AC David, MA Cavigelli, and ER Garrity, Autonomic response characteristics of porcine airway smooth muscle in vivo. J Appl Physiol 1985; **58**(4): p. 1176-88.

204. Garssen, J, H Van Loveren, CM Gierveld, H Van der Vliet, and FP Nijkamp, Functional characterization of muscarinic receptors in murine airways. Br J Pharmacol 1993; **109**(1): p. 53-60.

205. Barnes, PJ, JA Nadel, JM Roberts, and CB Basbaum, Muscarinic receptors in lung and trachea: autoradiographic localization using [3H]quinuclidinyl benzilate. Eur J Pharmacol 1982; **86**(1): p. 103-6.

206. van Koppen, CJ, WM Blankesteijn, AB Klaassen, JF Rodrigues de Miranda, AJ Beld, and CA van Ginneken, Autoradiographic visualization of muscarinic receptors in human bronchi. J Pharmacol Exp Ther 1988; **244**(2): p. 760-4.

207. Mak, JC and PJ Barnes, Autoradiographic visualization of muscarinic receptor subtypes in human and guinea pig lung. Am Rev Respir Dis 1990; **141**(6): p. 1559-68.

208. Homma, I, H Onimaru, M Oouchi, and S Ichikawa, The effects of high-frequency inflation and high-frequency deflation on respiration in rabbits. Neurosci Lett 1985; **60**(3): p. 307-11.

209. Kubin, L, GF Alheid, EJ Zuperku, and DR McCrimmon, Central pathways of pulmonary and lower airway vagal afferents. J Appl Physiol 2006; **101**(2): p. 618-27.

210. Coleridge, HM and JC Coleridge, Neural regulation of bronchial blood flow. Respir Physiol 1994; **98**(1): p. 1-13.

211. Haxhiu, MA, E Van Lunteren, and NS Cherniack, Influence of ventrolateral surface of medulla on tracheal gland secretion. J Appl Physiol 1991; **71**(5): p. 1663-8.

212. Haxhiu, MA, NS Cherniack, and KP Strohl, Reflex responses of laryngeal and pharyngeal submucosal glands in dogs. J Appl Physiol 1991; **71**(5): p. 1669-73.

213. Castenfors, J and T Sjostrand, Circulatory control via vagal afferents. I. Adjustment of heart rate to variations of blood volume in the rat. Acta Physiol Scand 1972; **84**(3): p. 347-54.

214. Golder, FJ, DD Fuller, PW Davenport, RD Johnson, PJ Reier, and DC Bolser, Respiratory motor recovery after unilateral spinal cord injury: eliminating crossed phrenic activity decreases tidal volume and increases contralateral respiratory motor output. J Neurosci 2003; **23**(6): p. 2494-501.

215. larrabee, M and G knowlton, Excitation and Inhibition of phrenic motoneurons by inflation of the lungs. Am J Physiol 1946; **147**: p. 90-96.

216. Naidu, KA, S Viswanatha, and MK Krishnakumari, Cardiotoxic effects of dichlorvos (DDVP) in albino rats. Indian J Physiol Pharmacol 1987; **31**(1): p. 19-24.

217. Karki, P, JA Ansari, S Bhandary, and S Koirala, Cardiac and electrocardiographical manifestations of acute organophosphate poisoning. Singapore Med J 2004; **45**(8): p. 385-9.

218. Smith, EC, B Padnos, and CJ Cordon, Peripheral versus central muscarinic effects on blood pressure, cardiac contractility, heart rate, and body temperature in the rat monitored by radiotelemetry. Pharmacol Toxicol 2001; **89**(1): p. 35-42.

219. Ben-Ami, H, SA Ben-Haim, Y Edoute, G Hayam, and U Taitelman, Direct effects of phosphamidon on isolated working rat heart electrical and mechanical function. Toxicol Appl Pharmacol 1991; **110**(3): p. 429-34.

220. Marshall, JM and JD Metcalfe, Influences on the cardiovascular response to graded levels of systemic hypoxia of the accompanying hypocapnia in the rat. J Physiol 1989; **410**: p. 381-94.

221. Nadel, JA, GA Cabezas, and JH Austin, In vivo roentgenographic examination of parasympathetic innervation of small airways. Use of powdered tantalum and a fine focal spot x-ray tube. Invest Radiol 1971; **6**(1): p. 9-17.

222. Nadel, JA and PJ Barnes, Autonomic regulation of the airways. Annu Rev Med 1984; **35**: p. 451-67.

223. Murao, H, Nervous regulation of the bronchial vascular system. Jpn Circ J 1965; **29**(9): p. 855-65.

224. Gal, TJ and PM Suratt, Atropine and glycopyrrolate effects on lung mechanics in normal man. Anesth Analg 1981; **60**(2): p. 85-90.

225. Wilson, PS, PL Khimenko, JW Barnard, TM Moore, and AE Taylor, Muscarinic agonists and antagonists cause vasodilation in isolated rat lung. J Appl Physiol 1995; **78**(4): p. 1404-11.

226. Merrick, A, WM Hadley, and TL Holcslaw, The effect of large doses of atropine sulfate on heart rate and blood pressure in rats. Res Commun Chem Pathol Pharmacol 1979; **25**(1): p. 13-22.

227. Merrick, BA and TL Holcslaw, Direct vasodilator activity of atropine in the rat perfused hindlimb preparation. Clin Exp Pharmacol Physiol 1981; **8**(3): p. 277-81.

228. Urso, R, G Segre, E Bianchi, G Bruni, P Dal Pra, and AI Fiaschi, Plasma kinetics of atropine and ipratropium in rats after different routes of administration evaluated by a radioreceptor assay. Eur J Drug Metab Pharmacokinet 1991; **Spec No 3**: p. 111-5.

229. Baile, EM, S Osborne, and PD Pare, Effect of autonomic blockade on tracheobronchial blood flow. J Appl Physiol 1987; **62**(2): p. 520-5.

230. Raff, H, Evaluation of a blood sample-transfusion protocol in rats: blood gases, renin, and ACTH. Am J Physiol 1988; **255**(5 Pt 2): p. R851-4.

231. Guntheroth, WG and I Kawabori, Hypoxic apnea and gasping. J Clin Invest 1975; **56**(6): p. 1371-7.

232. St John, WM, D Zhou, and RF Fregosi, Expiratory neural activities in gasping. J Appl Physiol 1989; **66**(1): p. 223-31.

233. Yang, L, MH Weil, M Noc, W Tang, T Turner, and RJ Gazmuri, Spontaneous gasping increases the ability to resuscitate during experimental cardiopulmonary resuscitation. Crit Care Med 1994; **22**(5): p. 879-83.

234. Manole, MD, RW Hickey, N Momoi, K Tobita, JP Tinney, GP Suciu, MJ Johnnides, RS Clark, and BB Keller, Preterminal gasping during hypoxic cardiac arrest increases cardiac function in immature rats. Pediatr Res 2006; **60**(2): p. 174-9.

235. St John, WM and D Bartlett, Jr., Comparison of phrenic motoneuron activity during eupnea and gasping. J Appl Physiol 1981; **50**(5): p. 994-8.

236. St John, WM, Neurogenesis, control, and functional significance of gasping. J Appl Physiol 1990; **68**(4): p. 1305-15.

237. Ramirez, JM, SW Schwarzacher, O Pierrefiche, BM Olivera, and DW Richter, Selective lesioning of the cat pre-Botzinger complex in vivo eliminates breathing but not gasping. J Physiol 1998; **507 (Pt 3)**: p. 895-907.

238. St John, WM, Rostral medullary respiratory neuronal activities of decerebrate cats in eupnea, apneusis and gasping. Respir Physiol 1999; **116**(1): p. 47-65.

239. Potts, JT and JF Paton, Optical imaging of medullary ventral respiratory network during eupnea and gasping in situ. Eur J Neurosci 2006; **23**(11): p. 3025-33.

240. Lieske, SP, M Thoby-Brisson, P Telgkamp, and JM Ramirez, Reconfiguration of the neural network controlling multiple breathing patterns: eupnea, sighs and gasps [see comment]. Nat Neurosci 2000; **3**(6): p. 600-7.

241. Watt, JG, D P.R., and C J.H., Effects of inhalation of 100 per cent ocygen upon respiration of ananesthetized dogs before and after chemoreceptor denervation. . Am J Physiol 1942; **138**: p. 610-617.

242. Coles, SK and TE Dick, Neurones in the ventrolateral pons are required for post-hypoxic frequency decline in rats. J Physiol 1996; **497 (Pt 1)**: p. 79-94.

243. Fung, ML, W Wang, and WM St John, Medullary loci critical for expression of gasping in adult rats. J Physiol 1994; **480 (Pt 3)**: p. 597-611.

244. Wright, AS, DH Hutson, and MF Wooder, The chemical and biochemical reactivity of dichlorvos. Arch Toxicol 1979; **42**(1): p. 1-18.

245. Blair, D, C Hoadley, and DH Hutson, The distribution of dichlorvos in the tissues of mammals after its inhalation or intravenous administration. Toxicol Appl Pharmacol 1975; **31**(2): p. 243-53.

246. *Toxical profiles of dichlorvos*, U.S.D.O.H.A.H. SERVICES, Editor. 1997, Agency for Toxic Substances and Disease Registry.

247. Arieli, R, D Kerem, and Y Melamed, Hyperoxic exposure affects the ventilatory response to hypoxia in awake rats. J Appl Physiol 1988; **64**(1): p. 181-6.

248. Arieli, R, Normoxic, hyperoxic, and hypoxic ventilation in rats continuously exposed for 60 h to 1 ATA O2. Aviat Space Environ Med 1994; **65**(12): p. 1122-7.

249. Chang, E, K Hornick, KI Fritz, OP Mishra, and M Delivoria-Papadopoulos, Effect of hyperoxia on cortical neuronal nuclear function and programmed cell death mechanisms. Neurochem Res 2007; **32**(7): p. 1142-9.

250. Dean, JB, DK Mulkey, RA Henderson, 3rd, SJ Potter, and RW Putnam, Hyperoxia, reactive oxygen species, and hyperventilation: oxygen sensitivity of brain stem neurons. J Appl Physiol 2004; **96**(2): p. 784-91.

251. Kolbitsch, C, IH Lorenz, C Hormann, M Hinteregger, A Lockinger, PL Moser, C Kremser, M Schocke, S Felber, KP Pfeiffer, and A Benzer, The influence of hyperoxia on regional cerebral blood flow (rCBF), regional cerebral blood volume (rCBV) and cerebral blood flow velocity in the middle cerebral artery (CBFVMCA) in human volunteers. Magn Reson Imaging 2002; **20**(7): p. 535-41.

252. St-John, WM, Neurogenesis of patterns of automatic ventilatory activity. Prog Neurobiol 1998; **56**(1): p. 97-117.

253. Richter, DW, Generation and maintenance of the respiratory rhythm. J Exp Biol 1982; **100**: p. 93-107.

254. Badr, MS and A Kawak, Post-hyperventilation hypopnea in humans during NREM sleep. Respir Physiol 1996; **103**(2): p. 137-45.

255. Mangin, P, J Krieger, and D Kurtz, Apnea following hyperventilation in man. J Neurol Sci 1982; **57**(1): p. 67-82.

256. Prabhakar, NR, J Mitra, JL Overholt, and NS Cherniack, Analysis of postinspiratory activity of phrenic motoneurons with chemical and vagal reflexes. J Appl Physiol 1986; **61**(4): p. 1499-509.

257. Tryba, AK, F Pena, SP Lieske, JC Viemari, M Thoby-Brisson, and JM Ramirez, Differential modulation of neural network and pacemaker activity underlying eupnea and sigh-breathing activities. J Neurophysiol 2008; **99**(5): p. 2114-25.

258. Lydic, R, HA Baghdoyan, and Z Lorinc, Microdialysis of cat pons reveals enhanced acetylcholine release during state-dependent respiratory depression. Am J Physiol 1991; **261**(3 Pt 2): p. R766-70.

259. Pickering, AE and JF Paton, A decerebrate, artificially-perfused in situ preparation of rat: Utility for the study of autonomic and nociceptive processing. J Neurosci Methods 2006; **155**(2): p. 260-71.

260. Ma, J, R Xiao, J Li, X Zhao, B Shi, and S Li, Determination of organophosphorus pesticides in underground water by SPE-GC-MS. J Chromatogr Sci 2009; **47**(2): p. 110-5.

261. St-Jacques, R and WM St-John, Transient, reversible apnoea following ablation of the pre-Botzinger complex in rats. J Physiol 1999; **520 Pt 1**: p. 303-14.

262. Reiner, E, B Krauthacker, V Simeon, and M Skrinjaric-Spoljar, Mechanism of inhibition in vitro of mammalian acetylcholinesterase and cholinesterase in solutions of 0,0-dimethyl 2,2,2-trichloro-1-hydroxyethyl phosphonate (Trichlorphon). Biochem Pharmacol 1975; **24**(6): p. 717-22.

263. Bellingham, MC and MF Ireland, Contribution of cholinergic systems to state-dependent modulation of respiratory control. Respir Physiol Neurobiol 2002; **131**(1-2): p. 135-44.